



Ross University School of Veterinary Medicine  
One Health Center for Zoonoses and Tropical Veterinary Medicine

Universidad de Granada, Instituto de Biotecnología  
Departamento de Parasitología

Dual Doctoral Thesis  
PhD by Research - RUSVM  
Programa de Doctorado en Biología Fundamental y de Sistemas – UGR

***Trichuris trichiura*: Assessment of potential alternative diagnostic  
methods and efficacy of treatments in the African Green  
Monkey animal model (*Chlorocebus sabaeus*).**

Presented by:  
Katalina Cruz DDS, MSc One Health  
Opting for the PhD degree

**Supervisors**

Patrick Kelly DVM, PhD  
Antonio Osuna Carrillo de Albornoz, PhD  
María Trelis Villanueva, PhD

October, 2021





Ross University School of Veterinary Medicine  
One Health Center for Zoonoses and Tropical Veterinary Medicine

Universidad de Granada, Instituto de Biotecnología  
Departamento de Parasitología

Dual Doctoral Thesis  
PhD by Research - RUSVM  
Programa de Doctorado en Biología Fundamental y de Sistemas – UGR

***Trichuris trichiura*: Assessment of potential alternative diagnostic  
methods and efficacy of treatments in the African Green  
Monkey animal model (*Chlorocebus sabaeus*).**

Presented by:  
Katalina Cruz DDS, MSc One Health  
Opting for the PhD degree

**Supervisors**

Patrick Kelly BVSC, PhD  
Antonio Osuna Carrillo de Albornoz, PhD  
María Trelis Villanueva, PhD

October, 2021

Editor: Universidad de Granada. Tesis Doctorales  
Autor: Katalina Cruz  
ISBN: 978-84-1117-312-4  
URI: <http://hdl.handle.net/10481/74611>



## Funding

Ross University School of Veterinary Medicine, through the One Health Center for Zoonoses and Tropical Veterinary Medicine, provided the funding for this doctoral thesis together with Universidad de Granada and Universitat de Valencia.

## The results from the doctoral thesis have been presented in

Cruz, K., Kelly, P., Vandenplas, M., Trelis, M., Marcilla, A. (2019, August 31 - September 1). Exploring how helminth extracellular vesicles (EVs) influence African green monkeys in St. Kitts, West Indies. Parasitic Helminths: New perspectives in Biology and Infection. Helminth EV Workshop. Hydra, Greece.

Cruz, K., Marcilla, A., Kelly, P., Vandenplas, M., Osuna A., Trelis, M. (2019, July 10 – 13). Salivary Diagnostics for the human whipworm (*Trichuris trichiura*), exploring the usefulness of the humoral response. ACACPMT Congress 2019. St. Kitts, West Indies.

Cruz, K., Trelis, M., Vandenplas, M., Marcilla, A., Osuna A., Verocai, GG., Kelly, P. (2019, April 7-10). 100 years later: Molecular characterization of *Primasubulura* sp. on St. Kitts, West Indies. Molecular Helminthology Conference, An Integrated Approach. San Antonio, Texas, USA.

Cruz, K., Marchi, S., Vandenplas, M., Beierschmitt, A., Trelis, M., Marcilla, A., Osuna, A. (2017, Octubre 27 - 31). Potencialidad del modelo animal: Mono Verde Africano (*Chlorocebus Sabaeus*) - *Trichuris trichiura* para el desarrollo de nuevos métodos inmunológicos de diagnóstico y seguimiento de la infección. Sociedad Española de Medicina Tropical y Salud Internacional Bilbao, España.

Also, the results from this thesis have been published in the following scientific publications:

Cruz, K., Marcilla, A., Kelly, P., Vandenplas, M., Osuna, A., & Trelis, M. (2021). *Trichuris trichiura* egg extract proteome reveals potential diagnostic targets and immunomodulators. *PLOS Neglected Tropical Diseases*, *15*(3), e0009221.

Cruz, K., Corey, T. M., Vandenplas, M., Trelis, M., Osuna, A., & Kelly, P. J. (2021). Case report: Control of intestinal nematodes in captive *Chlorocebus sabaesus*. *The Onderstepoort Journal of Veterinary Research*, *88*(1).

*Manuscript in preparation:*

Cruz, K., Marcilla, A., Kelly, P., Vandenplas, M., Osuna A., Trelis, M. (2021). *Trichuris trichiura* derived synthetic peptides with potential for the diagnosis of trichuriasis.

*To mom, Luci and Luis, for their resilience and unconditional love.*



## Acknowledgements

A few years ago, I was a dentist with an MSc One Health degree and the motivation to become part of the solution. It took a dream and a leap of faith to fly to Spain to meet Dr. María Trelis in Majadaonda, Spain for this day to be a reality. Dreams are certainly manifested with our intentions and daily actions.

First, I acknowledge the higher unified force of faith and light for the guidance I received through prayer, gratitude, and meditation.

I thank María Trelis, my University of Valencia supervisor for her devoted teaching, her patience and her resilient source of motivation. It did not matter if we were sharing the bench at the lab, the desk in her office or an ocean apart, her kindness and support was consistent. Her insurmountable positive energy and drive lit my path during the hardest times.

I thank Pat Kelly, my Ross University supervisor, for his patience and selfless dedication to my success with unconditional support. Pat offered me an open door when many closed, from the crack of dawn he proved to be a great listener and help me focus on the solution. He thought me the value of simplicity.

I thank Antonio Osuna, my University of Granada supervisor for his kindness and his support through the years. Being a UGR graduate is a dream that could not have been possible without his guidance, opportunities, and trust.

I thank Michel Vandenplas for his scientific enthusiasm and his knowledgeable support. Through the years he believed in me, and he stood up for my right to be recognized and respected as a professional PhD student.

I thank my tutor Dr. Susana Vilchez for her administrative support navigating the University of Granada doctoral program and the RUSVM research office team for their effort while adjusting to a dual bilingual PhD program.

I thank Dr. Antonio Marcilla, for his unique guidance and mentorship. He unlocked a world network of support that seemed surreal at times, but his companionship and example showed me that the best move forward is always to be myself!

To my laboratory buddies, from U of Valencia, Susi, Cristian, Theffy and Gemma; from U of Granada, Alexa, Luismi, Gloria, Lia, Samir, Albert, Alberto, Juan and Jenifer. Thank you for bringing a smile to my face, from endless Q&A sessions to bench ping pong, ice cube fights and dance contests you made my day!

Susi, you could easily be my Spanish twin – I adore you! Gloria and Luismi thank you for your mentorship, your time, and your motivation to make the most of every day. Lia and Alexa, the America girls, thank you for friendship, for listening and help me troubleshoot day and night, 24/7 always!

To my family in Costa Rica, my dad, brothers, and sister; thank you for your companionship along the way, your prayers and thoughts made 2500km or 5000km seem so much closer.

Grandma mami, you taught me that serving a bigger purpose was the path to find one's true passion. So, I did. Thank you. I love you.

Mom, I am grateful for your life, for beating cancer while I pushed the thesis forward, we did both together. Your resilience is my greatest teacher.

Luis and Luci, you are the foundation and light of our little family, and this is a merit to us. For leaning on each other as we grew and for the amazing life we have created together.

## Extended Summary – English

There are limited data on the efficacy of antiparasitic treatments and husbandry methods that can be used to control nematode infections in captive populations of African Green Monkeys (AGMs); *Chlorocebus sabaeus*. In routine Fecal Egg Count (FEC) testing, and post-mortem helminth examinations we determined the nematodes present in AGMs captured from the large (up to 50,000) feral population on the island of St. Kitts, West Indies. The most common nematode species identified in the AGMs FEC were *Capillaria* sp., followed by *Trichuris trichiura*, and strongylid species specifically (hookworm and *Trichostrongylus* spp.), but also *Strongyloides fuelleborni*.

After obtaining the data on parasitization by nematodes, we evaluated the anthelmintic efficacy of two different treatment regimens and the husbandry methods routinely employed at the animal facility. The first treatment regimen evaluated was praziquantel (5 mg/kg, given intramuscular) and albendazole (15 mg/kg, given orally) repeated after 2 weeks (PRAL), and the second one was ivermectin (300 µg/kg, given subcutaneously) and albendazole (10 mg/kg, given orally) daily for 3 days (IVAL). Both regimens were repeated at 3 – 5 month intervals. The PRAL treatment results had limited effect with only 2/12 (17%) AGMs negative at 2 months post-treatment, 1/7 (14%) at 4-5 months post-treatment and none (0%) negative at 10 to 24 months post initial treatment. The IVAL treatment regimen was more effective with 7/11 (64%) of the recipients negative at 3 months after the first treatment. The four that remained infected were cleared of *T. trichiura* after the second round of treatment but three appeared to have been reinfected with *Capillaria*.

Husbandry methods to control reinfection consisted of a daily cage washing with water and biweekly cage sanitation using a combination of steam (>82 °C), a quaternary-based disinfectant and an accelerated hydrogen peroxide foam. The facility's water is sanitized, filtered, and treated with ultraviolet light; therefore, thorough washing of fruits and vegetables, maintenance of pest control practices and controlled monitoring of social enclosure times could further limit potential sources of reinfection that can impact optimal health and behavior of study animals. It is important to note that regular FECs will not detect all nematode infections and full advantage should be

taken of necropsied animals for parasite detection and surveillance. Our results support and confirm that for *T. trichiura* there is no correlation between fecal egg counts and worm counts.

Worldwide, most cases of trichuriasis remain undiagnosed, chronic infections remain undetected and an overall lack of understanding of potential zoonotic exposures prevails. Therefore, early diagnosis of trichuriasis and diagnostic methods that do not rely on inconsistent clinical signs or fecal analysis are crucial to detect infections following accidental ingestion and during prolonged prepatent period of the parasite. The difficulty of access to the parasitic material (feces and adult nematodes) and biological samples from the hosts, further threatens the development of alternative diagnostic methods. With our work, we show that the St. Kitts green monkey being naturally infected with *T. trichiura*, serves as a predictive disease modeling test system that facilitates preclinical evaluation having similar immunological responses as humans.

Embryonated eggs are the infectious developmental stage of *T. trichiura* and are the primary stimulus for the immune system of the host. The intestinal-dwelling *T. trichiura* affects an estimated 465 million people worldwide with an estimated global burden of disease of 640,000 DALYs (Disability Adjusted Life Years). In Latin America and the Caribbean, trichuriasis is the most prevalent soil transmitted helminthiasis in the region (12.3%). The adverse health consequences impair childhood school performance and reduce school attendance, resulting in lower future wage-earning capacity. The accumulation of the long-term effects translates into poverty promoting sequelae and a cycle of impoverishment.

Each infective *T. trichiura* egg carries the antigens needed to face the immune system with a wide variety of proteins present in the shell, larvae's surface, and the accompanying fluid that contains their excretions/secretions. We used a proteomic approach with tandem mass spectrometry to investigate the proteome of soluble non-embryonated Egg Extracts (EE) of *T. trichiura* obtained from naturally infected AMG. A total of 231 proteins were identified, 168 of them with known molecular functions. The proteome revealed common proteins families which are known to play roles in energy and metabolism; the cytoskeleton, muscle and motility; proteolysis; signaling; the stress response and detoxification; transcription and translation; and lipid binding and transport. In addition to the study of the *T. trichiura* non-embryonated egg proteome, the antigenic profile of the *T. trichiura* EE and soluble Female Extract (FE) proteins against serum and saliva antibodies

from *C. sabaesus* naturally infected with trichuriasis was investigated. We used an immunoproteomic approach by Western blot and tandem mass spectrometry from the corresponding SDS-PAGE gels. Vitellogenin N and VWD and DUF1943 domain containing protein, poly-cysteine and histidine tailed protein isoform 2, carbohydrate-Binding Module 14 domain containing protein, kunitz bovine basic pancreatic trypsin inhibitor domain containing protein and heat shock protein 70, glyceraldehyde-3-phosphate dehydrogenase, actin, and enolase, were among the potential immunoactive proteins.

To identify possible cross-reactions of *T. trichiura* and other helminthic antigens, Western blots were performed on soluble protein extracts from other helminths, nematodes (*Primasubulura* sp., *Anisakis simplex*, *Aspicularis tetraptera*) and trematodes (*Fasciola hepatica*, *Dicrocoelium dendriticum* and *Gnathosoma hispidium*) with serum from *T. trichiura* naturally infected AGMs.

A total of four synthetic peptides were designed based on the amino acid sequences deduced from the candidate proteins present in the EE and, FE and recognized by saliva and serum antibodies from *C. sabaesus* naturally infected with *T. trichiura*. The final candidate proteins from which the peptides were designed were: Vitellogenin N and VWD and DUF1943 domain containing protein, CBM 14 domain containing protein, Kunitz BPTI domain containing protein, Poly-cysteine and histidine tailed protein isoform 2. The diagnostic feasibility of the selected peptides derived from the four final protein candidates VgNVD (YRSLAIDDLVLTETAP), KBDCP (QERCVATLPASVICRLP), CBM14 (SAPTTVTTQLSPVDCVTL), and PCHTP-2 (TECVKPPAHDCPAFG) was evaluated with 19 serum and 19 saliva samples from *T. trichiura* naturally infected AGMs and 6 negative human sample controls.

In both, the saliva and the serum samples, the peptides that elicited the strongest recognition by antibodies were the KBDCP (QERCVATLPASVICRLP), which is an FE stage specific protein of low abundance, and the VgNVD (YRSLAIDDLVLTETAP), which is an EE stage specific protein. The egg protein CBM14 (SAPTTVTTQLSPVDCVTL), and the most abundant protein in all developmental stages of the parasite PCHTP-2 (TECVKPPAHDCPAFG) presented the weakest signals (optical density, OD). Overall, the saliva samples showed strongest optical density values and lower cutoff values than the serum samples.

To our knowledge, this is the first study on the *T. trichiura* non-embryonated egg proteome as a novel source of information on potential targets for immunodiagnostics and immunomodulators from a neglected tropical disease. This initial list of *T. trichiura* non-embryonated egg proteins (proteome and antigenic profile) can be used in future research on the immunobiology and pathogenesis of human trichuriasis and the treatment of human intestinal immune-related diseases.

## Resumen Extendido – Español

Existe escasez de información acerca de la eficacia de los tratamientos antiparasitarios y los métodos de vigilancia y seguimiento que deben usarse para controlar las infecciones por nematodos en poblaciones cautivas de monos verdes africanos (African Green Monkeys; AGM); *Chlorocebus sabaues*. En los ensayos para el diagnóstico parasitario en heces (Fecal Egg Count; FEC), así como en los exámenes de intestino grueso realizados post-mortem para la identificación de presencia o ausencia de helmintos, logramos cuantificar la presencia de nematodos en AGMs capturados de una gran población salvaje (aproximadamente 50.000) en la isla de St. Kitts, Antillas Menores. Las especies de nematodos más comunes identificadas en las heces fueron *Capillaria* sp., seguida de *Trichuris trichiura*, especies de strongylidos (anquilostoma y *Trichostrongylus* spp.), y también *Strongyloides fuelleborni*.

Después de obtener los datos sobre la parasitación por nematodos, evaluamos la eficacia antihelmíntica de dos regímenes de tratamientos diferentes, así como los métodos de cuidado y mantenimiento empleados rutinariamente en la institución donde residen los animales. El primer régimen de tratamiento evaluado fue praziquantel (5 mg/kg, intramuscular) y albendazol (15 mg/kg, oral) repetido a las 2 semanas (PRAL), y el segundo método fue ivermectina (300 µg/kg, subcutáneo) y albendazol (10 mg/kg, oral) a diario por 3 días (IVAL). Ambos regímenes se repitieron a intervalos de 3 a 5 meses. Los resultados del tratamiento de PRAL tuvieron un efecto limitado con solo 2/12 (17%) AGMs con resultados negativos a los 2 meses post-tratamiento, 1/7 (14%) a los 4-5 meses post-tratamiento, y ninguno negativo de los 10 a los 24 meses desde del tratamiento inicial. El régimen de tratamiento IVAL fue más eficaz con 7/11 (64%) de los AGMs negativos a los 3 meses después del primer tratamiento. Los cuatro AGMs que permanecieron infectados lograron eliminar la infección con *T. trichiura* después de una segunda tanda de tratamiento, sin embargo, tres AGMs aparecieron reinfectados con *Capillaria* sp.

Los métodos de estabulado de los animales empleados para controlar la reinfección consistieron en el lavado diario de las jaulas con agua y la desinfección con vapor (>82°C), y un desinfectante de base cuaternaria y espuma de peróxido de hidrógeno cada dos semanas. En la institución, el agua se desinfecta, se filtra y se trata con luz ultravioleta, junto con ello, el lavado de frutas y

vegetales, el mantenimiento de las buenas prácticas de control de plagas y el monitoreo de los tiempos en jaulas de grupos, podrían limitar aún más las posibles fuentes de reinfección que pueden afectar la salud y el comportamiento óptimo de los animales. Es importante recalcar que a pesar de realizarse exámenes de heces frecuentes no se detectarán todas las infecciones por nematodos y se debe aprovechar al máximo a los animales sometidos a necropsia para la detección y vigilancia parasitaria. Nuestros resultados apoyan y confirman que para *T. trichiura* no existe una correlación entre el número de huevos en el diagnóstico en heces, por los métodos tradicionales de conteo de huevos, y el número de parásitos en el intestino grueso.

A nivel mundial, la mayoría de casos de trichuriasis permanecen sin diagnosticar, las infecciones crónicas no son detectadas, y prevalece una falta general de comprensión en cuanto a su potencial zoonótico. Por lo tanto, el diagnóstico temprano de trichuriasis unido a métodos de diagnóstico que no se basen en signos clínicos inespecíficos o únicamente en análisis de heces son cruciales para detectar infecciones accidentales especialmente durante el prolongado periodo prepatente del parásito. La dificultad de acceso al material parasitario (heces y nematodos), y a muestras biológicas de los hospedadores, complica aún más el desarrollo de métodos de diagnóstico alternativos. Con nuestro trabajo, demostramos que el mono verde de St. Kitts, al estar naturalmente infectado con *T. trichiura*, facilita su uso como un modelo para la evaluación preclínica de la enfermedad al tener una respuesta inmunológica similar a la de los humanos.

Los huevos embrionados de *T. trichiura* son el estadio infectivo de este nematodo y representan el primer estímulo para el sistema inmunitario del hospedador. El parásito intestinal *T. trichiura* se estima que afecta a 465 millones de personas a nivel mundial, con una carga de enfermedad de 640.000 DALYs (años de vida ajustados a la discapacidad). En América Latina y el Caribe, *T. trichiura* es el geohelminto más prevalente de la región (12.3%). Las consecuencias adversas para la salud afectan al rendimiento escolar de la niñez y reducen la asistencia a la escuela, lo que resulta en una menor capacidad para obtener ingresos en el futuro adulto. La acumulación de efectos a largo plazo se traduce en secuelas promotoras de pobreza y en un ciclo de empobrecimiento.

Cada huevo embrionado de *T. trichiura* contiene los antígenos necesarios para enfrentarse al sistema inmunitario, una gran variedad de proteínas presentes en su cubierta, en la superficie de



la larva que contiene y en el líquido de excreción/secreción que acompaña a los componentes del huevo. Se utilizaron herramientas de proteómica mediante espectrometría de masas en tándem para investigar el proteoma de las proteínas solubles del extracto del huevo no embrionado (EE) de *T. trichiura* obtenido de AGM infectados naturalmente. Se identificaron un total de 231 proteínas, 168 de ellas con funciones celulares conocidas. El proteoma reveló familias de proteínas comunes, que son conocidas por su relación con la obtención de energía, en el metabolismo; el citoesqueleto, el músculo y la movilidad; la proteólisis; la señalización; la respuesta al estrés y la detoxificación; la transcripción y la traducción; y la unión de lípidos y el transporte celular. Además del estudio del proteoma del huevo de *T. trichiura*, se investigó el perfil antigénico de las proteínas solubles, tanto del huevo (EE) como de la hembra (FE) de *T. trichiura*, sobre los anticuerpos presentes en el suero y en la saliva de *C. sabaesus* naturalmente infectados con trichuriasis. Para ello, se utilizó un enfoque inmunoproteómico con *Western blot* y espectrometría de masas en tándem de los geles SDS-PAGE correspondientes. La proteína vitellogenina N con dominios de VWD y DUF1943, la proteína poli-cisteína e histidina isoforma 2, la proteína con dominio de módulo de unión a carbohidratos 14, la proteína kunitz con dominio de inhibidor de la tripsina pancreática bovina, la proteína de choque térmico 70 (HSP-70), la gliceraldehído-3-fosfato deshidrogenasa, la actina y la enolasa, son las proteínas propuestas en nuestro estudio como las potencialmente immunoactivas.

Para identificar posibles reacciones cruzadas entre antígenos de *T. trichiura* y otras especies de helmintos, se realizaron Western blots con extractos de las proteínas solubles de otros helmintos, nematodos (*Primasubulura* sp., *Anisakis simplex*, *Aspicularis tetraptera*) y trematodos (*Fasciola hepatica*, *Dicrocoelium dendriticum* and *Gnathosoma hispidium*) contra suero de AGM naturalmente infectados con *T. trichiura*.

Un total de cuatro péptidos sintéticos se diseñaron basados en las secuencias de aminoácidos deducidas de las proteínas candidatas presentes en EE y FE, y que eran potencialmente reconocidas por anticuerpos de saliva y suero de *C. sabaesus* naturalmente infectados con *T. trichiura*. Las proteínas candidatas finales de donde fueron diseñados los péptidos son: vitellogenina N con dominios de VWD y DUF1943 (VgNVD), la proteína la proteína con dominio de módulo de unión a carbohidratos 14 (CBM14), la proteína kunitz con dominio de inhibidor de la

tripsina pancreática bovina (KBDCP) y la proteína poli-cisteína e histidina isoforma 2 (PCHTP-2). La capacidad diagnóstica de los péptidos derivados de las cuatro proteínas candidatas VgNVD (YRSLAIDDLTETAP), KBDCP (QERCVATLPASVICRLP), CBM14 (SAPTTVTTQLSPVDCVTL), and PCHTP-2 (TECVKPPAHDCPAFG) fue evaluada contra 19 muestras de suero y 19 muestras de saliva de AGM naturalmente infectados con *T. trichiura*, y 6 muestras de saliva y suero control negativas de humano.

En ambos grupos de muestras, saliva y suero, los péptidos que provocaron el mayor reconocimiento por anticuerpos fueron KBDCP (QERCVATLPASVICRLP), una proteína específica de la hembra adulta (FE) y de poca abundancia y la VgNVD (YRSLAIDDLTETAP) una proteína específica del huevo (EE) de *T. trichiura*. Otra proteína encontrada en el EE de *T. trichiura* CBM14 (SAPTTVTTQLSPVDCVTL), y la proteína más abundante en todos los estados de desarrollo del parásito, la PCHTP-2 (TECVKPPAHDCPAFG) presentaron las respuestas más débiles (densidad óptica, OD). En resumen, las muestras de saliva obtuvieron los valores de densidades ópticas más pronunciados, y los valores de cut-off más bajos en comparación con las muestras de suero.

Hasta la fecha, este es el primer estudio del proteoma de los huevos de *T. trichiura* y el uso de estos como una fuente alternativa de información sobre posibles moléculas diana para inmunodiagnóstico e inmunomodulación de esta enfermedad tropical desatendida.

## Table of Contents

<b>1</b>	<b>Introduction.....</b>	<b>14</b>
<b>1.1</b>	<b>Human helminthiasis: Nematoda (roundworms) .....</b>	<b>14</b>
1.1.1	Soil-Transmitted Helminths (STHs): Global burden and relevance in public health	15
1.1.2	Soil-Transmitted Helminths strategies for control .....	18
1.1.3	Zoonotic potential of STHs and reservoirs.....	19
<b>1.2</b>	<b><i>Trichuris trichiura</i>.....</b>	<b>20</b>
1.2.1	Classification and Taxonomy .....	20
1.2.2	Life cycle and Transmission.....	21
1.2.3	Morphology of developmental stages.....	22
1.2.3.1	<i>Trichuris trichiura</i> egg anatomy .....	22
1.2.3.2	<i>Trichuris trichiura</i> larval stages .....	24
1.2.3.3	<i>Trichuris trichiura</i> adult female and male.....	26
1.2.4	Genomics and Proteomics .....	27
<b>1.3</b>	<b>Trichuriasis .....</b>	<b>32</b>
1.3.1	Epidemiology of the disease and population at risk.....	32
1.3.2	Clinical disease in humans and nonhuman primates .....	33
1.3.2.1	Humans .....	33
1.3.2.2	Nonhuman primates .....	34
1.3.3	Diagnostics .....	35
1.3.3.1	Parasitological methods.....	35
1.3.3.2	Immunological diagnostic methods.....	37
1.3.4	Treatments.....	37
1.3.4.1	Humans .....	37
1.3.4.2	Nonhuman primates .....	38
<b>1.4</b>	<b>Host immune response against <i>Trichuris trichiura</i> infection .....</b>	<b>39</b>
1.4.1	Antibody Response .....	40

1.4.2	T helper lymphocytes.....	42
1.4.3	Co-infections .....	43
<b>2</b>	<b>Justification and Objectives .....</b>	<b>44</b>
<b>2.1</b>	<b>General Objective .....</b>	<b>44</b>
<b>2.2</b>	<b>Specific Objectives .....</b>	<b>44</b>
<b>3</b>	<b>Materials and Methods .....</b>	<b>45</b>
<b>3.1</b>	<b>Ethical statements .....</b>	<b>45</b>
<b>3.2</b>	<b><i>Trichuris trichiura</i>.....</b>	<b>45</b>
3.2.1	Adults .....	45
3.2.2	Adults extracts (AE).....	46
3.2.3	<i>Trichuris trichiura</i> non-embryonated (NE) egg extracts (EE) .....	47
3.2.4	Protein quantification of parasite extracts .....	48
3.2.5	Preparation for Scanning Electron Microscopy (SEM).....	48
<b>3.3</b>	<b>African green monkeys (AGM; <i>Chlorocebus sabaues</i>) .....</b>	<b>48</b>
3.3.1	Animals.....	48
3.3.2	Feces and analysis.....	49
3.3.3	Sera .....	49
3.3.4	Saliva .....	49
3.3.5	Human sera and saliva .....	50
<b>3.4</b>	<b>Case report on nematode control of captive AGMs.....</b>	<b>50</b>
3.4.1	Animals and Facilities.....	50
3.4.2	Treatments.....	51
3.4.3	Monitoring of treatments .....	52
3.4.4	Morphological identification .....	52
<b>3.5</b>	<b>Identification of immunogenic proteins of diagnostic value in <i>T. trichiura</i> adults and eggs</b>	<b>54</b>

3.5.1	Indirect ELISA for detection of specific antibodies anti- <i>Trichuris</i> in sera and saliva of infected animals.....	54
3.5.2	One dimensional <i>SDS-PAGE</i> electrophoresis (1-DE) gel staining and Western-blot with serum and saliva .....	54
3.5.3	Two-dimensional <i>SDS-PAGE</i> electrophoresis (2-DE), gel staining and Western-blot with serum .....	55
<b>3.6</b>	<b>Proteomic analysis of <i>T. trichiura</i> AE and EE .....</b>	<b>56</b>
3.6.1	Sample preparation .....	57
3.6.2	Liquid chromatography and tandem mass spectrometry (LC-MS/MS).....	57
3.6.3	Bioinformatic analysis.....	58
3.6.4	Proteomic results interpretation glossary .....	59
3.6.5	Proteomic analysis: Protein identification.....	61
3.6.5.1	First analysis: for data base construction .....	61
3.6.5.2	Second Analysis: homology determination in relation to other nematodes ...	63
3.6.5.3	Third analysis: Study of immunogenic potential of each protein and its peptides. 65	
3.6.5.4	Fourth analysis: Study of immunogenic potential of each selected peptide ...	67
3.6.5.5	Fifth analysis: Final BLAST analysis of the individual peptide sections selected from the 15 preliminary protein candidates. ....	70
<b>3.7</b>	<b>Design and evaluation of <i>T. trichiura</i> derived synthetic peptides for diagnosis.....</b>	<b>71</b>
3.7.1	Selection and design of final peptide candidates for ELISA.....	71
3.7.2	Synthetic peptides .....	72
3.7.3	Indirect ELISA for testing the applicability of designed peptides .....	72
<b>4</b>	<b>RESULTS.....</b>	<b>73</b>
<b>4.1</b>	<b>Efficacy of treatment analysis and egg to worm correlation in captive <i>C. sabaesus</i> ..</b>	<b>73</b>
<b>4.2</b>	<b><i>Trichuris trichiura</i> egg extract proteome reveals potential diagnostic target and immunomodulators .....</b>	<b>78</b>
4.2.1	Proteomic characterization of the <i>T. trichiura</i> egg extract (EE) .....	78

4.2.2	Gene ontology (GO) .....	78
4.2.3	1-DE and immunoblot analysis of <i>T. trichiura</i> EE and FE .....	82
<b>4.3</b>	<b>Identification of immunogenic proteins of diagnostic value .....</b>	<b>87</b>
4.3.1	Specificity Immunoblot analysis .....	87
4.3.2	2-DE SDS-PAGE electrophoresis and Western-Blot with serum antigenic profile ...	88
<b>4.4</b>	<b>Selection and evaluation of applicability of designed synthetic peptides.....</b>	<b>89</b>
4.4.1	Final protein candidates and derived peptide selection .....	90
4.4.1.1	Vitellogenin N and VWD and DUF1943 domain containing protein .....	90
4.4.1.2	CBM 14 domain containing protein .....	95
4.4.1.3	Kunitz BPTI domain containing protein .....	98
4.4.1.4	Poly-cysteine and histidine tailed protein isoform 2 .....	102
4.4.2	Synthetic peptides diagnostic feasibility evaluation through Indirect ELISA .....	104
<b>4.5</b>	<b><i>Trichuris trichiura</i> Scanning Electron Microscopy (SEM) images .....</b>	<b>109</b>
<b>4.6</b>	<b>Histopathology .....</b>	<b>111</b>
<b>5</b>	<b>Discussion .....</b>	<b>112</b>
<b>5.1</b>	<b>Control of nematode infections in captive <i>Chlorocebus sabaesus</i> .....</b>	<b>112</b>
5.1.1	Nematode species present in captive <i>Chlorocebus sabaesus</i> .....	112
5.1.2	Treatment and control outcomes.....	114
<b>5.2</b>	<b><i>Trichuris trichiura</i> immunogenic proteins of diagnostic value.....</b>	<b>118</b>
5.2.1	Diagnostic challenges to overcome .....	118
5.2.2	<i>Trichuris trichiura</i> genome and other helminths provide insights into the egg proteome. ....	118
5.2.2.1	EE proteome proteins with the largest numbers of distinct peptides .....	119
5.2.2.2	Antigenic profile of <i>T. trichiura</i> EE and FE extracts and identification of the top immunodominant proteins.....	121
5.2.2.3	Diagnostic applicability of the synthetic peptides designed from FE and EE .	125
<b>6</b>	<b>Conclusions.....</b>	<b>127</b>

<b>7</b>	<b>Appendices .....</b>	<b>129</b>
7.1	Appendix I. Karnovsky's fixative protocol .....	129
7.2	Appendix II. Double centrifugation with Sheather's sugar flotation solution .....	130
7.3	Appendix III. Standard Operating Procedure for saliva collection .....	132
7.4	Appendix IV. Saliva conservation mix .....	134
7.5	Appendix V. List of brand names and commercial addresses used .....	135
7.6	Appendix VII. IACUC approvals for African green monkey samples .....	137
7.7	Appendix VIII. IRB approvals for human samples .....	140
<b>8</b>	<b>References .....</b>	<b>143</b>
<b>9</b>	<b>Annexes .....</b>	<b>168</b>
9.1	Supplementary table 1.....	168

## List of Figures

Figure 1.1 Nematoda, Soil-Transmitted Helminths (STH) in the perspective of helminth family.	15
Figure 1.2 Distribution of STHs infection prevalence in 2010 by parasitic species. ....	16
Figure 1.3 Life cycle of <i>Trichuris trichiura</i> . ....	21
Figure 1.4 <i>Trichuris trichiura</i> egg anatomy. ....	23
Figure 1.5 Larval developmental stages ....	24
Figure 1.6 Larval developmental stages (continuation) ....	25
Figure 1.7 <i>Trichuris trichiura</i> adult anatomy ....	26
Figure 1.8 Bayesian tree showing most up to date relationships among <i>Trichuris</i> species. ....	29
Figure 1.9 Type 2 immunity ....	40
Figure 3.1 <i>Trichuris trichiura</i> uterus dissection guide. ....	47
Figure 3.2 Morphologic identification of nematode eggs species found. ....	53
Figure 3.3 Example of Proteins Detected Table from bioinformatics analysis database. ....	60
Figure 3.4 Example of UniProt page accessed per protein for information retrieval during bioinformatic analysis. ....	62
Figure 3.5 FASTA sequence format example. ....	63
Figure 3.6 Example of protein (VNVD) FASTA sequence format analysis by protein BLAST. ....	64
Figure 3.7 Example of the GenBank data from the National Center for Biotechnology Information database (NCBI). ....	65
Figure 3.8 Example of predicted B cell epitope results from the B cell epitope prediction data base. ....	66
Figure 3.9 Example of secondary BLAST analysis of 1 out of 13 peptide sequences identified for the VNVD protein. ....	67
Figure 3.10 Example of the antigenic analysis results obtained from the selected peptide sequences. ....	68
Figure 3.11 Example of Parker Hydrophilicity prediction result for the peptide YRSLADDVLTETAP. ....	69
Figure 3.12 Example of Kolaskar & Tongaonkar antigenicity scale prediction tool result for the peptide YRSLADDVLTETAP. ....	70



Figure 3.13 Example of final blast analysis for the peptide YRSLAIDDLVLTETAP.....	71
Figure 4.1 Prevalence of nematode species found in captive St. Kitts African green monkeys. .	73
Figure 4.2 Lack of correlation between eggs per gram of feces (EPG) and total adult <i>T. trichiura</i> counts from the 26 <i>C. sabaeus</i> . .....	75
Figure 4.3 Lack of correlation between eggs per gram of feces (EPG) and total female <i>T. trichiura</i> counts from the 26 <i>C. sabaeus</i> . .....	76
Figure 4.4 Main biological processes of the identified proteins in the non-embryonated egg extract proteome of <i>T. trichiura</i> according to information obtained from the Gene Ontology (GO) database. ....	82
Figure 4.5 Major immunogenic proteins detected in <i>T. trichiura</i> extracts. ....	83
Figure 4.6 Western blot showing AGMs sera antibodies in nematodes and trematodes extracts. ....	88
Figure 4.7 2-DE SDS-PAGE electrophoresis and Western-Blot with serum. Antigenic profile detected in <i>T. trichiura</i> egg extracts (EE).....	89
Figure 4.8 3D model Vitellogenin N and VWD and DUF1943 domain containing protein .....	93
Figure 4.9 Alignment of known protein identities.....	94
Figure 4.10 3D model CBM 14 domain containing protein model. ....	97
Figure 4.11 Alignment of known protein identities.....	97
Figure 4.12 3D model Kunitz BPTI domain containing protein.....	100
Figure 4.13 Alignment of known protein identities.....	101
Figure 4.14 3D model Poly-cysteine and histidine tailed protein isoform 2. ....	103
Figure 4.15 Alignment of known protein identities.....	104
Figure 4.16 Optical densities from 19 saliva samples from <i>Trichuris trichiura</i> infected AGMs analyzed with indirect ELISA against peptides VgNVD (YRSLAIDDLVLTETAP), KBDCP (QERCVATLPASVICRLP). ....	105
Figure 4.17 Optical densities from 19 saliva samples from <i>Trichuris trichiura</i> infected AGMs analyzed with indirect ELISA against peptides CBM14 (SAPTTVTTQLSPVDCVTL), and PCHTP-2 (TECVKPPAHDCPAFG).....	106

Figure 4.18 Optical densities from 19 serum samples from <i>Trichuris trichiura</i> infected AGMs analyzed with indirect ELISA against peptides VgNVD (YRSLAIDDLVLTETAP), KBDCP (QERCVATLPASVICRLP). .....	107
Figure 4.19 Optical densities from 19 serum samples from <i>Trichuris trichiura</i> infected AGMs analyzed with CBM14 (SAPTTVTTQLSPVDCVTL) and PCHTP-2 (TECVKPPAHDCPAFG)...	108
Figure 4.20 Adult female <i>Trichuris trichiura</i> anterior and posterior. ....	109
Figure 4.21 Adult <i>Trichuris trichiura</i> female and male reproductive structures. ....	110
Figure 4.22 Crypts of Lieberkühn within normal limits. ....	111
Figure 5.1 Graphical representation of treatment results evaluated in captive AGM.....	117

## List of tables

Table 1.1 Estimated global numbers infected with soil transmitted helminths and overall prevalence. ....	17
Table 1.2 Parasitological diagnostic methods for <i>Trichuris trichiura</i> . ....	36
Table 3.1 Convenience samples used to prepare protein extracts for the specificity assays.....	46
Table 3.2 Final candidate proteins and respective peptide selection. ....	72
Table 4.1 Outcome of the praziquantel and albendazole treatment regimen (PRAL) on fecal eggs identified 2 to 24 months later and visual identification of adult <i>Trichuris trichiura</i> in the large intestine at necropsy.....	74
Table 4.2 Fecal egg count (FEC) results and adult <i>Trichuris trichiura</i> found at necropsy in animals treated with ivermectin and albendazole (IVAL). ....	77
Table 4.3 Main proteins identified in the EE proteome (10 or more distinct peptides) organized by functional annotation. ....	80
Table 4.4 Potential identity of the EE proteins targeted by serum and salivary antibodies based on the MW data of the EE proteome. ....	84
Table 4.5 Protein identities, in decreasing abundance, in immunodominant bands 1W and 2W in Western blots with EE as antigen. Proteins were identified by LC-MS/MS of corresponding areas in SDS-PAGE gels, 1G and 2G.....	85
Table 4.6 Protein identities, in decreasing abundance within FE excised gel areas (3G, 4.1G, 4.2G) with suitable MW matching Western blot band areas 3W and 4W. ....	86

## List of Abbreviations, Acronyms, and Initialisms

Abbreviation	Meaning
1-DE	One Dimensional Electrophoresis
2-DE	Two Dimensional Electrophoresis
AAALAC	Association for Assessment and Accreditation of Laboratory Animal Care International
ACN	Acetonitrile
AE	Adult Extract
AGM	African Green Monkey
APV	Association of Primate Veterinarians
ATP	Adenosine Triphosphate
BE	Equilibration Buffer
BLAST	Basic Local Alignment Search Tool
BSA	Bovine Serum Albumin
CBM14	Carbohydrate-Binding Module 14 domain containing protein
CDC	Centers for Disease Control and Prevention
CEGMA	Core Eukaryotic Genes Mapping Approach
CHAPS	Cholamidopropyl dimethylammonium-1-propanesulfonate
CIC	Center for Scientific Instrumentation
CIDA	Chronic Iron Deficiency Anemia
DALYs	Disability Adjusted Life Years
DNA	Deoxyribonucleic Acid
DTT	Dithiothreitol
EE	Egg Extract
EGF	Epidermal Growth Factor
ELISA	Enzyme Linked Immunosorbent Assay
EMBL-EBI	European Bioinformatics Institute
EPG	Eggs Per Gram

ERR	Egg Reduction Rates
ES	Excretion/Secretion
EVs	Extracellular Vesicles
FA	Formic Acid
FASTA	Fast-All
FE	Female Extract
FEC	Fecal Egg Counts
GAPDH	Glyceraldehyde-3-Phosphate Dehydrogenase
GO	Gen Ontology
HSP-70	Heat Shock Protein 70
IAA	Iodoacetamide
IACUC	Institutional Animal Care and Use Committee
IDA	Information Dependent Acquisition Mode
IEF	Isoelectric Focusing
IFN- $\gamma$	Interferon $\gamma$
IL	Interleukin
IRB	Institutional Review Board
ITS	Internal Transcribed Spacers
IVAL	Ivermectin and Albendazole
KBDCP	Kunitz Bovine Basic Pancreatic Trypsin Inhibitor (BPTI) domain containing protein
LAMP	Loop-Mediated Isothermal Amplification
LC-MS/MS	Liquid Chromatography and Tandem Mass Spectrometry
MDA	Mass Drug Administration
MS/MS	Tandem Mass Spectrometry
MSP	Major Sperm Proteins
MW	Molecular Weight
NCBI	National Center for Biotechnology Information

NE	Non-Embryonated
NHP	Nonhuman Primate
NTDs	Neglected Tropical Diseases
OD	Optical Density
OPD	O-Phenylenediamine dihydrochloride
PBS	Phosphate Buffered Saline
PBST	PBS - Tween
PCHTP-2	Polycysteine and Histidine Tailed Protein isoform 2
PCR	Polymerase Chain Reaction
PO	<i>Per orem</i> "by mouth"
PRAL	Praziquantel and Albendazole
RUSVM	Ross University School of Veterinary Medicine
SCSIE	Servei Central de Suport a la Investigació Experimental
SD	Standard Deviation
SDS-PAGE	Sodium Dodecyl Sulphate–Polyacrylamide Gel Electrophoresis
SEM	Scanning Electron Microscopy
SKBRF	Saint Kitts Biomedical Research Foundation
SLPI	Secretory Leukocyte Protease Inhibitor
SQ	Subcutaneous
STH	Soil-Transmitted Helminth
TDS	<i>Trichuris</i> Dysentery Syndrome
TFA	Trifluoroacetic Acid
T <sub>H</sub> 1	T helper Lymphocyte 1
T <sub>H</sub> 2	T helper Lymphocyte 2
T <sub>H</sub> 9	T helper Lymphocyte 9
VgNVD	Vitellogenin N and VWD and DUF1943 domain containing protein
WAP	Whey Acidic Protein
WB	Western Blot

WHO	World Health Organization
YLDs	Years Lived with Disability

**List of Appendices**

- Appendix I      Karnovsky's fixative
- Appendix II     Double centrifugation with Sheather's sugar flotation solution
- Appendix III    Standard Operating Procedure for saliva collection
- Appendix IV     Saliva conservation mix
- Appendix V      Brand names and addresses of materials used
- Appendix VI     IACUC approvals for African green monkey samples
- Appendix VII    IRB approvals for human samples

**List of Annexes**

- Annex I          Supplementary table 1

# 1 Introduction

## 1.1 Human helminthiasis: Nematoda (roundworms)

### Key concepts

- Soil-transmitted helminth (STH) infections are a major group of nematodes amongst the most common infections in humans worldwide.
- Mainly caused by the whipworm *Trichuris trichiura*, *Ascaris lumbricoides* and the hookworms; *Necator americanus* and *Ancylostoma duodenale*.
- They infect the host by accidental ingestion of eggs present in human or nonhuman primate (NHP) feces or by active infections after skin penetration of the larvae (*N. americanus* and *A. duodenale*).
- Eggs and larvae can contaminate food, water, and soil, especially in areas where sanitation is poor.
- Approximately 1.5 billion people are infected with STH worldwide (Pullan *et al.*, 2014).
- 4.98 million years lived with disability (Years Lost to Disability (YLDs)) are attributed to STH (Pullan *et al.*, 2014).
- Infected children are nutritionally, physically, and cognitively impaired. During adulthood, they will face reduced worker productivity and quality of life.
- Control is based on periodical deworming through Mass Drug Administration (MDA) campaigns, preventive health education and improved sanitation conditions.
- Diagnosis is based on the detection of eggs in feces using a variety of fecal analysis techniques.
- *Strongyloides stercoralis* is also part of the STH but requires different diagnostic methods and treatment, for this reason, is usually underrepresented, underdiagnosed, and not impacted by MDA programs as the other STH.

Human parasitic helminths are classified into three main groups as represented in **Figure 1.1** Nematodes, trematodes and cestodes.



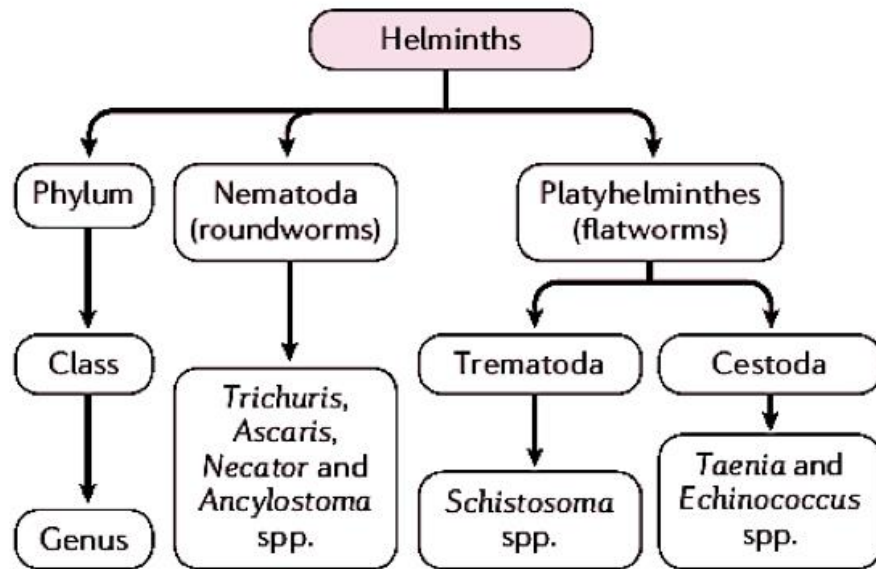


Figure 1.1 Nematoda, Soil-Transmitted Helminths (STH) in the perspective of helminth family.

Adapted from Else *et al.*, 2020

Human helminthiasis is an umbrella term for these multicellular endoparasites, and STH are the most common nematode infections in humans.

### 1.1.1 Soil-Transmitted Helminths (STHs): Global burden and relevance in public health

Globally an estimated 2000 million people are infected with STHs (World Health Organization (WHO), 2018) and the number of global deaths associated with high-intensity infections adds up to 12,000 to 135,000 per year (Salaam-Blyther *et al.*, 2011; WHO, 2012b). Infections are broadly distributed in all continents, but almost 70% of the infections occur in Asia (Pullan *et al.*, 2014). *Ascaris lumbricoides* shows the widest distribution with the highest transmission rate observed in Cameroon (30.8%); hookworms (*Ancylostoma duodenale* and *Necator americanus*) highest transmission observed in the Central African Republic (30.5%), and *T. trichiura* infections reached the highest prevalence in Malaysia (49.9%) (Figure 1.2 and Table 1.1).

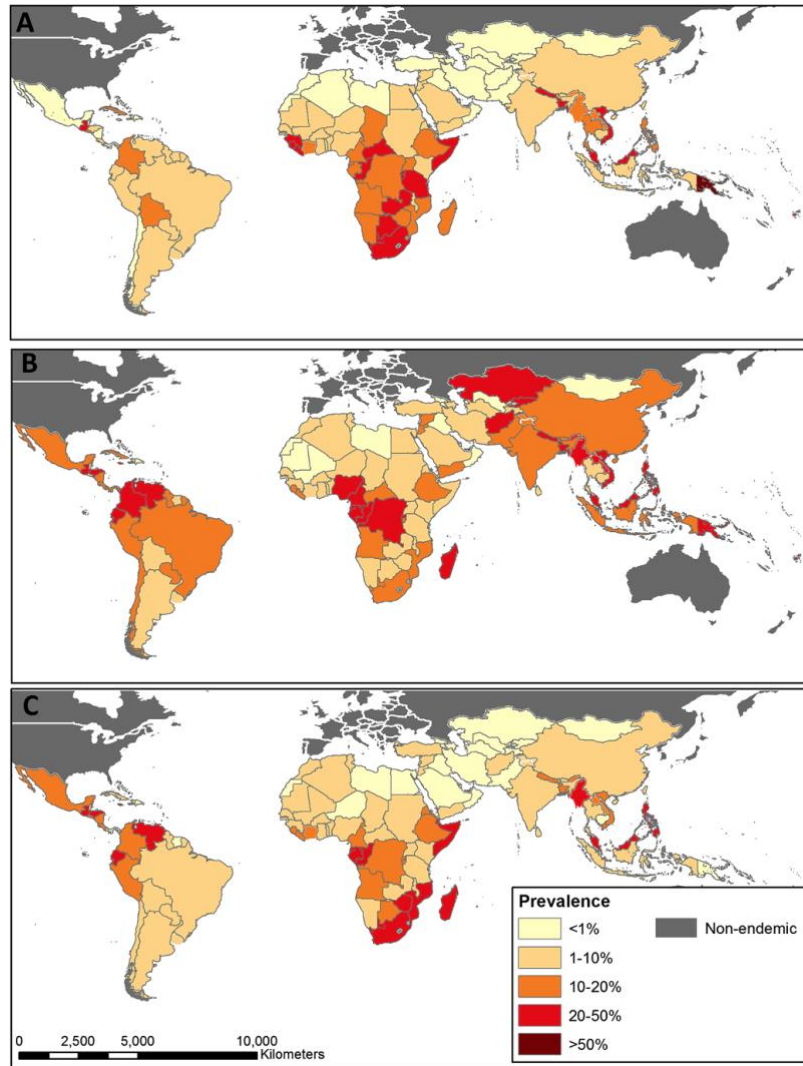


**Figure 1.2 Distribution of STHs infection prevalence in 2010 by parasitic species.**

(A) Hookworm, (B) *Ascaris lumbricoides* and (C) *Trichuris trichiura*; based on geostatistical models for sub-Saharan Africa and available empirical information for all other regions (Pullan *et al.*, 2014).

Human STHs have been a part of our life's since before the era of our earliest recorded history, their eggs can be found in mummified feces of humans dating back thousands of years (Evans, 1996; Hotez *et al.*, 2008; Else *et al.*, 2020). They are a part of the 20 major Neglected Tropical Diseases (NTDs) identified by the World Health Organization. Although they are endemic in low-middle income developing countries of Africa, Asia, and America with warm, humid tropical or subtropical climates, developed countries are also affected in socioeconomically disadvantaged groups (WHO, 2018; Mutombo *et al.*, 2019).

Table 1.1 Estimated global numbers infected with soil transmitted helminths and overall prevalence.

Table 4 Estimates of global numbers infected with soil-transmitted helminths in 2010, by region

REGION	Total population (millions)	Infected Populations in millions (95% CI <sup>1</sup> )			Overall prevalence (95% CI)		
		Hookworm	<i>A. lumbricoides</i>	<i>T. trichiura</i>	Hookworm	<i>A. lumbricoides</i>	<i>T. trichiura</i>
<b>Asia</b>	<b>3736.7</b>	<b>281.8 (249.5-318.5)</b>	<b>589.0 (524.4-660.3)</b>	<b>282.3 (248.5-323.5)</b>	<b>7.5% (6.7-8.7%)</b>	<b>15.8% (14.5-17.7%)</b>	<b>7.6% (6.6-8.7%)</b>
Central Asia	80.7	0.1 (0.01-0.2)	6.0 (5.1-6.9)	0.1 (0.2-25)	0.1% (0.0-0.3%)	7.4% (6.4-8.5%)	0.1% (0.0-0.3%)
East Asia	1424.4	64.5 (44.9-87.3)	158.4 (124.7-194.1)	66.2 (41.9-93.5)	4.5% (3.3-5.5%)	11.1% (8.8-13.6%)	4.6% (3.0-6.6%)
South Asia	1621.1	140.2 (117.2-173.0)	297.8 (263.8-345.4)	100.7 (80.3-129.8)	8.7% (5.2-6.6%)	18.4% (16.3-21.9%)	6.2% (5.0-8.0%)
Southeast Asia	610.5	77.0 (69.2-84.9)	126.7 (116.0-137.4)	115.3 (106.8-125.3)	12.6% (11.3-13.9%)	20.8% (19.0-22.5%)	18.9% (17.5-20.5%)
<b>LAC</b>	<b>586.0</b>	<b>30.3 (25.5-35.5)</b>	<b>86.0 (78.2-95.6)</b>	<b>72.2 (66.0-80.0)</b>	<b>5.2% (4.4-6.1%)</b>	<b>14.7% (13.4-16.3%)</b>	<b>12.3% (11.3-13.7%)</b>
Caribbean	39.7	2.1 (1.81-2.36)	3.2 (2.8-3.7)	2.8 (2.5-3.1)	5.2% (4.5-5.9%)	8.1% (7.0-9.4%)	7.0% (6.3-7.7%)
Andean LA	52.7	2.3 (1.73-2.91)	10.6 (9.2-12.3)	10.3 (9.0-12.0)	4.3% (3.3-5.5%)	20.1% (17.5-23.3%)	19.6% (17.1-22.7%)
Central LA	230.3	13.5 (12.04-15.15)	41.8 (38.1-45.7)	44.0 (40.4-47.6)	5.9% (5.2-6.6%)	18.1% (16.6-19.9%)	19.1% (17.6-20.7%)
Southern LA	57.9	1.4 (1.00-1.92)	5.9 (5.1-7.0)	2.1 (1.5-2.7)	2.5% (1.7-3.3%)	10.2 (8.7-12.2%)	3.5% (2.5-4.8%)
Tropical LA	205.4	11.0 (6.83-15.77)	24.5 (18.0-32.5)	13.0 (8.1-19.4)	5.4% (3.2-7.7%)	11.9% (8.7-15.8%)	6.4 (3.9-9.5%)
<b>SSA</b>	<b>866.0</b>	<b>117.7 (111.1-125.9)</b>	<b>117.9 (108.7-127.1)</b>	<b>100.8 (94.1-108.0)</b>	<b>13.6% (12.9-14.6%)</b>	<b>13.6% (12.6-14.8%)</b>	<b>11.6% (10.9-12.6%)</b>
Central SSA	98.0	19.3 (16.5-22.2)	21.0 (17.8-24.7)	16.5 (13.6-20.1)	19.7% (16.6-22.6%)	21.4% (18.1-25.2%)	16.9% (13.9-20.5%)
East SSA	358.7	49.5 (45.7-54.3)	34.4 (30.3-38.8)	42.2 (37.9-46.8)	13.8% (12.8-15.2%)	9.6% (8.5-10.9%)	11.8% (10.6-13.1%)
Southern SSA	70.4	14.9 (12.9-17.3)	8.6 (6.7-10.7)	23.3 (20.7-26.0)	21.2% (19.1-25.8%)	12.2% (10.1-5.9%)	33.1% (30.8-38.7%)
West SSA	339.0	34.0 (30.0-38.9)	53.9 (46.7-60.7)	18.8 (15.3-23.2)	10.0% (8.9-11.5%)	15.9% (13.8-17.9%)	5.5% (4.5-6.8%)
<b>North Africa and Middle East</b>	<b>477.4</b>	<b>4.6 (4.0-7.1)</b>	<b>24.3 (22.6-28.5)</b>	<b>8.7 (7.3-10.7)</b>	<b>1.0% (0.9-1.6%)</b>	<b>5.4% (5.31-6.4%)</b>	<b>1.9% (1.6-2.4%)</b>
<b>Oceania</b>	<b>9.6</b>	<b>4.6 (4.3-3.8)</b>	<b>1.9 (1.6-2.2)</b>	<b>0.6 (0.6-0.7)</b>	<b>47.9% (44.7-51.0%)</b>	<b>19.7% (16.6-23.1%)</b>	<b>6.4% (5.8-7.0%)</b>
<b>GLOBAL<sup>2</sup></b>	<b>5,631.4</b>	<b>438.9 (406.3-480.2)</b>	<b>819.0 (771.7-891.6)</b>	<b>464.6 (429.6-508.0)</b>	<b>7.8% (7.2-8.5%)</b>	<b>14.5% (13.7-15.8%)</b>	<b>8.3% (7.6-9.0%)</b>

<sup>1</sup>Credible interval, based on within-admin2 variation generated by Bayesian linear mixed model. LAC, Latin America and the Caribbean. SSA, sub-Saharan Africa.

<sup>2</sup>Global prevalence includes populations in Asia, LAC, SSA, North Africa and the Middle East and Oceania as the denominator.

Highest overall worldwide in Latin America and the Caribbean (12.3%) highlighted in red (From Pullan *et al.*, 2014).

The intestinal-dwelling *T. trichiura* affects an estimated 465 million people worldwide with a global burden of disease of 640,000 DALYs (Disability Adjusted Life Years) (Pullan *et al.*, 2014) and 337,000 YLDs (Years Lost to Disability) (Vos *et al.*, 2017), although lower estimates have also been north recently reported (James *et al.*, 2018). In Latin America and the Caribbean, STHs are present in all countries with an estimated 26.3 million school-age children at risk of infection with an overall prevalence of trichuriasis which is the highest in the region (12.3%) (Table 1.1) (Lustigman *et al.*, 2012; Pullan *et al.*, 2014).

The adverse health consequences of STHs impair childhood school performance and reduce school attendance, resulting in a lower future wage-earning capacity (Stephenson *et al.* 2000; Humphries *et al.*, 2021). The accumulation of the long-term effects translates into poverty promoting sequelae that explains why poor communities remain in a cycle of impoverishment (Hotez *et al.*, 2008).

Children of school years represent the majority of clinically significant cases, and worm

burden tends to decline significantly in adulthood (Else *et al.*, 2020). This decline of infection burden in adulthood has been related to a combined acquired immunity and/or a lower exposure to infection due to changes in behavior with an improvement in hygiene habits (Stephenson *et al.*, 2000; Hotez *et al.*, 2008, Humphries *et al.*, 2021).

### 1.1.2 Soil-Transmitted Helminths strategies for control

During the 2001 World Health Assembly, the resolution WHA54.19 was endorsed urging endemic countries to increase their efforts for controlling STHs. The strategies focus on morbidity control through the implementation of periodic Mass Drugs Administration (MDA) campaigns integrated with school health programmes for populations at risk. Treatment campaigns target preschool and school-age children, women of reproductive age, including pregnant women in the second and third trimesters, breastfeeding women, and adults in high-risk occupations (WHO, 2018). Also, the health and hygiene education campaigns help reduce transmission and reinfection by encouraging healthy behaviors and by finding alternatives despite not always having adequate sanitation, which is a concern in resource-poor settings. In 2018, endemic countries treated over 676 million school-aged children (53% of all children at risk), following the United Nations guidelines endorsed by the WHO regarding STH global targets by 2030 (WHO, 2018):

1. Achieve and maintain the elimination of STH morbidity in pre-school and school-age children.
2. Reduce the number of tablets needed in preventive chemotherapy for STH.
3. Increase domestic financial support to preventive chemotherapy for STH.
4. Establish an efficient STH control programme in adolescents, pregnant and lactating women.
5. Establish an efficient strongyloidiasis control programme in school-age children.
6. Ensure universal access to at least basic sanitation and hygiene by 2030 in STH-endemic areas.

A large volume of research has explored social, environmental, and behavioral determinants of STH infection; however, understanding correlations between these factors can

provide some new ideas in terms of strategies for control. For example, large scale variability in the prevalence and distribution of *T. trichiura* together with other co-infections is important for defining control programs based on location-specific treatment needs (Sturrock *et al.*, 2017). While countries with the highest prevalence of multiple NTDs, including trichuriasis, may benefit from MDA programmes as a rapid impact approach, other countries, with a more scattered distribution of trichuriasis, and regional variability such as the Americas would be better candidates for targeted treatment efforts with previous diagnosis and determination of worm burdens (Lustigman *et al.*, 2012).

Additionally, recent reviews of randomized controlled trials questioned the effectiveness of current MDA programs and policies (Taylor-Robinson *et al.*, 2015, 2017; Jourdan *et al.*, 2018). These reviews concluded that the population-level effect of deworming was absent on a range of child health outcomes such as growth and hemoglobin levels (Taylor-Robinson *et al.*, 2015, 2017; Jourdan *et al.*, 2018). Others caution that elimination of STHs transmission can have an unintended but significant impact on the increased risk of autoimmune diseases, a phenomenon known as the hygiene hypothesis (Jouvin *et al.*, 2012; Wammes *et al.*, 2014).

### 1.1.3 Zoonotic potential of STHs and reservoirs

The zoonotic potential of STH infections and the variety of reservoirs has been a topic of great debate. Molecular analyses have made it possible to identify potential zoonoses with a higher degree of confidence, especially when morphological differences between eggs, larvae, or adult nematodes does not allow for species identification (Nejsum *et al.*, 2012). The overall consensus is that further sampling of species from humans, NHPs, and domesticated animals, such as dogs and pigs, from different geographic distributions, combined with molecular analysis is warranted to continue determining the extent and importance of the potential STHs zoonotic transmissions (Betson *et al.*, 2015; Mutombo *et al.*, 2019).

In the specific case of trichuriasis, most human cases are attributed to *T. trichiura*, but reports of human infection with *Trichuris vulpis* (Areekul *et al.*, 2010), the species of canids, and *Trichuris suis* (Summers *et al.*, 2005), the species of swine, were confirmed using molecular techniques. Under experimental conditions, *T. suis* cross-infection can occur, and although infections seem

to establish only temporary (Nejsum *et al.*, 2012), one study found fully grown adults in a study volunteer (Williams *et al.*, 2017). The complexity of *T. trichiura* phylogenetic relationships between humans and NHPs is explained in detail in the genomics section (**1.2.4 Genomics and Proteomics**).

## 1.2 *Trichuris trichiura*

### 1.2.1 Classification and Taxonomy

*Trichuris trichiura* under the helminth umbrella, belongs to the phylum Nematoda and the genus *Trichuris*.

Phylum: Nematoda

Class: Enoplea

Order: Trichinellida

Superfamily Trichinelloidea

Family: Trichuridae

Genus: *Trichuris*

Species: *Trichuris trichiura* (Linnaeus, 1758).

The genus *Trichuris* belongs to the class Enoplea and the order Trichinellida together with *Trichinella spiralis*. A superfamily of nematodes, including the following roundworms that are parasitic in humans: *Trichinella spiralis*, the trichina worm (family Trichinellidae); *T. trichiura*, the human whipworm; *Capillaria hepatica*, the capillary liver worm; and *Capillaria philippinensis*.

Over 70 *Trichuris* spp. are recognized in different mammalian hosts, including the etiological agent of trichuriasis, *T. trichiura* and *T. suis* in pigs are the most closely related species (Betson *et al.*, 2015). Although the scientific name *Trichuris* given by Johann Georg Roederer in 1761 means, “hair tail”, the thin portion of the parasite’s body is the head (Else *et al.*, 2020). While various authors have used the term *Trichocephalus* which is morphologically precise, the correct taxonomic denomination is *Trichuris* (Acha *et al.*, 2003).

## 1.2.2 Life cycle and Transmission

*Trichuris trichiura* life cycle as a soil-transmitted helminth, with equal routes of transmission, mainly fecal-oral, in humans and nonhuman primates is shown in **Figure 1.3**.

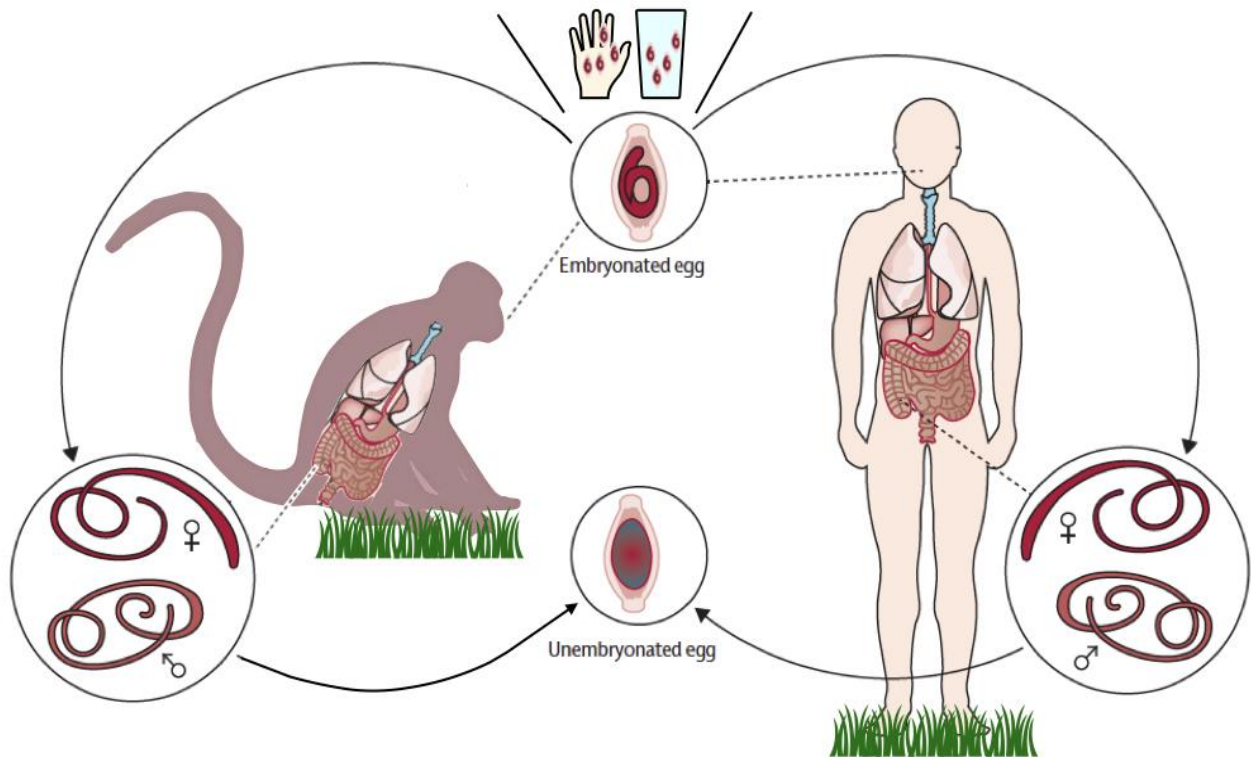


**Figure 1.3** Life cycle of *Trichuris trichiura*.

Adapted from Jourdan *et al.* (2018).

After the accidental ingestion of the embryonated eggs from contaminated hands, food, soil, or water, larvae (L1) hatch in the proximal small bowel and migrate aborally to the colon and cecum where they penetrate the epithelial cells at the crypts of Lieberkühn base, creating an intracellular niche where they undergo four molts (L2, L3, L4). However, by the L3 stage, the parasite is no longer fully intracellular, because as it grows in length, it reemerges to the intestinal lumen, but remains attached to the mucosa (Bundy and Cooper, 1989; Else *et al.*, 2020). The last larvae (L4) mature to adults in 4 to 16 weeks, survive from 1 to 8 years, and measure 3 – 5 cm (Bundy and Cooper, 1989; Hansen *et al.*, 2016; Else *et al.*, 2020). Their thick posterior ends are free in the intestinal lumen while their anterior part remains attached to the mucosa, surrounded

by a syncytial tunnel within the epithelium cells, which biology remains unknown (Else *et al.*, 2020). After copulation, the adult females oviposit thousands of eggs: 2-20,000 eggs/day (Bundy and Cooper, 1989); 18,000 eggs/female per day (Hansen *et al.*, 2016), expelled in their unembryonated (not infectious) form in the feces. To embryonate, they require 2-4 weeks in the appropriate soil and/or ambient conditions that allow the development of the larvae into the infectious developmental stage: the embryonated egg containing L1 larvae (Else *et al.*, 2020). *T. trichiura* eggs measure 50-60 µm in length and 20-30 µm in width, they do not develop in direct sunlight and perish below 9°C or above 52°C (Bundy and Cooper, 1989; Stephenson *et al.*, 2000; CDC, 2013).

There is no direct person to person transmission, or direct infection from fresh feces, because the eggs require the right ambient conditions and time to embryonate and become infective (Bundy and Cooper, 1989). *T. trichiura* does not multiply in the human host (autoinfection), reinfection occurs only as a result of accidental ingestion of an embryonated egg (Bundy and Cooper, 1989).

Interestingly, in the mouse model, the close relationship between *Trichuris muris* and the composition of the gut microbiota has been explored in regards to egg hatching triggers and the successful establishment of infection (Hayes *et al.*, 2010). Throughout its life cycle *T. trichiura* excrete and secrete a variety of molecules that interact with the host environment (Bancroft *et al.*, 2019; Cruz *et al.*, 2021). Some are antigenic and some are immunomodulatory, and the functions of many of them are still to be identified (Bancroft *et al.*, 2019, Cruz *et al.*, 2021).

### **1.2.3 Morphology of developmental stages**

#### **1.2.3.1 *Trichuris trichiura* egg anatomy**

The lemon-shaped, bile-stained egg contains three layers. First, an outer vitelline layer derived from the fertilized oocyte's vitelline membrane. The vitelline layer develops the entire egg, including the bipolar plugs. After, a middle chitinous layer with high tensile strength adapted to protect the enclosed embryonic material and larva, and lastly, an inner lipid layer. The clear bipolar plugs are composed of the same three layers: vitelline, chitinous, and lipid, and are supported by



a "collar" composed of the middle chitinous layer that fans out from the shell (Appleton and White, 1990) (Figure 1.4).

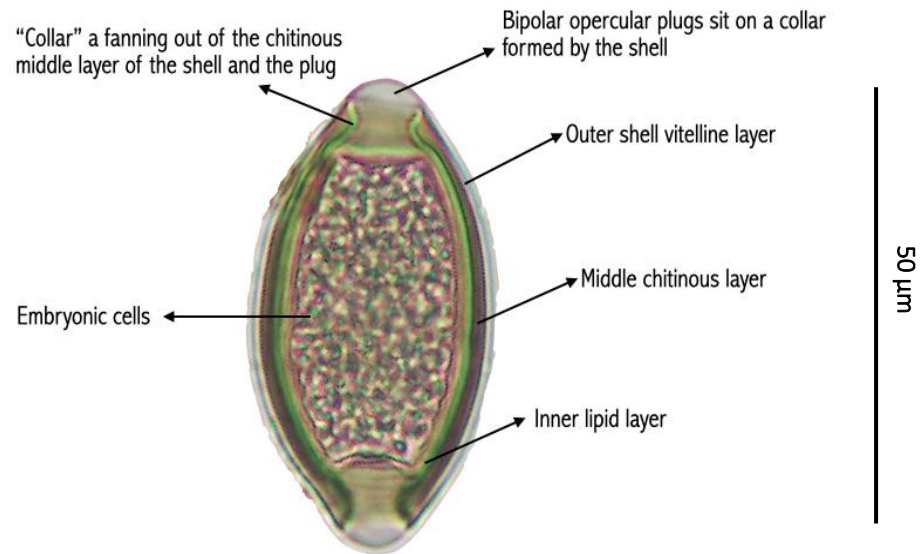
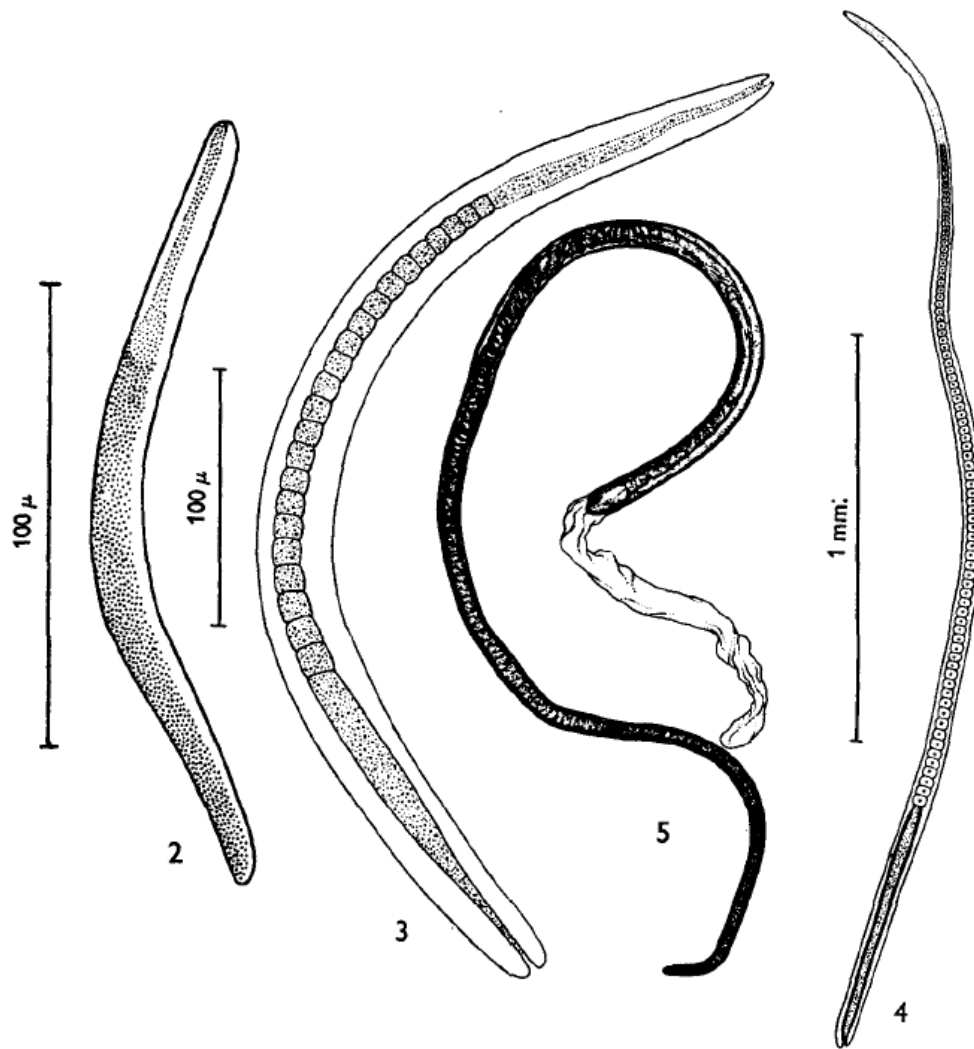


Figure 1.4 *Trichuris trichiura* egg anatomy.

### 1.2.3.2 *Trichuris trichiura* larval stages

The larval developmental stages, as described by Fahmy (1954), show the L1 (2) larvae recently released from the egg as early as 2 hrs and 30 min post-infection. Nine days post-infection (3), the L1 showing a more defined esophagus and intestine structures. The L2 larvae (4) after the first molt with distinct esophageal cells and the same L2 larvae in the process of molting for the second time (5) (Figure 1.5).



**Figure 1.5 Larval developmental stages**

(2) newly hatched larva (L1), (3) 9 days after infection, (4) at 17 days, (5) Larva in the process of molting (23 days post-infection) (Adapted from *T. muris* in Fahmy (1954)).

After the second molt, the L3 larvae displays well developed reproductive organs. The spicule and testis can be identified in the male (6) with the characteristic coiled posterior and an overall smaller length. The long and thick posterior end with the vulva opening, the ovary, and the oviduct are identified in the slender and longer female (7) (Figure 1.6).

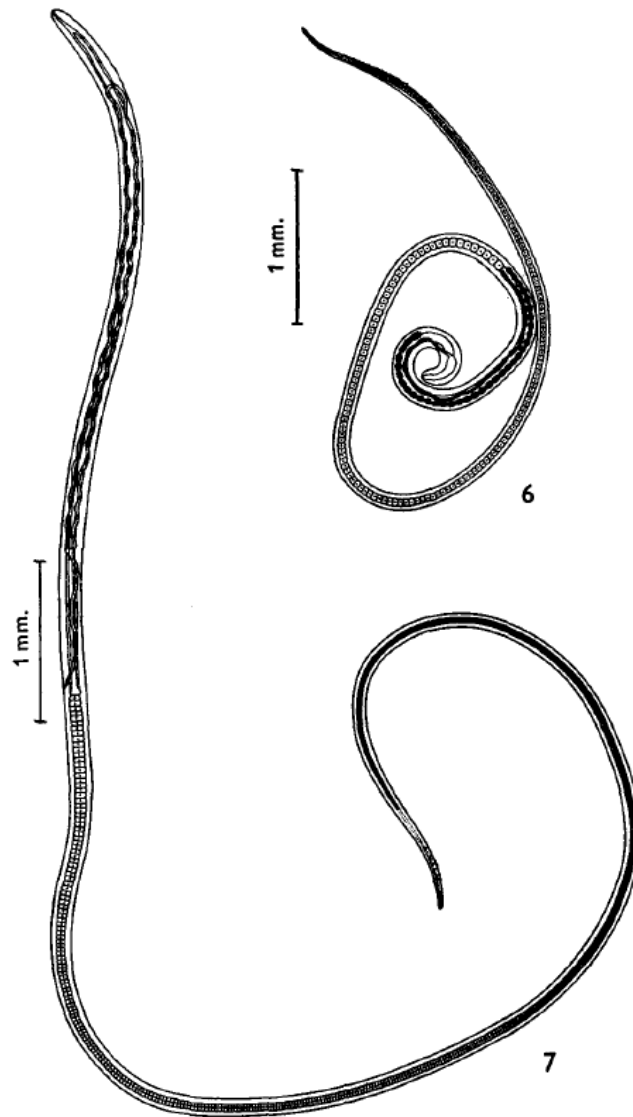


**Figure 1.6 Larval developmental stages (continuation)**

L3 Larvae 27 days post-infection (6) Male larva (7) Female larva (Adapted from *T. muris* in Fahmy (1954)).

### 1.2.3.3 *Trichuris trichiura* adult female and male

The fully developed adult trichuris, male and female, display a long and slender anterior portion and a wide and thick posterior, giving the whip's appearance. The male is smaller than the female, and in both, the esophagus extends two-thirds of the body length composed by a single layer of stichocytes (Figure 1.7).

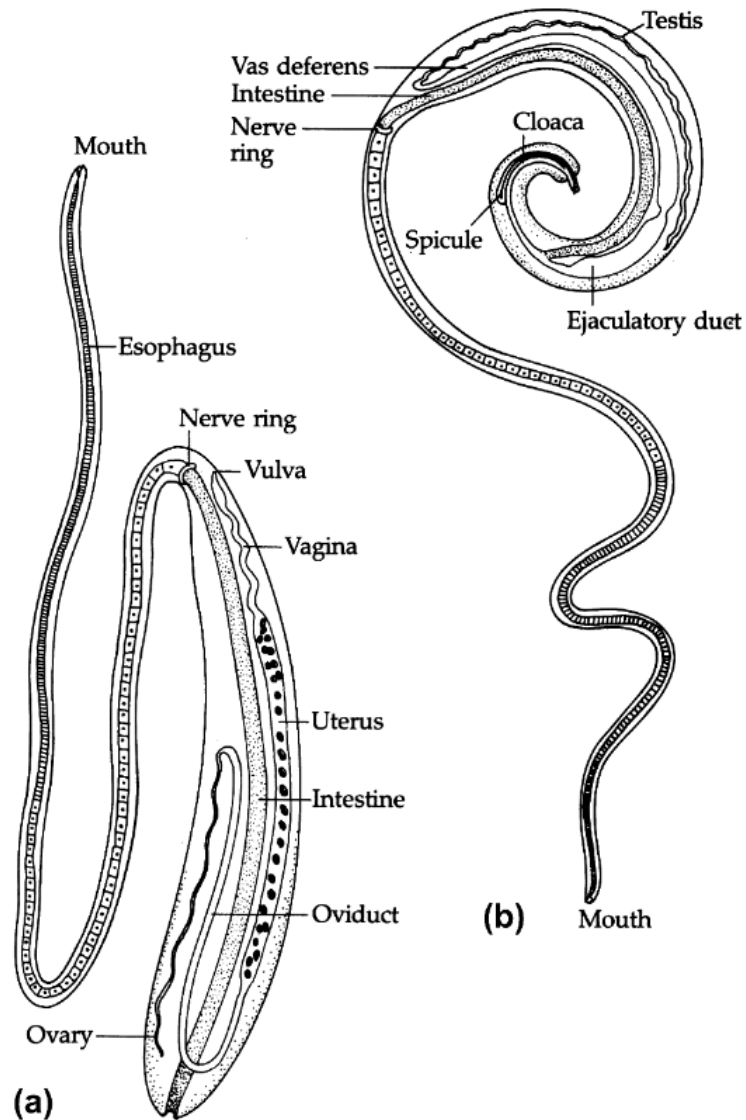


Figure 1.7 *Trichuris trichiura* adult anatomy

(A) female (B) male 32 post-infection (Adapted from Bogitsh *et al.* (2013))

#### 1.2.4 Genomics and Proteomics

The understanding of *Trichuris trichiura* genome and proteome to date represent the basis of the work presented here. We have used them to identify gene families and respective processes associated with host invasion and drivers of *T. trichiura* infection.

The *Trichuris* genus has a wide geographical distribution which makes it a likely candidate to contain cryptic species, that is those that cannot be distinguished using conventional morphological examination methods (Betson *et al.*, 2015). Whipworms in humans are traditionally designated as *T. trichiura*, but the possibility of several species affecting humans and some of these being shared with nonhuman primates (NHPs) has been explored (Cavallero *et al.*, 2019; Di Filippo *et al.*, 2020). Hawash (2016) and Rivero (2021) described how genetic similarities between species found in humans and NHPs also suggests that species of *Trichuris* found in humans represent an heirloom parasite, meaning a parasite inherited from our primate ancestors.

The inference of the phylogenetic relationship between nematodes based on ITS sequences can be problematic, which is why it is recommended to supplement this type of analysis with other genetic markers such as mitochondrial DNA (mtDNA) genes (Callejón *et al.*, 2013). Sequencing of nuclear and mitochondrial markers from a range of wild and captive NHP host species has clarified this taxonomic relationship between worms and the potential zoonoses. Ravasi (2012) compared Internal Transcribed Spacers (ITS1-5.8S-ITS2) sequences from South Africa's adult *Trichuris* sp. from wild baboons and humans, finding a potential cross-infection as both *Trichuris* sequences shared the same two distinct clades. Ghai (2014) compared *Trichuris* full mtDNA genome from humans in China and Uganda to adult nematodes from captive baboons in the USA and Denmark, finding that there was more than one species involved in these infections based on the genetic distances observed. Cavallero (2015) integrated new phylogenetic results from *Macaca fuscata* and *Cercopithecus aethiops* with Ravasi (2012) and Callejón (2013) findings, providing further evidence of the distinct clades and subclades confirming the existence of additional separated taxa amongst NHP and human *Trichuris* species.

Cavallero (2019) presented the largest dataset to date (*rrnL* gene, the large subunit rRNA-encoding gene from the mitochondrial (mt) large subunit ribosomal RNA (rRNA)) and the most representative phylogenetic tree showing two main clades and of relevance to our work. The first,

named clade 1 CPGOB, grouped *Trichuris* species isolated from European zoological parks including nonhuman primate species (*Chlorocebus sabaesus*, *Chlorocebus aethiops*, *Colobus* sp.) and pig (**Figure 1.8**). The second clade, named clade 2, includes 4 branches: subclade Clade 2A (*Papio hamadryas*, *Macaca fuscata*, *Chlorocebus sabaesus* (St. Kitts isolate), *Papio* sp. and humans); subclade MF (*M. fuscata*); subclade H (humans) and a sister branch of *Trichuris* infecting *Trachypitecus francoisi*. It is of note that all *Trichuris* sequences from the *rrnL* gene from the genus *Chlorocebus* clustered together in Clade 1, except for the isolates obtained from the monkeys studied in our current work. The Saint Kitts *C. sabaesus*, is clustered in Clade 2, subclade 2A (Cavallero *et al.*, 2019), suggestive of a *C. sabaesus* species that has developed isolated in the island of St. Kitts (**Figure 1.8**). Whipworms in humans, therefore, represent multiple *Trichuris* species, some of which we share with NHPs.

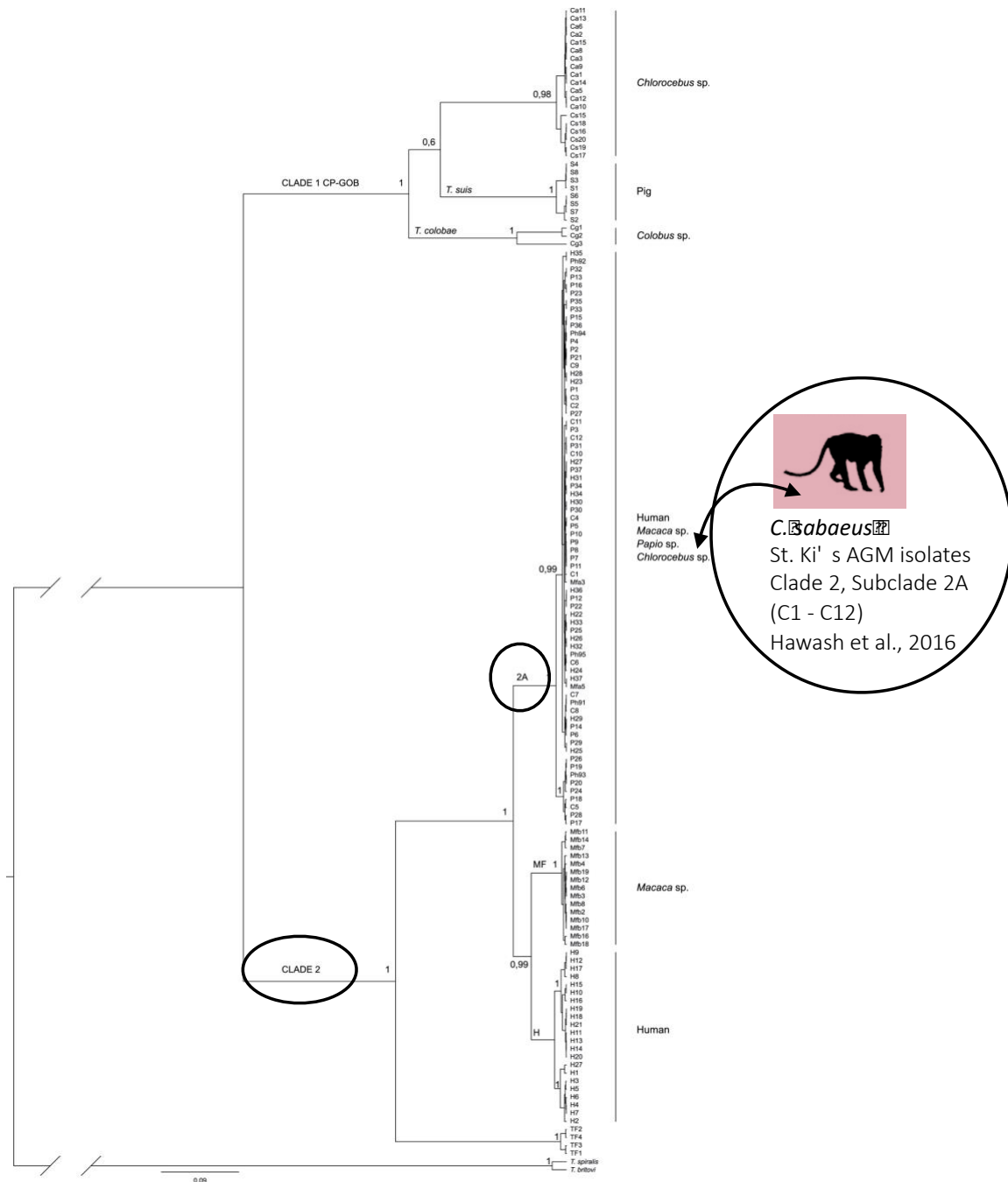


**Figure 1.8** Bayesian tree showing most up to date relationships among *Trichuris* species. Based on the analysis of the Dataset *rnl*, including sequences used as outgroup (*Trichinella spiralis* and *T. britovi*), with indications on host affiliation and assignment to clades and subclades, following the nomenclature used in previous papers (Ravasi *et al.*, 2012; Callejón *et al.*, 2013; Cavallero *et al.*, 2015). Adapted from Caballero *et al.* (2019).

In 2014, Foth and collaborators produced and published the draft genome assembly (75.2 Mb) from one adult male *T. trichiura* predicting, 9,650 genes, 2,350 of those genes being species-specific to *T. trichiura*. While this genome is considered to be 94.8% complete using Core Eukaryotic Genes Mapping Approach (CEGMA), the complete genome of the human whipworm is an ongoing project started in 2017 and led by the Wellcome Sanger Institute [PRJEB535](#).

According to Foth (2014), the 2,350 species specific genes were dominated by hypothetical proteins of no known function. Specifically, a total of 2,014 hypothetical proteins were encoded by *T. trichiura*, with 253 (12.6%) proteins predicted to contain signal peptides, and 359 (17.8%) sequences predicted to contain transmembrane domains. These data represent a large number of proteins secreted and transported outside of the cell from which function remains unknown, including some of the proteins identified in our work.

From other sequences with known functional annotations extracted through the Gene Ontology (GO) term enrichment analysis, it was inferred that extracellular proteins, proteases, and protease inhibitors were particularly abundant among the remaining species-specific proteins (Foth *et al.*, 2014). In particular, serine proteases such as chymotrypsin A-like serine proteases were most abundant in both, gene number and gene expression (encoded by 75 genes) than other protease families, which is not the case in other nematodes such as *N. americanus* (Cantacessi *et al.*, 2010) and *S. stercoralis* (Marcilla *et al.*, 2010, Marcilla *et al.*, 2012). Therefore, chymotrypsin A-like serine proteases are the single largest group of proteases in the *T. trichiura* proteome and of relevance to the work presented here, because the stichosome and bacillary band in the anterior region are involved in the nutrient uptake, digestion, and host-parasite interactions (Foth *et al.*, 2014). Consequently, serine proteases could serve both; digestive and host-immunomodulatory functions as well as degrade host intestinal mucins that act as a physical barrier to the parasite (Foth *et al.*, 2014).

The *T. trichiura* genome also featured 20 genes encoding Whey Acidic Protein (WAP) domains, the Secretory Leukocyte Protease Inhibitor (SLPI)-like proteins, being the most abundant protease inhibitor transcripts in the anterior portion of the parasite, but surprisingly only one of them: TTRE\_0000351901, in which the WAP domain contained the established eight cysteine residues recognized for this domain. The rest of the proteins containing the WAP domains present



a novel adaptation of six cysteine residues instead of eight, and the specifics of this modification in the function of the proteins remains unknown.

In addition to the protease inhibitor activity, SLPI-like proteins have anti-inflammatory, immunomodulatory, and antimicrobial properties on the host epithelial cells as it is invaded and wounded by the parasite, representing an important immunomodulatory function triggered in the innate immune defense and wound healing processes of the host (Wilkinson *et al.*, 2011; Foth *et al.*, 2014). It is of note that no other parasitic helminth lineage presents SPLI-like proteins, meaning that the corresponding genes are robustly and particularly expressed by the whipworm anterior portion (Foth *et al.*, 2014). As described above, the majority of these proteins are secreted, suggesting that this family of proteins could carry a nematode clade I-specific function focused on inhibition of inflammation in the host response during invasion and establishment of the parasite (Foth *et al.*, 2014), relevant to our findings for Kunitz BPTI domain containing protein.

Transcripts for DNase-II-like proteins were also prevalently expressed in the whipworm anterior region (Foth *et al.*, 2014). Normally, in other animals including *Caenorhabditis elegans*, free-living nematode, these proteins are involved in apoptotic DNA degradation and development (Lai *et al.*, 2009), but the phylogenetic tree positioning observed by Foth (2014) leaves an open-ended question concerning the potential biological role of DNase II-like proteins in *Trichuris* species.

The draft genome of *T. trichiura* also revealed male-specific expression of transcripts encoding proteins with Major Sperm Protein (MSP) domains, thought to have a role in the locomotion of the sperm (Tarr *et al.*, 2005), and proteins with casein kinase-related and epidermal growth factor (EGF) like domains, these proteins are likely involved in male mating behaviors and functions (Hu *et al.*, 2006). In contrast with male-specific proteins, transcripts for proteins with chitin-binding domains which are relevant to our findings for CBM 14 domain containing protein, were upregulated in the female whipworm. Nematode eggshells commonly contain chitin (Johnston *et al.*, 2010); therefore, it is likely that these proteins are linked to the process of the egg formation (Foth *et al.*, 2014).

Larvae L2 and L3 transcriptional landscape resembles that of the anterior region of the adult stages of the whipworm, likely due to the shared intraepithelial location and absence of the

reproductive and sex-specific transcripts that dominate the posterior portions of the adult *T. trichiura* (Foth *et al.*, 2014). Also, larval stages had high expression of transcripts for ribosomal, collagen and fibronectin related proteins; most likely associated with the protein and cuticle synthesis necessary for the fast growth that these life stages undergo during their development (approximately 5,000-fold increase in body/muscle volume over a 35-day period) (Foth *et al.*, 2014; Bancroft *et al.*, 2019). These findings are relevant to polycysteine and histidine protein the most abundant found in our work.

The majority of *T. trichiura* genes are orthologs shared by both *T. muris* and *T. trichiura*, with 5,060 one-to-one protein orthologs presenting an average amino acid identity of 76% (Foth *et al.*, 2014).

## 1.3 Trichuriasis

### 1.3.1 Epidemiology of the disease and population at risk

*Trichuris trichiura* infections favor the warm and moist conditions in tropical and subtropical regions where the appropriate temperature and humidity allow the life cycle of the soil-transmitted nematode to continue (Bundy and Cooper, 1989; Else *et al.*, 2020). Transmission requires the excreted unembryonated and noninfectious eggs to embryonate and become infectious under ideal environmental conditions (Bundy and Cooper, 1989; Else *et al.*, 2020), this fundamental aspect of its biology determines a set of transmission dynamics that are different from other human nematodes (Hotez *et al.*, 2008). Consequently, temperature, humidity, and population density geographical information system tools have been used to enable prediction and estimation of the geographical distribution of parasite (Else *et al.*, 2020).

Trichuriasis is considered a disease of the poor, where lack of education and sanitation infrastructure favors transmission. In these environments, the prevalence of infection, determined by the intensity of infection measured by Eggs Per Gram of feces (EPG) found in a single fecal sample, can be 90% and mainly affecting children of school age (5-15 years old) (Stephenson *et al.*, 2000; Else *et al.*, 2020). Historical data shows that the prevalence peaks earlier in life due to age-related risk exposure, and there is a decline in prevalence observed after school age and in

adults with lower risk exposure and potential age-acquired immunity (Stephenson *et al.*, 2000; Else *et al.*, 2020). Morbidity is associated with the number of worms infecting the host rather than the presence or absence of infection (Hotez *et al.*, 2008).

Epidemiological characteristics surrounding the parasitized patient such as age, sex, type of job, contact with soil, soil temperature, the consumption of potential contaminated food or water, weather conditions, and housing type, are essential when describing the population at risk (Mutombo *et al.*, 2019). Three main categories determine an increased risk factor (Stephenson *et al.*, 2000, Hotez *et al.*, 2008; Sturrock *et al.*, 2017)

- a. Environmental risk factors such as temperature, precipitation, soil conditions, and humidity.
- b. Human socioeconomic risk conditions such as water access, sanitation, and population density.
- c. Human behavior risk factors such as food preparation, hand washing, and hygiene education and geophagy.

Therefore, improvement in the above categories has demonstrated to be vital for the elimination and control of Soil-Transmitted Helminths (STHs), such as the case of industrialized countries (Lustigman *et al.*, 2012).

### **1.3.2 Clinical disease in humans and nonhuman primates**

#### **1.3.2.1 Humans**

Clinical disease is caused by the inflammation of the cecum and the large intestine, due to the adult worm induced local inflammatory response and blood loss (estimated to be 0.005 mL per worm per day) (Else *et al.*, 2020). The clinical signs in humans are related to worm burden (Else *et al.*, 2020). In human infections, low-level infections (< 15 worms) are often asymptomatic, but moderate to high infections (hundreds of worms) can cause a range of symptoms including intestinal discomfort with abdominal pain, colitis, vomiting, and bloody diarrhea (Stephenson *et al.*, 2000; Else *et al.*, 2020). Infections in children can result in severe anemia, general malaise and weakness, stunted growth, and poor school performance (Stephenson *et al.*, 2000; Else *et al.*,

2020). Infections of very high intensity can cause intestinal obstruction that can require surgical interventions to avoid rectal prolapse (WHO, 2018). Sequalae nutritional impairment includes loss of iron, protein and an overall reduction of nutritional intake that can cause dysentery (Stephenson *et al.*, 2000; Else *et al.*, 2020).

*Trichuris* Dysentery Syndrome (TDS) results from very high intensity infections (several hundreds to thousands of worms) (Cooper *et al.*, 1986; Stephenson *et al.*, 2000). This severe illness, also known as massive infantile trichuriasis, is associated with iron deficiency anemia, chronic mucoid diarrhea, rectal bleeding, rectal prolapse, consequence of increased straining and/or peristalsis, and finger clubbing (Khuroo *et al.*, 2010; Kaminsky *et al.*, 2015). In adults however, TDS has been identified recently to be the causative agent of severe iron deficiency anemia, reflecting the poor clinical recognition of trichuriasis in general but mostly in communities with severe poverty, not included in MDA programs (Khuroo *et al.*, 2010; Else *et al.*, 2020). Colonoscopy reports from patients with this diagnosis revealed associated mucosal changes including, edema, petechial lesions, blotchy mucosal hemorrhages, active mucosal oozing, and luminal narrowing (Khuroo *et al.*, 2010; Wang *et al.*, 2013).

The quality of life is the most affected by chronic infections, contributing to the long term nutritional morbidity and affecting the cognitive development of infected children (Else *et al.*, 2020).

#### 1.3.2.2 Nonhuman primates

The clinical disease of nonhuman primates has not been studied in depth despite *Trichuris* being a highly prevalent parasite species amongst captive and wild populations (Abee *et al.*, 2012; Calle and Joslin, 2014); therefore, human *Trichuris* literature is commonly used as guidance. Whipworms are the most common nematodes found in AGMs in previous reports, and they mainly focused on the description of treatment outcomes (Munene *et al.*, 1998; Muriuki *et al.*, 1998; Mutani *et al.*, 2003; Gillespie *et al.*, 2004., Legesse *et al.*, 2004; Petrášová *et al.*, 2010; Gaetano *et al.*, 2014; Kooriyama *et al.*, 2014; Amenu *et al.*, 2015; Li *et al.*, 2015; Wren *et al.*, 2015; Dalimi *et al.*, 2016; Valenta *et al.*, 2017; Teklemariam *et al.*, 2018 and Barbosa *et al.*, 2020).

*Trichuris trichiura* is the species generally thought to be present in AGMs, and this has been confirmed to be the species infecting *C. sabaesus* on St. Kitts (Hawash *et al.*, 2016; Yao *et al.*, 2018). While light infections in NHPs are often subclinical, the heavy infection produces severe enteritis with non-responsive gray mucoid diarrhea and inappetence, which have been reported in fatal *trichuris* infections with hemorrhagic typhlitis and ileal intussusception found at necropsy (Hennessy *et al.*, 1994; Emikpe *et al.*, 2002; Eo *et al.*, 2018). In addition, chronic infections have been reported to exacerbate hepatopathology caused by *Schistosoma mansoni* and a higher female worm burden (Le *et al.*, 2020) and have been associated with behavioral shifts (Chapman *et al.*, 2016) where the AGMs had reduced rates of movement and socialization.

### 1.3.3 Diagnostics

#### 1.3.3.1 Parasitological methods

Diagnosis of trichuriasis relies on the examination of a fecal sample in order to determine presence or absence of eggs and, if possible, a quantification of the eggs present in the sample analyzed. To date, the WHO recommends using the Kato-Katz and direct microscopy fecal examination method including a two slide preparations per sample analyzed (WHO, 2018).

Other parasitological diagnostic methods (**Table 1.2**) include formol-ether concentration, FLOTAC, mini-FLOTAC, McMaster and double centrifugation with Sheather's sugar solution, but the sensitivity of these methods depends directly on the variability of the infection intensity experienced by the host (Nikolay *et al.*, 2014; Else *et al.*, 2020).

Molecular-based parasitological diagnostic methods, with superior sensitivity, have been developed in an effort to counter the overall reduced sensitivity of microscopy-based parasitological methods (Else *et al.*, 2020; Fernández-Soto *et al.*, 2020). However, the requirement of specific and more expensive equipment and DNA extraction from stool samples limits the application in field settings and endemic areas with limited resources. The Loop-Mediated Isothermal Amplification (LAMP) test is a species-specific colorimetric isothermal assay (between 59 °C– 66 °C) that offers an alternative to traditional PCR in field conditions and low-income areas providing accessible, cost-effective, easy-to-perform method (Ngari *et al.*, 2020). Also, LAMP test

has shown to identify infections more than 15 days before the initial identification of eggs in the feces, and it is also applicable to urine samples (Fernández-Soto *et al.*, 2020). The ability to identify infections during the prepatent period of the parasite (that is, the time of infection to egg production identified in the feces) poses the biggest challenge to trichuriasis diagnosis to date (Cruz *et al.*, 2021).

**Table 1.2 Parasitological diagnostic methods for *Trichuris trichiura*.**

Test	Output	Sensitivity %	Specificity %	Advantages	Limitations
Direct microscopy	Egg detection	62.8	97.5	Low cost	Positive results only at high parasitic burden
Kato–Katz	Egg detection and egg quantification	62.8–91.0	97.5	Relatively low cost; possible to determine the burden of infection	Overall low sensitivity (Especially at light infection intensities). Need for a qualified microscopist.
Formol–ether	Egg detection	81.2	97.5	Relatively low cost	
FLOTAC	Egg detection and egg quantification	88.7–100	97.5	Detection of different STHs simultaneously	Requires centrifugation steps with two different rotors; relatively high cost
Mini- FLOTAC	Egg quantification	76.2–91.5	97.5	Detection of different STHs simultaneously	Limited sensitivity (Sensitivity comparable to that of the Kato–Katz method but lower than that of FLOTAC)
FECPAK	Egg quantification	59.8–65.8	97.5	Detection of different STHs simultaneously. simple procedure with results within an hour	Requires internet connection
Double centrifugation with Sheather’s sugar solution	Egg quantification	No data in humans	No data in humans	Relatively low cost. Detection of different STHs simultaneously, less common in human diagnostics. Widely used in Veterinary Medicine.	Requires two centrifugations steps; sugar solution can create sticky surfaces.
McMaster	Egg quantification	61.1–81.8	97.5	Possible to detect multiple infections by multiplexed assays; high specificity	Need for a special counting chamber
LAMP assay	Identification of DNA from <i>Trichuris</i> spp.	100	100	Possible to detect multiple infections by multiplexed assays; high specificity	Risk of low sensitivity due to the presence of inhibitors in the fecal sample; decreased sensitivity if formalin is used for fixation of samples, requires specialized equipment, and has restricted use in the field
qPCR	Quantification of DNA from <i>Trichuris</i> spp.	72.3–100	100		

Adapted from Nikolay *et al.* (2014) and Else *et al.* (2020).

### 1.3.3.2 Immunological diagnostic methods

The focus of immunological diagnostic methods to date is on research and discovery, to uncover the molecules excreted, secreted, or contained within all the developmental stages of *T. trichiura*. These parasite-derived molecules interact with the host environment during the prepatent period of the parasite, before the eggs appear in the feces (Bancroft *et al.*, 2019; Cruz *et al.*, 2021). The immunological diagnostic approach would allow the early diagnosis of trichuriasis and diagnostic methods that do not rely on inconsistent clinical signs or fecal analysis to detect infections (Else *et al.*, 2020; Cruz *et al.*, 2021). Novel immunological diagnostics are crucial to detect infections following accidental ingestion and during the prolonged prepatent period that can last anywhere between 8 to 16 weeks (Bundy and Cooper, 1989; Hansen *et al.*, 2016)

There are no commercially approved antibody detection tests for the diagnosis of *T. trichiura* (Mutombo *et al.*, 2019; Else *et al.*, 2020). The association between *T. trichiura* infections and anti-*Trichuris* salivary IgG was explored by Needham (1996) and collaborators in the 90's. Their findings using saliva samples and crude antigen extract for their indirect ELISA assay, showed a correlation between age and infection intensity allowing for diagnosis at the community level, but not individual diagnosis.

Challenges on antibody detection assays remain in the differentiation of active and past infections as well as their ability to correlate with worm burden (Mutombo *et al.*, 2019).

### 1.3.4 Treatments

#### 1.3.4.1 Humans

The WHO recommendations include preventive chemotherapy with the implementation of a biannual single-dose of albendazole (400 mg) or mebendazole (500 mg) when the baseline prevalence is over 50%, and annual therapy when the baseline prevalence is lower than 50% (WHO, 2017). This regimen is recommended as a public health intervention for children 2 to 12 years old, for all adolescent girls 10 to 19 years old, and non-pregnant women of reproductive age (15 - 49 years old). The same regimen is also applied for pregnant women after the first trimester in areas of high STHs prevalence (WHO, 2017). These regimens have shown efficacy (based on Egg

Reduction Rates (ERR)) of 99.9% for *A. lumbricoides*, 92.4% for hookworms, and 64.4% for *T. trichiura* (WHO, 2013), and are also followed during MDA campaigns without a previous individual diagnosis to all the at-risk groups to reduce morbidity, worm burden, and help maintain a low intensity of infection (WHO, 2018).

#### 1.3.4.2 Nonhuman primates

*Chlorocebus sabaeus*, African green monkeys (AGMs) of the Cercopithecidae family, widely found in Africa, were introduced onto the Caribbean island of St. Kitts in the 17th century (McGuire., 1974). There is little data on the parasites of the vast feral population of AGMs (perhaps 50,000) (Dore *et al.* 2021), which commonly come into contact with people and may play a role in the epidemiology of human zoonotic parasitic infections common on the island (Berger, 2020). Incomplete Caribbean studies have reported island AGMs to be infected with *Trichuris trichiura* (Yao *et al.* 2018), *Strongyloides* spp. (Ritchie *et al.* 1967; Gallagher *et al.* 2019), *Primasubulura* sp. (Cameron, 1930) and *Schistosoma mansoni* (Cameron, 1928).

There is limited data on anthelmintic treatments for AGMs and husbandry recommendations to control parasitic infections in captive research animals. Research facilities require effective parasite treatment and prevention protocols to minimize infections that may confound research outcomes and cause unnecessary stress, which lowers the quality of life of study animals. Ritchie *et al.* (1967) reported that thiabendazole (two 50 mg/kg doses PO 14 days apart) significantly reduced or eliminated *Strongyloides* spp. eggs in the feces. Kagira *et al.* (2011), reported that a three-day regimen of albendazole (7 mg/kg, PO) and ivermectin (300 µg/kg, SQ) reduced the Fecal Egg Counts (FECs) of *T. trichiura* and strongyles by 100% consistently after 7, 14 and 28 days. Chapman *et al.* (2016) reported that two doses of ivermectin (300 µg/kg, PO) five days apart resulted in a 100% cure rate for nematodes in wild AGMs, with no eggs found in the feces 1-month post-treatment.

Unfortunately, evaluation of nematode infections is challenging because of inadequate data on drug efficacy in AGMs and the lack of studies with prolonged follow-up which is needed to detect confounding factors (autoinfection, reinfection, larval transplacental or colostrum transmission, dormant stages, and autoinfection due to parthenogenesis) (Reichard *et al.*, 2017).



Also, FECs can be unreliable, and studies that enable necropsy evaluations are relevant in the absence of a 'gold standard' (Geary *et al.*, 2010).

#### 1.4 Host immune response against *Trichuris trichiura* infection

Eggs contain the first antigens of *T. trichiura* that are presented to a naïve host's immune system and would thus seem to be the most important in the development of an early and effective immune response to limit infection (Cruz *et al.*, 2021). Also, once the adult worms are tethered to the intestinal mucosa, they secrete and excrete an abundance of proteins that have been shown to elicit protective immune responses (Lillywhite *et al.*, 1995; Santos *et al.*, 2013) and immunomodulate the host immune response to facilitate their parasitism in the host (Foth *et al.*, 2014).

Bancroft and collaborators (2019) described how the major secreted protein of *T. muris*, p43, also the most abundant in our work presented here for *T. trichiura*, PCHTP-2, (Cruz *et al.*, 2021), is able to bind the host IL-13 and separate the cytokine within the host extracellular matrix, preventing it from activating the type 2 immune response.

There is however, limited available information of T<sub>H</sub>1 and T<sub>H</sub>2 immune responses from humans and nonhuman primates infected solely with *T. trichiura*, as polyparasitism is the most usual presentation of the disease (Else *et al.*, 2020). Nevertheless, it is strongly inferred that *T. trichiura* induces a type 2 immunity response and that acquired immunity requires type 2 protective immune responses that develops slowly after prolonged exposure (Else *et al.*, 2020).

It is also understood that epithelial cells on the host frequently produce SPLs proteins when responding to inflammation in order to modulate the inflammatory process, the cytokine secretion, and the cell recruitment and to favor T<sub>H</sub>1-type immune response (Foth *et al.*, 2014). Interestingly as described in section 1.2.4., this family of proteins appears to carry a nematode clade I-specific function that inhibits the inflammatory responses on the host during invasion and establishment of the parasite (Foth *et al.*, 2014).

Furthermore, in recent years the role of Extracellular Vesicles (EVs) in *Trichuris* spp. infection has been described. Extracellular vesicles are a population of lipid-enclosed spherical vesicles that participate in the communication between cells and organisms (Mardahl *et al.*, 2019).

They are released by cells into the extracellular space and contain bioactive components (Mardahl *et al.*, 2019). In 2015, it was described for the first time that EVs were released from whipworms and that L1 larvae of *T. suis* secrete small RNAs apparently involved in host-parasite interactions (Hansen *et al.*, 2015). In 2018, Shears and collaborators described how fractions of excretion/secretion (ES) products of *T. muris* elicited long-lasting immunity against reinfection, showing that EVs induced a mixed  $T_H1$  and  $T_H2$  response.

Challenges including genetic heterogeneity, undefined infection history, exposure intensities, and co-infections continue to blur the clear picture of *T. trichiura* host immune responses (Else *et al.*, 2020; Hayon *et al.*, 2021).

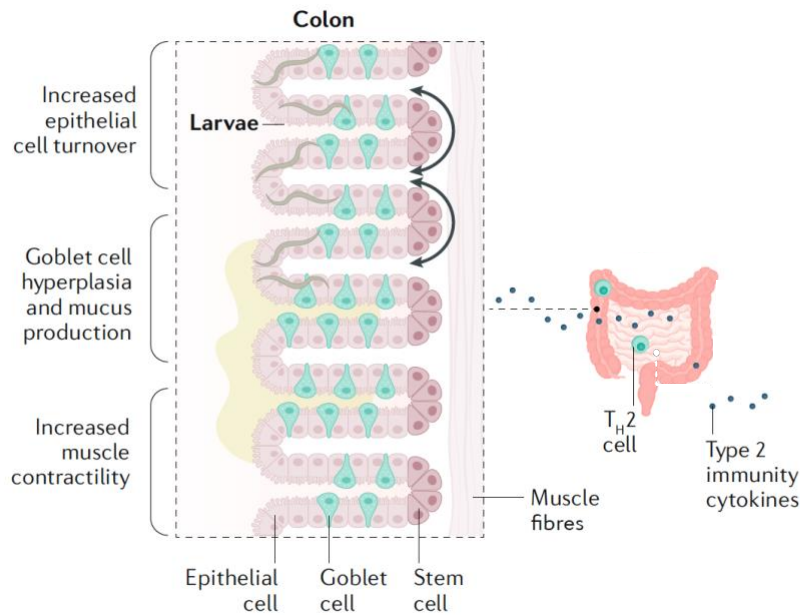


**Figure 1.9 Type 2 immunity**

Type 2 immunity cytokines (IL-4, IL-5, IL-9, and IL-13) increase the rate of epithelial turnover, the goblet cell numbers, and mucus production, and increase in muscle contractility resulting in epithelial turnover and parasite expulsion (Adapted from Else *et al.*, 2020).

### 1.4.1 Antibody Response

Although antibody response to *T. trichiura* has not been studied in-depth due to limitations inherited from the lack of an adequate animal model and the difficulties obtaining the parasite

material (Else *et al.*, 2020), Lillywhite (1991) and collaborators showed that infection with *T. trichiura* evokes a strong humoral immune response of serum IgG, IgA, and IgE classes.

Lillywhite (1991) found that the predominant humoral response was mediated by IgG, showing a correlation to infection intensity that was later confirmed by Needham (1994). Serum IgE antibody responses also studied by Needham (1994) were difficult to interpret as the antibody signals were negligible to the crude antigen extract used. Also, serum IgA antibodies showed a vigorous unspecific response during early childhood, and adulthood, in low and high transmission areas suggesting a potential association with acquired immunity to *T. trichiura* (Needham *et al.*, 1994).

Further, Needham (1996) investigated the salivary antibody responses based on the concept of a common mucosal immune system where antibodies secreted in the saliva, and other mucosal secretions would be expected to reflect the same gut-associated antigen responses. The salivary IgA levels showed a weak but significant negative correlation with infection intensity and an increase with age, suggesting the confirmation of its association with acquired immunity (Needham *et al.*, 1996).

Faulkner and collaborators (2002) showed that serum IgE levels were strongly associated with an age-dependent decrease in *T. trichiura* infection intensity (the older and less heavily infected study subjects had greater levels of serum IgE), while serum IgG and IgA were inconsistent in mirroring infection intensity and age correlation.

Self-infection studies showed that serum IgA and IgG anti-*Trichuris* antibody levels remained below detection levels before *T. trichiura* infection and peaked at the time of the establishment of infection while remaining above the detection levels for the remaining of the study inclusive of the post-treatment period (Dige *et al.*, 2016).

Of note, the few studies described above that have studied *T. trichiura* antibody responses to date used crude antigen preparations because the nature and functional characteristics of *T. trichiura* adults, larval and egg life stages were largely unknown. Not until 2014, Foth and collaborators published the first draft genome for *T. trichiura*, while the complete human *T. trichiura* genome project is still an ongoing effort.

### 1.4.2 T helper lymphocytes

The T helper 2 ( $T_H2$ ) or T helper 1 ( $T_H1$ ) immune response in the host determines the possibility to resist ( $T_H2$ ) or be susceptible ( $T_H1$ ) to *Trichuris* infection (Hayon *et al.*, 2021). Based on animal models,  $T_H2$  cytokines are associated with resistance to infection and the mechanisms needed to trigger the immune-mediated parasite expulsion from the host (Hayon *et al.*, 2021). Cytokines IL-4, IL-5, IL-9, and IL-13 have been represented as the promoters of *Trichuris* control inducing gut hypercontractility (IL-9 - recently moved from  $T_H2$  to  $T_H9$ ), increasing mucus production, and promoting epithelial turnover (IL-13) for the rapid expulsion of the parasites (Hayon *et al.*, 2021). For example, IL-4 receptor blockage polarized to a  $T_H1$  immune response and promotes chronic infection, whereas administration of IL-4 to susceptible mouse strains results in a predominant  $T_H2$  response and clearance of infection, defining IL4 as a critical mediator to enhance antibody responses (Briggs *et al.*, 2018; Hayon *et al.*, 2021). In contrast, during chronic trichuriasis (low dose prolonged infections), high concentrations of typical  $T_H1$  immune response interferon  $\gamma$  (IFN- $\gamma$ ), IL-12, and IL-18 have been identified, where IL-18 drives suppression of IL-4 and IL-13  $T_H2$  associated cytokines, reducing rapid parasite expulsion, and making the host more susceptible to persistent infection (Shears *et al.*, 2018; Hayon *et al.*, 2021). Furthermore, when IFN- $\gamma$  is depleted a reduction in IL-18 creates a more resistant host (Hayon *et al.*, 2021).

There is no analysis of type 1 and type 2 cytokines released by peripheral blood leukocytes and re-stimulated in vitro for *T. trichiura* because polyparasitism is the most common presentation in endemic populations where studies have been conducted (Else *et al.*, 2020; Hayon *et al.*, 2021). The challenges of understanding the role of T helper lymphocytes for isolated *T. trichiura* infections have been only recently elucidated with single-subject self-infection studies (Hansen *et al.*, 2016; Dige *et al.*, 2017). The longitudinal analysis of T cell subsets in mucosal biopsy samples and peripheral blood revealed a mixed mucosal T cell response ( $T_H1$ ,  $T_H2$ ,  $T_H17$ , and regulatory T ( $T_{reg}$ ) cells) while circulating T helper cells became predominantly  $T_H2$  cells (Hansen *et al.*, 2016; Dige *et al.*, 2017). In the *T. muris* model, high levels of local inflammatory  $T_H17$ -dependent IL-23 expression have been observed, highlighting the importance of its role for an accelerated worm expulsion. (Gomez-Samblas *et al.*, 2017).

There is an urgency to develop a vaccine against human whipworm (Hayon *et al.*, 2021). Significant efforts have led to discovering potential vaccine candidates; however, understanding the protective immunity of these candidates relies on preclinical models, like the murine model, which has led to a lack of consensus on the ideal development strategy (Hayon *et al.*, 2021). The challenges encountered with the murine model are the selection of the mouse strain to balance the host susceptibility to infection and how different *T. muris* strains or isolates can affect the success of the model (Hayon *et al.*, 2021).

### 1.4.3 Co-infections

Co-infections often affect children and are generally underdiagnosed as they remain associated with non-specific gastrointestinal symptoms (Else *et al.*, 2020). In endemic areas, chronic infections and misdiagnosis can lead to older adults experiencing Chronic Deficiency Anemia (CIDA) with hemoglobin levels less than 8 g/dL, iron deficiency, and TDS diagnosis upon confirmation of *Trichuris* infection (Khuroo *et al.*, 2010).

Co-infections in captive populations of AGMs are also common (Cruz *et al.*, 2021). They can remain undiagnosed as they can be associated with non-specific gastrointestinal symptoms that AGMs easily mask confounding daily observations and diagnoses (Cruz *et al.*, 2021). In the wild, naturally occurring co-infections are commonly described and understudied as most reports focus on the description of the treatment outcomes (Munene *et al.*, 1998; Muriuki *et al.*, 1998; Gillespie *et al.*, 2004., Legesse *et al.*, 2004; Petrášová *et al.*, 2010; Gaetano *et al.*, 2014; Kooriyama *et al.*, 2014; Amenu *et al.*, 2015; Wren *et al.*, 2015; Dalimi *et al.*, 2016; Valenta *et al.*, 2017; Teklemariam *et al.*, 2018).

## 2 Justification and Objectives

Trichuriasis represents a public health threat. Concerns on treatment efficacy, low cure rates, drug resistance, and chronic illness compromise the control and eradication efforts. Under-diagnosis and lack of understanding of potential zoonotic exposures due to human encroachment and wildlife interactions expose the urgent need for a suitable animal model that enables access to parasitic material (feces, adult nematodes) and biological samples (serum and saliva) that facilitate the study of *T. trichiura* alternative diagnostic methods.

### 2.1 General Objective

Identify *Trichuris trichiura* immunogenic proteins of diagnostic value and evaluate anthelmintic treatments for captive AGMs for their application in animal and human trichuriasis prevention and control programs.

### 2.2 Specific Objectives

1. Evaluate the use of albendazole and ivermectin as anthelmintic treatment for AGMs and describe the husbandry recommendations used to control *T. trichiura* infections in captive research animals.
2. Analyze the correlation between fecal examination egg counts results and total worm counts found post-treatment in the large intestine.
3. Characterize and describe the *T. trichiura* egg proteome.
4. Identify *T. trichiura* immunogenic proteins of diagnostic value and lay out the process of designing and selecting synthetic peptides for diagnostic use.
5. Study the humoral immune response in saliva and serum to monitor the treatment outcomes in naturally infected AGM.

### 3 Materials and Methods

#### 3.1 Ethical statements

The Institutional Animal Care and Usage Committee (IACUC) of the St. Kitts Biomedical Research Foundation (SKBRF) & Virscio Inc. (IACUC AC1875, Study code S00147) approved the collection of saliva and serum samples. The IACUC of Ross University School of Veterinary Medicine (RUSVM) approved postmortem tissue and sample collection from African green monkeys (2018 - Immunodiagnosics for *Trichuris trichiura*, P. Kelly).

Use of existing anonymous human saliva, serum and plasma samples from healthy volunteers were approved for use under RUSVM Institutional Review Board (IRB) exemption certifications No. 18 -11 EX and No. 18 -10 EX.

#### 3.2 *Trichuris trichiura*

##### 3.2.1 Adults

Adult worms were obtained at routine necropsy of naturally infected *C. sabaesus* that were humanely euthanized as part of other studies conducted at the SKBRF facility on St. Kitts. The abdominal cavity was opened, and the intestines ligated at the proximal duodenum and distal rectum before they were removed and placed in 0.9% saline for transport to the RUSVM Research Laboratory. Upon arrival, 4 grams of fecal material was extracted from the rectum for analysis and the large intestine separated from the small intestine. After the large intestine was opened longitudinally, a 2x2 cm full thickness section was removed from cecum and placed in 10% formalin for histopathology. The cecal samples were dehydrated in a series of ethanol solutions (30%, 50%, 70%, 80%, 90%, 95% and 100%) they were embedded in paraffin wax (BMJ-III embedding machine, Jiangsu, China) at 56 °C and sectioned. The 5 µm sections were stained with hematoxylin-and-eosin (H&E) and examined with an Olympus DP73 microscope (Tokyo, Japan) for morphological and structural changes. The remaining large intestine was soaked in saline solution (0.9%) for 2 hours at room temperature (30-32 °C) to loosen the intestinal contents and subsequently at 4 °C until analysis. Within 24h, any ingesta remaining attached to the mucosa was removed manually into the saline solution and the surface visually inspected for *T. trichiura* that remained attached.

The solution of the collected ingesta was filtered through a 100 µm sieve and the recovered material examined for adult nematodes under a stereomicroscope (7x – 10x magnification). The *T. trichiura* identified were counted, sexed, and washed five times for 5 min in Phosphate Buffered Saline (PBS; pH 7.4) before they were dried and preserved at -80 °C or, in the case of the most intact specimens, placed in Karnovsky's fixative (**Appendix I**) for Scanning Electron Microscopy. Other species of nematodes found were preserved in either 10% formalin or 70% ethanol for future morphological and molecular characterization.

### 3.2.2 Adults extracts (AE)

Adult females (n=10) and males (n=10) stored at -80 °C were defrosted at 4 °C, pooled by sex, and placed in PBS containing 1% protease inhibitors (cOmplete™ mini EDTA-free tablets, Roche, Mannheim, Germany) and 1% Triton™ x-100 (Sigma-Aldrich®, MO, USA). Five pulses, 30 s each, of a low speed mechanical rotor (Dremel®, Robert Bosh GMBH, Mount Prospect, IL, USA) was used to initially break down the worms which were maintained on ice during the procedure. After freezing at -20 °C and thawing at room temperature the nematodes were sonicated on ice with a Microson Ultrasonic Cell Disruptor XL™ (Misonix, NY, USA) using ten cycles of 10x 1-second pulses at maximum intensity. Following centrifugation (10,000 x *g* for 10 min at 4 °C) the supernatant containing the soluble proteins (the Adult Extract - AE) was removed and stored at -20 °C.

For the specificity assays, protein extracts from other species of helminths (see **Table 3.1**) were obtained, as above, from convenience samples of the following species:

**Table 3.1 Convenience samples used to prepare protein extracts for the specificity assays.**

<i>Sample species</i>	<i>Source</i>
<i>Fasciola hepatica</i> and <i>Dicrocoelium dendriticum</i>	adults were obtained from infected cow's livers from an abattoir in Valencia (Martínez Loriente S. A., Valencia, Spain) in collaboration with Dr. Fernando Cantalapiedra.
<i>Aspicularis tetraptera</i>	adults from mice were donated from concurrent studies at the Parasitology Department of University of Valencia.
<i>Anisakis simplex</i>	adults were obtained from whole cod bought commercially and examined in the parasitology laboratory as part of other projects.
<i>Gnathosoma hispidium</i>	adults were obtained from infected cows from the local abattoir in Valencia (Martínez Loriente S. A., Valencia, Spain) in collaboration with Dr. Fernando Cantalapiedra.
<i>Primasubulura</i> sp.	as described for <i>T. trichiura</i> , adults were obtained from ceca of AGMs at necropsy.



### 3.2.3 *Trichuris trichiura* non-embryonated (NE) egg extracts (EE)

The uteri were dissected and extracted (**Figure 3.1** (A) and (B)) from *T. trichiura* adult females (n=50) thawed from -80 °C at room temperature using a 30G ½” needle (BD Microlance™, Fraga, Huesca, Spain) (10x – 30x magnification) and placed in PBS. After, the uteri were opened with a longitudinal incision to facilitate the release of non-embryonated (NE) eggs which were pooled. After five washes in 1 mL PBS (10,000 x g; 1 min) the supernatant was removed and the NE resuspended in 700 µL PBS containing 1% protease inhibitors (cOmplete™ mini EDTA-free, Roche®) and 1% Triton™ x-100 (Sigma-Aldrich®). To ensure disruption of *Trichuris* eggshells, the homogenate was sonicated while frozen at -20 °C using ten cycles of 10 x 1-second pulses at maximum intensity with a Microson Ultrasonic Cell Disruptor XL™ (Misonix). Homogenates were checked for eggshell disruption under a stereomicroscope (10x - 30x magnification), centrifuged (10,000 x g for 10 min at 4 °C) and the supernatant containing the soluble NE egg proteins recovered (the *T. trichiura* NE egg extract - EE) and frozen at -20 °C until further analysis.

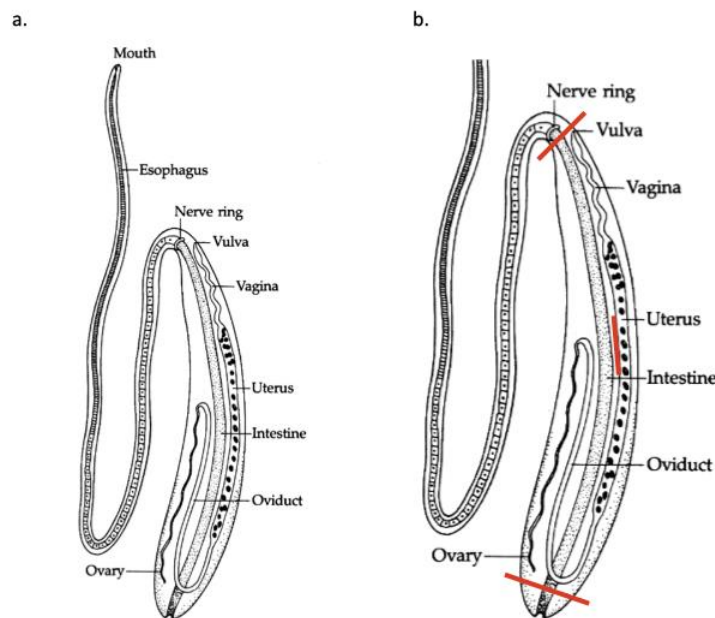


**Figure 3.1** *Trichuris trichiura* uterus dissection guide.

(A) Identification of anatomical landmarks. (B) identification of the three dissection zones.

### 3.2.4 Protein quantification of parasite extracts

The total protein concentrations of the extracts (AE and EE) were determined using a commercial Protein Assay (Bio-Rad®, CA, USA) according to the manufacturer's instructions with Bovine Serum Albumin (BSA) (Sigma-Aldrich®) as the standard. The assay uses the Bradford method (Bradford, 1976) to quantify soluble proteins (1-10 µg/mL) that is based on the binding of Coomassie Brilliant Blue G-250 dye to form a dye-protein complex which can be detected at 595 nm in a spectrophotometer (ELISA iMark Microplate Absorbance Reader (Bio-Rad®)) using the software Microplate Manager™ and quantitated against the BSA (Sigma-Aldrich®) standard quantification curve generated.

### 3.2.5 Preparation for Scanning Electron Microscopy (SEM)

Specimens were removed from Karnovsky's fixative and washed four times in 0.1 M cacodylate buffer (stock solution with 0.2 M sodium cacodylate to 1 L distilled H<sub>2</sub>O). Following dehydration in 50%, 70%, 80% and 90% ethanol for 15 min each and a final incubation in 100% ethanol for 1h, the specimens were dried in a Critical Point Dyer (Balzer Union, Balzers, Liechtenstein) and mounted on the carbon mounts sample plates. Gold palladium vaporation was carried out at 25 mA for 8 min. The samples were prepared and analyzed in a scanning electron microscope (Zeiss Auriga, FEI QemScan 650 F, Oberkochen, Germany) at the Center for Scientific Instrumentation (CIC) of the University of Granada.

## 3.3 African green monkeys (AGM; *Chlorocebus sabaeus*)

### 3.3.1 Animals

Apparently healthy juveniles and adult *C. sabaeus* (11 females and 22 males) humanely euthanized for other experiments performed at the SKBRF & Virscio were used for the collection of samples. Prior to euthanasia the animals were maintained and treated according to standard operating procedures in place at the facility for cleaning, feeding and enrichment activities (see section 3.4.1).

### 3.3.2 Feces and analysis

Feces were collected from individual *C. sabaesus* cages according to SKBRF & Virscio standard operating procedures. They were also collected from *C. sabaesus* following humane euthanasia as described in section 3.2.1. Aliquots (2 g) were examined within 48 h using the double centrifugation technique with Sheather's sugar flotation solution (spg 1.28) as described previously (Zajac & Conboy, 2012) (**Appendix II**).

### 3.3.3 Sera

Blood was drawn according to SKBRF & Virscio standard operating procedures as part of other studies. Sera were separated by centrifugation at 2,000 x *g* for 15 min at room temperature and stored at -80 °C until analysis.

### 3.3.4 Saliva

Saliva was collected following an in-house protocol (**Appendix III**). In short, when *C. sabaesus* were anaesthetized during the morning for other studies conducted at the SKBRF & Virscio with ketamine HCl 8 mg/kg (Bioniche Pharma USA LLC, IL, USA) and xylazine 1.6 mg/kg (AnaSed® Akorn, Inc., IL, USA). Cotton rolls (Richmond™, NC, USA) were placed along the upper and lower mucobuccal folds and left for 5 min before being placed in 3 mL sterile syringes (BD Luer-Lok™ tip, NJ, USA) for transport on ice to the RUSVM research laboratory. Within 3 h of collection, each syringe with its cotton roll was placed, needle-attachment site down, into a 15 mL centrifuge tube (Falcon™, NY, USA) and centrifuged for 20 min at 1,500 x *g* at 4 °C. The supernatant saliva was removed from the Falcon™ tube, mixed with equal volumes of saliva conservation mix (PBS, cComplete™ mini EDTA-free Roche® and ProClin® Sigma-Aldrich) (**Appendix IV**), and stored at -80 °C until analysis.

### 3.3.5 Human sera and saliva

Saliva and sera from humans to be used as negative controls were obtained from other studies where the study subjects or volunteers had agreed to their anonymized samples being used for other research. The samples were stored at -80 °C until use.

## 3.4 Case report on nematode control of captive AGMs

### 3.4.1 Animals and Facilities

St. Kitts Biomedical Research Foundation (SKBRF) and translational research affiliate Virscio, Inc. are an Association for Assessment and Accreditation of Laboratory Animal Care International (AAALAC)-accredited biomedical research facility for integrated preclinical research and development with a multidisciplinary nonhuman primate translational focus. The facility houses approximately 1,000 *C. sabaesus*, primarily in outdoor social enclosures or indoor pair house caging designed according to regulations in the *Guide for the Care and Use of Laboratory Animals* (National Research Council of the National Academies, 2011).

All the *C. sabaesus* on which we collected data were being used in studies approved by the Institutional Animal Care and Use Committee of SKBRF & Virscio. The AGMs had entered the facility between January 2018 and July 2019 and were housed and cared for according to SKBRF standard operating procedures. All the animals were moved to individual stainless steel cages that meet the nonhuman primate requirements (National Research Council of the National Academies, 2011) for the duration of their study periods, except for AGM 20 that remained in paired housing and AGMs 21-26 with longest study periods of 12 – 24 months that spent a range of 4 to 14 months in social enclosures according to standard regulations (National Research Council of the National Academies, 2011). The individual cages have steel mesh floors lined with steel pans above the ground that meet standard non-human primate requirements (National Research Council of the National Academies, 2011) (minimum height 30 cm<sup>2</sup> and floor space 0.4 m<sup>2</sup>). The cages were washed down with water daily to remove feces, urine, and left-over food debris.

Every two weeks the AGMs were removed from the cages, which were then sanitized using a combination of steam (>82 °C) and a quaternary-based disinfectant (Consume Eco-Lyzer®,

Consume Nature's Way, Spartan Chemical Company Inc, Ohio, USA), or using an accelerated hydrogen peroxide foam (Peroxigard™, Virox® Technologies Inc. Ontario, Canada). The residual disinfectant was removed by power washing with cold water. The disinfectant used was alternated at each 2-week application, and sanitation effectiveness measured by routine Adenosine triphosphate (ATP) bioluminescence testing of randomly selected surfaces after cages had dried after the final power wash.

The main food provided once a day to the *C. sabaesus* was monkey chow (Envigo® Teklad 8773 primate biscuits, Indiana, USA) which was supplemented with seasonal fruits and vegetables sourced from on-site gardens or local farms. The fruits and vegetables were picked directly from the trees and washed if evidently soiled, they were provided for both nutrition and as an enrichment activity for the animals' wellbeing. Water, provided *ad libitum* with Lixit® (California, USA) water valves in the individual cages, was from the St. Kitts main water supply which the facility filtered (Neo-Pure PS-27097-05 9-3/4" standard efficiency pleated filter 5 µ, Neologic solutions®, South Carolina, USA) and treated with ultraviolet light (Sanitron® ultraviolet water purifiers, Atlantic Ultraviolet Corporation®, New York, USA). The water lines in the facility were sanitized monthly with a sodium hypochlorite flush delivered by an Edstrom automated watering system (Avidity Science®, Wisconsin, USA).

### 3.4.2 Treatments

Until recently, based on Association of Primate Veterinarians recommendations (APV) (Nonhuman primate formulary, 2018; Calle *et al.*, 2014), wild-caught *C. sabaesus* brought into the facility were routinely treated with intramuscular 5mg/kg praziquantel (Droncit®, Kansas, USA) and 15 mg/kg albendazole (Valbazen®, Michigan, USA) (PRAL treatment) delivered by nasogastric or orogastric gavage to chemically restrained animals (ketamine HCl, 8 mg/kg, Bioiniche Pharma USA LLC and xylazine, 1.6 mg/kg, AnaSed® Akorn, Inc.) animals. This treatment was repeated after 2 weeks and arbitrarily every 3-5 months for ongoing control.

In 2019, a new treatment regimen was introduced based on a report from Kenya (Kagira *et al.*, 2011) that a combination of ivermectin and albendazole (IVAL treatment) resulted in a 100

% fecal egg reduction rate for *T. trichiura* and strongyles. The IVAL treatment we used consisted of a three-day regimen of 300 µg/kg ivermectin (Noromectin®, Newry, Co. Down, Northern Ireland) SQ SID, and 10 mg/kg albendazole (Valbazen®) SID delivered by nasogastric or orogastric gavage following chemical restraint, as described above. The IVAL treatment was repeated when an animal had a positive fecal flotation result during routine screening after three months. The praziquantel treatment regimen remained used for cases diagnosed with cestode or trematode infections.

### 3.4.3 Monitoring of treatments

We monitored the success of the PRAL and IVAL treatments in *C. sabaesus* that required sampling and necropsy as part of studies in which they were enrolled and that had been approved by the Institutional Animal Care and Use Committee of SKBRF & Virscio. The *C. sabaesus* treated with the PRAL regimen (n= 26; 9 females, 17 males) had FECs (all AGMs) and counts of adult *T. trichiura* in the large intestine (15 AGMs – see below) performed at routine necropsies carried out 2, 4, 5, 10, 12, 15, 22 and 24 months after the initial PRAL treatment and at least 3–5 months after ongoing PRAL treatments in the case of the AGMs euthanized 10 – 24 months after the initial treatment.

The *C. sabaesus* treated with the IVAL regimen (n=11, all males) had FECs carried out on feces collected from their cages 3 months after the IVAL treatment. Animals with a positive result were given a second IVAL treatment and all animals tested by FEC and counts of adult *T. trichiura* in the large intestine at routine necropsies 6 or 8 months after the initial IVAL treatment.

### 3.4.4 Morphological identification

Parasites were identified to the species level whenever possible as detailed species-level taxonomic identification from microscopic analysis alone is not always feasible. Morphologic identification of *T. trichiura* eggs was based on size (50-60 x 20-30 µm), brown-bile green color, the presence of bipolar plugs, and the characteristic lemon-shaped unembryonated egg with a smooth shell, an important characteristic to differentiate from *Capillaria*. Specimens of *Capillaria*

spp. were identified based on size (50-60 x 20-30  $\mu\text{m}$ ), ovoid barrel-shaped unembryonated egg, light yellow/green color, bipolar prominences, and characteristic striated shell. Eggs were classified as *Strongyloides* spp. based on size (50-60 x 30-40  $\mu\text{m}$ ), lack of color, ellipsoidal shape, thin shells, and the presence of larvae coiled inside the eggs was regarded as an indication of *Strongyloides fuelleborni* (Acha *et al.*, 2003; Modrý *et al.*, 2015). Eggs were classified as strongylid based on their size (60-85 x 35-50  $\mu\text{m}$ ), ellipsoidal shape, and their smooth, thin shelled and colorless appearance. Strongylid eggs containing a morula were regarded as hookworms, while those slightly longer, with an early cleavage-stage embryo and one or both eggshell ends more pointed were classified as *Trichostrongylus* spp. (Hasegawa, 2009; Modrý *et al.*, 2015; CDC, 2016) (Figure 3.2).

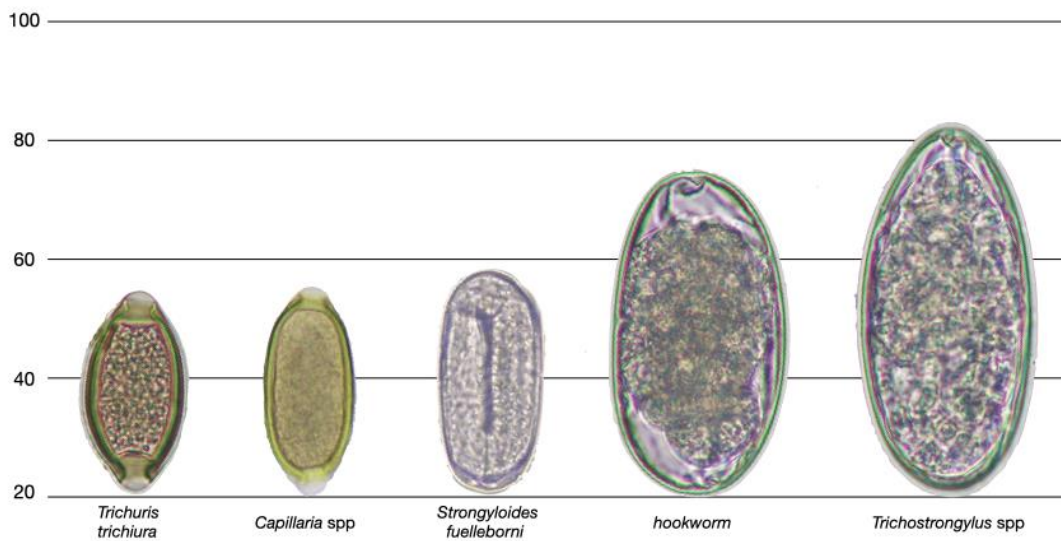


Figure 3.2 Morphologic identification of nematode eggs species found.

Measurements in  $\mu\text{m}$ .

### 3.5 Identification of immunogenic proteins of diagnostic value in *T. trichiura* adults and eggs

#### 3.5.1 Indirect ELISA for detection of specific antibodies anti-*Trichuris* in sera and saliva of infected animals.

Microtiter plates (96 well; Thermo Fisher Scientific, MA, USA) were coated with 5 µg of AE diluted in coating buffer 0.05 M, pH 9.5-9.6 (Na<sub>2</sub>CO<sub>3</sub>, NaHCO<sub>3</sub>) in a final volume of 100 µL per well. After overnight incubation at 4 °C the coating buffer was removed, and the plates were blocked with BSA (Sigma-Aldrich®) 0.05% in PBS-0.05% Tween 20® (Sigma-Aldrich®) (PBST) for 1h at 37 °C on an orbital shaker at 60 rpm. Duplicate samples of saliva (1/80 in PBST) and sera from infected AGMs and negative human controls (1/100 in PBST) were incubated in wells for 90 min at 37 °C on an orbital shaker at 60 rpm. After three washes in PBST the plates were incubated for 1h at 37 °C on an orbital shaker at 60 rpm and reactive antibodies in AGM samples detected with peroxidase labeled goat anti-primate IgA or IgG (Novusbio™ Novus Biologicals LLC, CO, USA) (1/5,000 in PBST), and for human samples goat anti-human IgA or IgG (Abcam®, Cambridge, UK) (1/5,000 in PBST). After washing as above, immune complexes formed were revealed with OPD substrate (o-Phenylenediamine dihydrochloride) (Sigma-Aldrich®) 0.4% mg/mL in 0.05 M, pH 5 citrate -phosphate buffer (0.1 M C<sub>6</sub>H<sub>8</sub>O<sub>7</sub>/0.2M NaHPO<sub>4</sub> 0.2 M/30% H<sub>2</sub>O<sub>2</sub>). After 5 min at room temperature (21°C), the reaction was stopped with 3N HCl and the colorimetric reaction assessed photometrically at 490 nm using iMark Microplate reader (Bio-Rad®) and Microplate Manager 6.0 (Bio-Rad®).

Each sample was tested in duplicate, and the results expressed as mean optical densities (OD) with their standard deviations (SD). The cutoff was established as the mean OD of the negative controls plus 3 SDs.

#### 3.5.2 One dimensional *SDS-PAGE* electrophoresis (1-DE) gel staining and Western-blot with serum and saliva

The AE and EE (10 µg/well) was diluted in 4x Laemmli buffer (Bio-Rad®) (1:1), denatured at 100 °C for 5 min under reducing conditions and separated by electrophoresis in Mini-Protean® TGX precast acrylamide gels (4-15% gradient, 10 well comb, 50 µL/well) (Bio-Rad®) with 80 – 120



V in a Mini-PROTEAN Tetra System electrophoresis system (Bio-Rad®). Samples were run simultaneously with molecular weight markers (4 µL) (Precision Plus Protein™ Dual Color Standards, Bio-Rad®). Following electrophoresis, half of the gel was stained with Coomassie brilliant blue R-250 (Bio-Rad®) and the other mirror half transferred onto nitrocellulose filters (Trans-Blot Turbo™ transfer pack, Mini Format, 0,2 µm Nitrocellulose, single application, cat # 1704158, Bio-Rad®) using a Trans-Blot® Turbo™ transfer system (Bio-Rad®) as per manufacturer's instructions for mixed MW for 7 min. The blotted membrane was stained in acidic Ponceau S (99 mL distilled water, 0.5 g Ponceau S (Sigma-Aldrich®), 1 mL glacial acetic acid) and after the proteins were visualized, the membrane was washed with distilled water, blocked with 5% skimmed milk in PBST for 2 h at room temperature, and incubated overnight at 4° C with a pool of either saliva or serum samples diluted 1:10 or 1:500 in PBST, respectively. Following three washes, each of 30 min in PBST, the membranes were incubated for 4 h at room temperature with the secondary antibody (peroxidase-labeled goat anti-primate IgG (1:5000 in PBST) or IgA (1:1000 in PBST), (Novusbio™), washed three times in PBST (30 min each) and the assay developed using Clarity™ Western ECL substrate (Bio-Rad®) mixed in a 1:1 ratio. The positive reactions were determined by the appearance of defined protein bands detected by chemiluminescence with an Amersham™ Imager 600 (GE Healthcare®, IL, USA). The relative molecular masses of the recognized protein fractions were determined by comparison with molecular weight markers (kDa) and data analysis was completed as previously described (Bernal *et al.*, 2006).

### **3.5.3 Two-dimensional SDS-PAGE electrophoresis (2-DE), gel staining and Western-blot with serum**

Egg extract (1 µg/µL) was purified with the 2-D Clean-up Kit (GE Healthcare®, New Jersey, USA) following the manufacture's protocol. After the final centrifugation step, the protein pellets were resuspended in lysis buffer (7 M Urea, 2 M thiourea, 4% CHAPS), and quantified (1 µg/µL) with the RC DC™ Protein Assay (Bio-Rad®).

The EE (10 µg for Coomassie staining, and 30 µg for 2-DE Immunoblotting) was diluted 1:1 in sample buffer containing 65 mM dithiothreitol (DTT) and 1% ampholytes, loaded onto previously hydrated (125 µL DeStreak™ and 1 % ampholytes) 7 cm, pH 3-11 strips (Immobile

DryStrips™ GE Healthcare) for first dimension separation. The protein samples were separated according to isoelectric point (pI) values through Isoelectric focusing (IEF), using a Ettan IPGphor 3 (GE Healthcare®) at 20 °C as follows: (i) 300 V for 30 min (step and hold), (ii) 1000 V for 30 min (gradient), (iii) 5,000 V for 80 min (gradient) and (iv) 5,000 V until 4,000 Vh (step and hold) (current limit of 70 µA/IPG strip).

After focusing, the strips were equilibrated in two steps in a reswelling tray (Immobiline™ Drystrip Reswelling Tray, Pharmacia Biotech AB®, Uppsala, Sweden) at room temperature. The first step comprised 15 min in equilibration buffer (BE) (6 M Urea/ 50 mM Tris/HCL, pH 8.8/ 29.3% Glycerol/ 2% SDS/ 0.002% Bromophenol blue) with 2% DTT (GE healthcare®), and the second step was carried out for 15 min in BE with 2.5% iodoacetamide (IAA) (GE healthcare®). The two-dimensional SDS-PAGE was performed with 12.5 % acrylamide separating gels in a Mini-PROTEAN Tetra Cell electrophoresis chamber (Bio-Rad®) at 60 – 120 V for 120 min (Bio-Rad®). The samples were run simultaneously with 5 µL of the molecular weight marker (Precision Plus Protein™ Dual Xtra Standards; Bio-Rad®) in the Coomassie gel and 2 µL in the 2D WB gel.

After 2-DE, resultant EE gels were stained with Coomassie brilliant blue R-250 (Bio-Rad®) or transferred to nitrocellulose paper (Amersham™ Hybond™-ECL, GE healthcare®) using the Mini Protean™ transfer system (Bio-Rad®) at 200 mA for 2 h. The blotted membrane was processed for Western blotting as described for 1-DE above except the incubation period of the secondary antibody was 4 h.

### 3.6 Proteomic analysis of *T. trichiura* AE and EE

Sample preparation, liquid chromatography, tandem mass spectrometry and initial proteomic analysis of MS/MS fragmentation data was performed for the study of *T. trichiura* complete egg proteome and immunogenic bands from egg (EE) and adult (AE) extracts by the proteomics facility of *Servei Central de Suport a la Investigació Experimental (SCSIE)* of University of Valencia (Burjassot, Spain) that belongs to ProteoRed, PRB2-ISCI, supported by grant PT13/001.

### 3.6.1 Sample preparation

Following electrophoresis, the strip of gel containing the all the EE products was cut and digested with 500 ng of sequencing grade trypsin (Promega, WI, USA), a proteolytic enzyme, in 200  $\mu$ L of ammonium bicarbonate solute. The selected immunogenic bands visible and non-visible (in the case of immunogenic bands that are not clearly visible in the SDS-PAGE due to lower abundance) were identified on the SDS-PAGE Coomassie gels and cut for digestion with 100 ng of sequencing grade trypsin (Promega) in 100  $\mu$ L of ammonium bicarbonate solution as described elsewhere (Shevchenko *et al.*, 1996). Digestion was stopped with 1% trifluoroacetic acid (TFA) and a double extraction with acetonitrile (ACN) performed as previously described (Bernal *et al.*, 2006). The final peptide solutions were vacuum dried in a rotatory evaporator and resuspended with 25  $\mu$ L of 2% ACN and 0.1% TFA (pH 2) for EE and 9  $\mu$ L 2% ACN and 0.1% TFA (pH 2) for the individual bands.

### 3.6.2 Liquid chromatography and tandem mass spectrometry (LC-MS/MS)

To initiate the elution process, 5  $\mu$ L of the final peptide solution was loaded onto a trap column (Nano-LC Column, 3 $\mu$ m C18-CL, 350  $\mu$ m x 0.5 mm, Eksigent<sup>®</sup>, AB SCIEX<sup>®</sup>, CA, USA) and desalted with 3  $\mu$ L/min 0.1% TFA over 5 min. The peptides were loaded onto an analytical column (LC Column, 3  $\mu$ m C18-CL, 75  $\mu$ m x 12 cm, Nikkyo, Nikkyo Technos Co., Ltd, Tokyo, Japan) equilibrated in 5% acetonitrile, 0.1% formic acid (FA) and eluted using a linear gradient (5-35%) of solvent B (0.1% FA in ACN) in A (0.1% FA) for 120 min for the EE and 30 min for the individual bands at a flow rate of 300 nL/min. The eluted peptides were analyzed with a nanoESI-Q-TOF mass spectrometer (5600 TripleTOF, AB SCIEX<sup>®</sup>) in an Information Dependent Acquisition Mode (IDA) as per manufacturer's instructions. An IDA method automatically runs experiments based on results obtained from previous experiments using Analyst<sup>®</sup>, AB SCIEX<sup>®</sup> software.

The eluted sample was ionized applying 2.8 kV to the spray emitter and survey MS1 scans were acquired from 350 to 1,250 m/z for 250 ms. The quadruple resolution was set to 'UNIT' for MS2 experiments, which were acquired 100–1,500 m/z for 50 ms in 'high sensitivity' mode. The following switch criterion was used: charge 2+ to 5+, minimum intensity, 70 counts per second

(cps). Up to 50 ions were selected for fragmentation after each survey scan. Dynamic exclusion was set to 15 s. The system sensitivity was controlled with 2 fmol of 6 proteins (LC Packings, A Dionex Company, Amsterdam, Netherlands).

### 3.6.3 Bioinformatic analysis

ProteinPilot™ Software (version 4.5.1, revision 2768; Paragon™ Algorithm 4.5.1.0, 2765; Applied Biosystems®/MDS Sciex, MA, USA) default parameters were used to generate the peak list directly from 5600 TripleTof .wiff files. All .wiff files from the sample were combined in a single search. ProteinPilot™ Software is a program used for analysis of peptide tandem mass spectrometry data by conducting protein inference analysis and relative quantification of proteins. The Paragon™ Algorithm (Shilov, I.V., *et al.*, 2007) included in ProteinPilot™ software was used for searching the National Center for Biotechnology Information (NCBI) protein database with the following parameters: tryptic specificity, cys-alkylation, Metazoa, Nematoda and *Trichuris trichiura* protein taxonomy restrictions. The Paragon™ scoring algorithm provides confidence levels for proteins hits.

Protein grouping was done by Pro Group™ algorithm. A protein group in a Pro Group™ Report is a set of proteins that share some physical evidence, meaning that they are groups of related and homologous proteins.

Unlike sequence alignment analyses where full length theoretical sequences are compared, the information of protein groups in Pro Group™ is guided entirely by observed peptides alone. Since the observed peptides are actually determined from experimentally acquired spectra, the grouping can be considered to be guided by usage of spectra. Therefore, unobserved regions of protein sequence play no role in explaining the data.

Identification was considered accurate when the ProteinPilot™ *Unused score* (see definition in section 3.6.4) greater than 1.3 was identified with ≥ 95% confidence according to the following equation:

$$\text{ProtScore} = -\log(1 - (\text{percent confidence}/100))$$

The resulting proteins identified in each sample are presented in the *Proteins Detected Table* (see definition in section 3.6.4) with the following information for each of them.

### 3.6.4 Proteomic results interpretation glossary

#### ***Proteins Detected Table***

The Proteins Detected Table lists the winner protein for each group, sorted by *Unused ProtScore*.

#### ***N***

The rank of the specified protein relative to all other proteins in the list of detected proteins.

#### ***Unused (ProtScore)***

The Unused ProtScore reflects the amount of total, unique peptide evidence related to a given protein. It is a measure of the protein confidence for a detected protein, calculated from the peptide confidence for peptides from spectra that are not already completely “used” by higher scoring winning proteins.

#### ***Total (ProtScore)***

A measure of the total amount of peptide evidence related to a detected protein. The Total ProtScore is calculated using all of the peptides detected for the protein. The Total ProtScore does not indicate anything about the confidence that a protein has been detected, because some or even all of the spectra contributing to the Total ProtScore may be better explained by higher ranked proteins.

#### ***% Cov (Coverage)***

The percentage of matching amino acids from identified peptides having confidence greater than 0 divided by the total number of amino acids in the sequence.

#### ***% Cov (60)***

The percentage of matching amino acids from identified peptides having confidence greater than or equal to 60% divided by the total number of amino acids in the sequence.

#### ***% Cov (95)***

The percentage of matching amino acids from identified peptides having confidence greater than or equal to 96% divided by the total number of amino acids in the sequence.

#### ***Accession #***

The accession number for the protein corresponding to the peptide sequence transcript ID code.

#### ***Name***

The name of the protein.

## Species

The species code for this protein. Not all FASTA files have species, so this column may be blank.

## Peptides (95%)

The number of distinct peptides having at least 95% confidence. Multiple modified and cleaved states of the same underlying peptide sequence are considered distinct peptides because they have different molecular formulas (Figure 3.3). Multiple spectra of the same peptide, due to replicate acquisition or different charge states, only count once.

N	Unused	Total	%Cov	%Cov(50)	%Cov(95)	Accession	Name	Species	Peptides(95%)
1	261.11	261.11	73.72999787	71.79999948	65.71000218	TTRE_0000643201-mRNA-1	transcript=TTRE_0000643201-mRNA-1 gene=TTRE_0000643201	0000643201-mRNA-1	470
2	6.04	6.04	10.88000014	9.296999872	7.710000128	TTRE_0000228401-mRNA-1	transcript=TTRE_0000228401-mRNA-1 gene=TTRE_0000228401	0000228401-mRNA-1	4
3	5.21	5.27	14.63000029	14.63000029	14.63000029	TTRE_0000521801-mRNA-1	transcript=TTRE_0000521801-mRNA-1 gene=TTRE_0000521801	0000521801-mRNA-1	4
3	4.24	4.26	20.64000007	18.60000044	11.63000017	TTRE_0000829301-mRNA-1	transcript=TTRE_0000829301-mRNA-1 gene=TTRE_0000829301	0000829301-mRNA-1	3
4	3.05	3.13	3.946999833	3.946999833	3.946999833	TTRE_0000682001-mRNA-1	transcript=TTRE_0000682001-mRNA-1 gene=TTRE_0000682001	0000682001-mRNA-1	2
5	2.17	2.18	40.63000083	23.52000028	13.16000074	TTRE_0000464201-mRNA-1	transcript=TTRE_0000464201-mRNA-1 gene=TTRE_0000464201	0000464201-mRNA-1	1
6	2	2	12.5	7.500000298	7.500000298	TTRE_0000189701-mRNA-1	transcript=TTRE_0000189701-mRNA-1 gene=TTRE_0000189701	0000189701-mRNA-1	1
7	1.68	1.72	1.095999964	1.095999964	1.095999964	TTRE_0000430801-mRNA-1	transcript=TTRE_0000430801-mRNA-1 gene=TTRE_0000430801	0000430801-mRNA-1	1
8	1.46	1.49	4.467000067	4.467000067	4.467000067	TTRE_0000107401-mRNA-1	transcript=TTRE_0000107401-mRNA-1 gene=TTRE_0000107401	0000107401-mRNA-1	1

Figure 3.3 Example of Proteins Detected Table from bioinformatics analysis database.

Because proteins can often share homology (similarity at the sequence level), there are often peptides identified in a database search that point to more than one protein. The Pro Group™ Algorithm works to try to resolve the complexity of reporting identified proteins by selecting only the ones that are truly present. After the peptide identification is complete a Pro Group Algorithm is run to assemble the list of proteins, the *Total ProtScore* of every protein is computed and then ranked. Starting at the top of the list, all the peptide evidence is assigned to the first protein, making the *Unused ProtScore* the same as the *Total ProtScore*. Then each protein down the list is analyzed and when shared peptide evidence is found for a protein that has already been used in a protein higher up the list, the score for that peptide is removed from the lower protein and the *Unused ProtScore* is recalculated. Therefore, the *Unused ProtScore* will be slightly less than the *Total ProtScore* and will reflect only the unique evidence that supports the presence of that protein.

### 3.6.5 Proteomic analysis: Protein identification

Protein identification from the *Proteins Detected table* of results with 95% confidence scores and highest numbers of distinct peptides were considered significant. For the EE complete proteome analysis, all proteins including those with only one distinct peptide were subject to further identification and for the specific immunogenic bands excised, only the top proteins with the highest number of distinct peptides (minimum of two distinct peptides) identified and highest > 95% coverage scores were subsequently analyzed for identification. The process of identification is described in detail below.

#### 3.6.5.1 First analysis: for data base construction

The protein identification for the construction of our own data base was conducted by following three main stages:

1. Entering the resulting peptide sequence transcript ID accession codes (e.g., TTRE\_0000643201-mRNA1) from the *Proteins Detected Table* into the Wormbase Parasite database (version WBPSS14 (WS271) <https://parasite.wormbase.org> accessed 2018 - 2019). This database includes 174 genomes including the *T. trichiura* genome (Foth *et al.*, 2014) produced by the Parasite Genomics group at the Wellcome Trust Sanger Institute in collaboration with Richard Grencis (University of Manchester). Assembly version [TTRE2.1](https://parasite.wormbase.org/Trichuris_trichiura_prjeb535/Info/Index/),  
Bio Project [PRJEB535](https://parasite.wormbase.org/Trichuris_trichiura_prjeb535/Info/Index/)  
([https://parasite.wormbase.org/Trichuris\\_trichiura\\_prjeb535/Info/Index/](https://parasite.wormbase.org/Trichuris_trichiura_prjeb535/Info/Index/)).
2. Recording the assigned UniProt accession code obtained from the Wormbase Parasite database <https://parasite.wormbase.org> accessed 2018 - 2019) (e.g., [A0A077ZE83](https://www.uniprot.org/entry/A0A077ZE83)).
3. Assigning from the UniProt database (<https://www.uniprot.org> accessed 2018-2019) their respective gene ontology (GO) information. The GO version 2018 and 2019 were used, Gene Ontology and GO Annotations are a branch of the European Bioinformatics Institute (EMBL-EBI), Europe's flagship laboratory for the life sciences accessed via embedded data on the UniProt database for each protein. For each protein, we recorded: protein description, molecular weight, signal peptide (if present), Genomic DNA translation

accession number, molecular function, subcellular location, and biological process when known (**Figure 3.4**).

UniProtKB - A0A077ZE83 (A0A077ZE83\_TRITR)

Submitted name: **Vitellogenin N and VWD and DUF1943 domain containing protein**

Gene: **TTRE\_0000643201**

Organism: *Trichuris trichiura* (Whipworm) (*Trichocephalus trichiurus*)

Status: Unreviewed - Annotation score: ●○○○○ - Protein predicted<sup>1</sup>

**Function<sup>1</sup>**

GO - Molecular function<sup>1</sup>

- lipid transporter activity <sup>1</sup> Source: InterPro

Complete GO annotation on QuickGO ...

**PTM / Processing<sup>1</sup>**

Molecule processing

Feature key	Position(s)	Description	Actions	Graphical view	Length
Signal peptide <sup>1</sup>	1 - 19	Sequence analysis <sup>1</sup>	Add BLAST		19
Chain <sup>1</sup> PRO_5001228075	20 - 1709	Sequence analysis <sup>1</sup>	Add BLAST		1690

**Sequence<sup>1</sup>**

Sequence status<sup>1</sup>: Complete.

A0A077ZE83-1 [UniParc] FASTA Add to basket

Show ▶

Length: 1,709  
 Mass (Da): 198,527  
 Last modified: October 29, 2014 - v1  
 Checksum<sup>1</sup>: DAB20E6866122981

BLAST GO

Sequence databases

Select the link destinations: HG806270 Genomic DNA Translation: CDWS8129.1

EMBL<sup>1</sup>

**Figure 3.4** Example of UniProt page accessed per protein for information retrieval during bioinformatic analysis.

<https://www.uniprot.org>

For the specific immunogenic bands of interest, the molecular weight of our Western Blot images (semi-log plot of the molecular weight markers against the distance of the migration of the proteins from gel well origin) were compared to the molecular weight of the proteins identified in the *Proteins Detected Table* obtained from UniProt (see mass (Da)) on the figure example above (**Figure 3.4**). Based on this initial molecular weight comparison, 15 preliminary protein candidates were targeted for further analysis. In the case of the complete EE proteome description, the data base constructed was used and described in: *Trichuris trichiura* egg extract proteome reveals potential diagnostic targets and immunomodulators (Cruz *et al.*, 2021).



### 3.6.5.2 Second Analysis: homology determination in relation to other nematodes

The 15 candidate proteins selected underwent the following three step analysis:

1. For each protein the FASTA sequence format was retrieved using the link embedded in UniProt database (Figure 3.5).

Example:

```
>tr|A0A077ZE83|A0A077ZE83_TRITR Vitellogenin N and VWD and DUF1943 domain
containing protein OS=Trichuris trichiura OX=36087 GN=TTRE_0000643201 PE=4 SV=1

MGLKVVILTLAALYAAAGRHQQRLKLLRDTVNYQNVQESYFRINQYKFKYNGQVKIGV
PDHSNQNSMTRFTAETVTLVKRSEEHFIIRVNNIRLGKQLGNSKQDEMASFEELEPVEIK
QSDLKILELPVEFTYAEGVQVQDLVQDDEEWSENLKRGIINLFQIKLQSTDRTSMEEEQ
SALNRIDTESKTNVGTAYRTREKTVEGECDTMYTVSAIDDDDDNSERGSRLVTKAIDM
KSCQRRPEVWWNFQFISPCPRCHQLPRSGERSVESSTTIRYQIRGKRDKFLIERVELSND
HVIAQQNADESAVVVKIKASLKLVSSESNDGSSEMSNFPATGQQRVSDLIYSTRDDEHFD
RFYAEQDQHYNDRLFRRQKGDKSAALAEIIMKMMRHMKDTADEKANRYFYKAVQLMRY
MSESEIRSTNEHHFGRQQSGMLTPEERERARNIMPNLLAQAGTSSFRQLADKIANGEIN
PLKAAIVITMMMDTPRVSKEIITELMRLDESQTVQRNEQLRRAILLTAGSMMRMTCAPQR
HQRQQRQESQNRDDIRTDNSNHQRCDEIKQRFVRTIADRLAASDRWEDQVILIRALGNA
GLDVSISELESIIIRNQDRRNPAAIRLEAILALRHKIDSLPQKTKNILLSAAAANRMESSAV
RMAAIQMLLQQNPDRMTIDQIGVIINHDPNRRVASFAYKLIRRLADSNQPCYEENKQKQKQ
TVAKSVRRRLQLPHSDMIFESVYDREKKTGFDFIMPMPYDMDDIVPKFMRAGINMVERG
ERNRNLFALEIGTSSLSNIISELLPDIEQNRQGGNTEIKMKLRRMAEETRRNGNRGSRQQ
QQQRQQQRQTKAWMSMKFRNQDIMLLTFNEDRLKQLTQQNRGAESLLLLIAKMASNRQG
SISIDEATLLRETVKIPTAIGSLSIRRKAPAFSAHGQASIGRNIPIQADIRARISTT
ISMVTDVSSRTPISTNGIYLIKNIKATVPVDMTISLDHRQEDELKIQMRNHGKDLLK
LESRPVIIYMRSQNPLAEAEKTVVAEKNVRMESFKRCMRGPLFGSEICMRGVITTPMCN
HNKLLHYMAPWFGPNKVTISAYMRRTEENENENENSRQVGLTIRSDSMQNKLELEYETSS
RSLIPTKVDALQQRQGHGQQRQEICINMKTQGKENDQRSEQTRRSSDININWGTQCNDEN
YIKARIETASRRNVWIEQRQSNAIQEDNEERDQKQIYGVSSEETAGYKIQIHRNVPEW
AVDKAEDIIRMLTSMNYWSTEIENKRQRYDSAERNRQRDEQSRAGEVRIQAIMRNEDKAD
VKIQTPRKTIRMNNVYIPTLLRKETYRRSNFMRLMNLVMGNKHAKGTCCIRQNSITTFDG
AIYRIPFSSCYTILARDEEDPKFAIMARRSREQPKKVVKLMTSDHEIELIPERGGGIE
VKVDGQRWDDQSKHHRAMRIRKRENEVTVDLKRPNVDVHYDGNIEITRVS DKYHGRQTG
MCGNLNADSSDEFKSNQKNRDIWETFNEMTIRTDDCQHPQRQEQQDSDSQQFSDYSDSDS
SNSYDSWEMARQHRSDSISYDDEEESMFSDSQQQQRDDQERNQHYSLAIDVLTET
APVRRNKVIDSRGRKCISMRPIESCPEHGYTARGEKEEKEVPYTKCANDELYHKIGRMQ RQG
TPMDLSNSEMSFTRKETVPRKCISIV
```

Figure 3.5 FASTA sequence format example.

2. Subsequently, each FASTA sequence format was analyzed by protein Basic Local Alignment Search Tool (BLAST) (<https://blast.ncbi.nlm.nih.gov/Blast.cgi>) and the results from each of the 15 selected preliminary protein candidates were recorded. Proteins with E-value of 0 and 100% homology to *T. trichiura* and no other nematodes were flagged for further analysis. Proteins showing > 55% of homology with other nematodes were excluded. An exception was made for *Trichuris suis* given the high percentage of homology between *T. trichiura* and *T. suis* genomes (Liu *et al.*, 2012). Although a few cases of temporary patent

*T. suis* infection have been observed in man (Nejsum *et al.*, 2012) the potential natural cross-transmission is not clear and it has not been studied in *C. sabaeus* (Figure 3.6).

Vitellogenin N and VWD and DUF1943 domain contain ing protein [Trichur - Protein - NCBI] NCBI Blast:Protein Sequence (1709 letters)

Sequences producing significant alignments:

Select: [All](#) [None](#) Selected:0

Alignments [Download](#) [GenPept](#) [Graphics](#) [Distance tree of results](#) [Multiple alignment](#)

Description	Max score	Total score	Query cover	E value	Ident	Access
<input checked="" type="checkbox"/> Vitellogenin N and VWD and DUF1943 domain contain ing protein [Trichuris trichiura]	3559	3559	100%	0.0	100%	CDW58129
<input type="checkbox"/> von Willebrand factor type D domain protein [Trichuris suis]	3055	3055	100%	0.0	87%	KHJ42225.
<input type="checkbox"/> hypothetical protein M513_05347 [Trichuris suis]	3033	3033	100%	0.0	85%	KFD53841.
<input type="checkbox"/> hypothetical protein M514_05347 [Trichuris suis]	3025	3025	100%	0.0	84%	KFD71631.
<input type="checkbox"/> Vitellogenin-5 [Caenorhabditis elegans]	351	351	97%	5e-95	22%	NP_508588
<input type="checkbox"/> Vitellogenin-4 [Caenorhabditis elegans]	350	350	97%	1e-94	22%	NP_508612
<input type="checkbox"/> Vitellogenin-3 [Caenorhabditis elegans]	344	344	97%	8e-93	22%	NP_001294
<input type="checkbox"/> put. vitellogenin [Caenorhabditis elegans]	337	337	97%	2e-90	22%	CAA26849.
<input type="checkbox"/> Vitellogenin-6 [Toxocara canis]	335	464	82%	1e-89	25%	KHN77828.
<input type="checkbox"/> hypothetical protein PRIPAC_54065 [Pristionchus pacificus]	327	420	81%	6e-87	25%	PDM60240
<input type="checkbox"/> hypothetical protein PRIPAC_43917 [Pristionchus pacificus]	325	445	81%	1e-86	25%	PDM70712
<input type="checkbox"/> hypothetical protein PRIPAC_45330 [Pristionchus pacificus]	324	423	77%	5e-86	25%	PDM66105
<input type="checkbox"/> vit-6 [Pristionchus pacificus]	323	432	81%	1e-85	25%	PDM70654
<input type="checkbox"/> hypothetical protein WR25_19855 [Diploscaptor pachys]	322	421	79%	2e-85	24%	PAV85180.
<input type="checkbox"/> hypothetical protein PRIPAC_45281 [Pristionchus pacificus]	318	368	71%	2e-84	24%	PDM66056
<input type="checkbox"/> lipoprotein amino terminal region [Oesophagostomum dentatum]	311	311	59%	5e-84	25%	KHJ98709.
<input type="checkbox"/> hypothetical protein PRIPAC_53880 [Pristionchus pacificus]	317	420	81%	8e-84	24%	PDM63523
<input type="checkbox"/> RecName: Full=Vitellogenin-6; Short=OTI-VIT-6; Contains: RecName: Full=VT3; Contains: RecName: Full=VT2; Flags: Precursor	310	408	78%	6e-82	24%	Q94637.2

Figure 3.6 Example of protein (VNVD) FASTA sequence format analysis by protein BLAST.

- For each of the 15 preliminary protein candidates we also recorded the GenBank data from the NCBI <https://blast.ncbi.nlm.nih.gov> accessed 2018-2019 (Figure 3.7).

**Vitellogenin N and VWD and DUF1943 domain containing protein [Trichuris trichiura]**  
 GenBank: CDW58129.1  
[Identical Proteins](#) [FASTA](#) [Graphics](#)  
 Go to:  
 LOCUS CDW58129 1709 aa linear INV 23-JUL-2014  
 DEFINITION Vitellogenin N and VWD and DUF1943 domain containing protein [Trichuris trichiura].  
 ACCESSION CDW58129  
 VERSION CDW58129.1  
 DBLINK BioProject: [PRJEB535](#)  
 DBSOURCE embl accession [HG806270.1](#)  
 KEYWORDS.  
 SOURCE Trichuris trichiura (human whipworm)  
 ORGANISM [Trichuris trichiura](#)  
 Eukaryota; Metazoa; Ecdysozoa; Nematoda; Enoplea; Dorylaimia; Trichinellida; Trichuridae; Trichuris.  
 REFERENCE 1  
 AUTHORS Foth,B.J., Tsai,I.J., Reid,A.J., Bancroft,A.J., Nichol,S.,Tracey,A., Holroyd,N., Cotton,J.A., Stanley,E.J., Zarowiecki,M., Liu,J.Z., Huckvale,T., Cooper,P.J., Grecis,R.K. and Berriman,M.  
 TITLE The whipworm genome and dual-species transcriptomics of an intimate host-pathogen interaction  
 JOURNAL Nature Genetics  
 REFERENCE 2 (residues 1 to 1709)  
 AUTHORS Aslett,M.  
 TITLE Direct Submission  
 JOURNAL Submitted (23-JAN-2014) Pathogen Sequencing Unit, Wellcome Trust, Sanger Institute, Wellcome Trust Genome Campus, Hinxton,CambridgeCambridgeshire. CB10 1SA, UNITED KINGDOM

Figure 3.7 Example of the GenBank data from the National Center for Biotechnology Information database (NCBI).

<https://blast.ncbi.nlm.nih.gov>

### 3.6.5.3 Third analysis: Study of immunogenic potential of each protein and its peptides.

Two step analyses for each of the 15 preliminary protein candidates:

1. We assessed the immunogenic potential of each protein FASTA sequence with the purpose of determining which parts of the protein are more immunogenic and from those peptide sequences which specific peptide sections can act as linear epitopes for B lymphocytes. This analysis could mean that the specific sections selected could activate B lymphocytes to produce antibodies and therefore highlight the potential use for antibody diagnostics. For this analysis we used a B Cell epitope prediction database <https://www.iedb.org> accessed 2018 and 2019 and selected only the peptide sequences with more than 25 amino acids (**Figure 3.8**).

### Vitellogenin N and VWD and DUF1943 domain containing protein [*Trichuris trichiura*]

No.	Start	End	Peptide	Length
43	1340	1365	LLRKETYRRSNFMRLMNLNMGKNHAK	26
1	21	47	HQQRLLKLRDVTNYYQNVQESYFRINQK	27
17	539	567	QRHQRRQQRQESQNRDDIRTDNSNHQRCDS	29
32	1031	1062	RSQNPLAEAEKKTVAEKNVRMESFKRCMRGP	32
3	94	127	RLGKQLGNSKDQDEMASFEELPVEIKQSDLKIL	34
6	167	200	KLQSTDRTSMEEEQSALNRIDTESKTVNGTAYRT	34
51	1668	1701	ANDELYHKIGRMQRQGTMPDLNSNEMSFTRKETV	34
38	1211	1245	RRNVIWEQRQSNAIQEDNEERDQKQIGYVSSEET	35
8	239	276	DMKSCQRRPEVWVNFQFISPCPRCHQLPRSGERSVESS	38
34	1104	1146	RRTEENENENENSRQVGLTIRSDSMQNKLELEYTSSRSLIPT	43
27	806	851	DIEQNQRGGNTEIKMKLRRMAEETRRNGNRGSRQQQQRQQQRQT	46
10	325	385	SSQESNDGSSEMSNFPATGQRVSDLIYSTRDDEHDFRYAEGDQHYNDRLFSRRQKGGQDKS	61
50	1535	1660	TDDCQHPQRQEQQDSDSQFDSYSDSDSNYSYDSEWEMARQHRSDDSISYDDEEESMFDSQDQQQRRDQERNQHYRSLAIDDLVTETAPVRRNKVIDSRGRKCISMRPIE SCEPHGYTARGEKEEKE	126

Figure 3.8 Example of predicted B cell epitope results from the B cell epitope prediction data base.

<https://www.iedb.org>

- We did a secondary BLAST analysis to each B cell epitope predicted peptide sequences selected from each of the 15 potential candidate proteins. We recorded the E-value and the percentage of homology with *T. trichiura* and with other nematodes for each peptide sequence. Peptides sequences with E-value < 10e and 100% homology with *T. trichiura* and no other nematode except for *T. suis* as explained in the second analysis, were included for further analysis (**Figure 3.9**).

No.	Start	End	Peptide	Length
50	1535	1660	TDDCQHPQRQEQQDSDSQFDSYSDSDSNYSYDSEWEMARQHRSDDSISYDDEEESMFDSQDQQQRRDQERNQHYRSLAIDDLVTETAPVRRNKVIDSRGRKCISMRPIESCEPHGYTARGEKEEKE	126

Sequences producing significant alignments:

Select: All None Selected:0

Alignments Download GenPept Graphics Distance tree of results Multiple alignment

Description	Max score	Total score	Query cover	E value	Ident	Accession
<input type="checkbox"/> Vitellogenin N and VWD and DUF1943 domain contain ing protein [Trichuris trichiura]	420	449	100%	2e-127	100%	CDW58129.1
<input type="checkbox"/> von Willebrand factor type D domain protein [Trichuris suis]	349	349	100%	5e-103	87%	KHJ42225.1
<input type="checkbox"/> hypothetical protein M513_05347 [Trichuris suis]	349	349	100%	5e-103	87%	KFD53841.1
<input type="checkbox"/> hypothetical protein M514_05347 [Trichuris suis]	349	349	100%	5e-103	87%	KFD71631.1
<input type="checkbox"/> uncharacterized protein LOC111711963 [Eurytemora affinis]	51.1	93.3	47%	0.002	42%	XP_023342221.1
<input type="checkbox"/> tetratricopeptide repeat protein [Rhodohalobacter barkolensis]	50.3	50.3	51%	0.003	38%	WP_101073064.1
<input type="checkbox"/> hypothetical protein [Nocardiosis dassonvillei]	49.4	49.4	40%	0.006	40%	WP_094801679.1
<input type="checkbox"/> hypothetical protein [Nocardiosis dassonvillei]	48.6	48.6	39%	0.011	40%	WP_013152261.1
<input type="checkbox"/> hypothetical protein, partial [Nocardiosis sp. CNS-639]	48.6	48.6	39%	0.011	40%	WP_036553146.1
<input type="checkbox"/> FAD-dependent monooxygenase, putative [Eimeria mitis]	48.1	74.2	54%	0.014	38%	XP_013355644.1
<input type="checkbox"/> hypothetical protein AC631_01793 [Debaryomyces fabryi]	47.3	77.2	36%	0.023	51%	XP_015468526.1
<input type="checkbox"/> lin1 family protein [Stemphylium lycopersici]	47.3	47.3	39%	0.024	38%	KNG48368.1
<input type="checkbox"/> hypothetical protein [bacterium 2013Arg42]	46.9	46.9	39%	0.033	49%	WP_092490676.1
<input type="checkbox"/> PREDICTED: muscleblind-like protein 1 isoform X8 [Drosophila kikkawai]	46.9	46.9	54%	0.034	35%	XP_017027134.1
<input type="checkbox"/> PREDICTED: myb-like protein Q isoform X7 [Drosophila kikkawai]	46.9	46.9	54%	0.034	35%	XP_017027133.1
<input type="checkbox"/> PREDICTED: myb-like protein Q isoform X6 [Drosophila kikkawai]	46.9	46.9	54%	0.034	35%	XP_017027132.1
<input type="checkbox"/> hypothetical protein PTSG_07134 [Salpingoeca rosetta]	46.9	46.9	53%	0.035	33%	XP_004992551.1
<input type="checkbox"/> hypothetical protein cubi_01695 [Cryptosporidium ubiquitum]	46.4	88.2	33%	0.044	42%	OII72745.1
<input type="checkbox"/> hypothetical protein IMG5_181440 [Ichthyophthirius multifiliis]	46.0	46.0	26%	0.056	48%	XP_004027560.1
<input type="checkbox"/> putative uncharacterized protein [Blautia sp. CAG-237]	46.0	46.0	28%	0.058	100%	CDP36688.1
<input type="checkbox"/> Midasin [Wickerhamomyces ciferri]	46.0	46.0	38%	0.058	100%	CDP36688.1

Questions/comment

Figure 3.9 Example of secondary BLAST analysis of 1 out of 13 peptide sequences identified for the VNVD protein.

### 3.6.5.4 Fourth analysis: Study of immunogenic potential of each selected peptide

1. For each selected peptide from each of the 15 potential candidate proteins.

We analyzed their individual antigenic sites using <http://www.bioinformatics.nl/cgi-bin/emboss/antigenic> accessed 2018 -2019. Resulting Peptide sections with 15 to 20

amino acids in length and 1.1 antigenicity score were included for further analysis (**Figure 3.10**).

```
OUTPUT FILE outfile
#####
# Program: antigenic
# Rundate: Thu 2 Apr 2020 23:07:16
# Commandline: antigenic
# -auto
# -sequence /var/lib/emboss-explorer/output/613540/.sequence
# -minlen 6
# -outfile outfile
# -rformat2 motif
# Report_format: motif
# Report_file: outfile
#####

#=====
#
# Sequence:      from: 1   to: 125
# HitCount: 4
#=====

Max_score_pos at "*"

(1) Score 1.119 length 19 at residues 74->92
      *
Sequence: YRSLAIDDLTETAPVRRN
          |                   |
          74                 92
Max_score_pos: 80

(2) Score 1.071 length 6 at residues 4->9
      *
Sequence: CQHPQR
          |   |
          4   9
Max_score_pos: 7

(3) Score 1.070 length 7 at residues 100->106
      *
Sequence: RKCISMR
          |   |
          100 106
Max_score_pos: 105

(4) Score 1.068 length 8 at residues 108->115
      *
Sequence: IESCPHEG
          |   |
          108 115
Max_score_pos: 113

#-----
#-----
```

Figure 3.10 Example of the antigenic analysis results obtained from the selected peptide sequences.

2. The hydrophobicity of each selected peptide section was analyzed using the Parker Hydrophilicity Prediction tool <http://tools.iedb.org/bcell/> (Parker *et al.*, 1986), the cutoff was established at 1.4 (**Figure 3.11**).

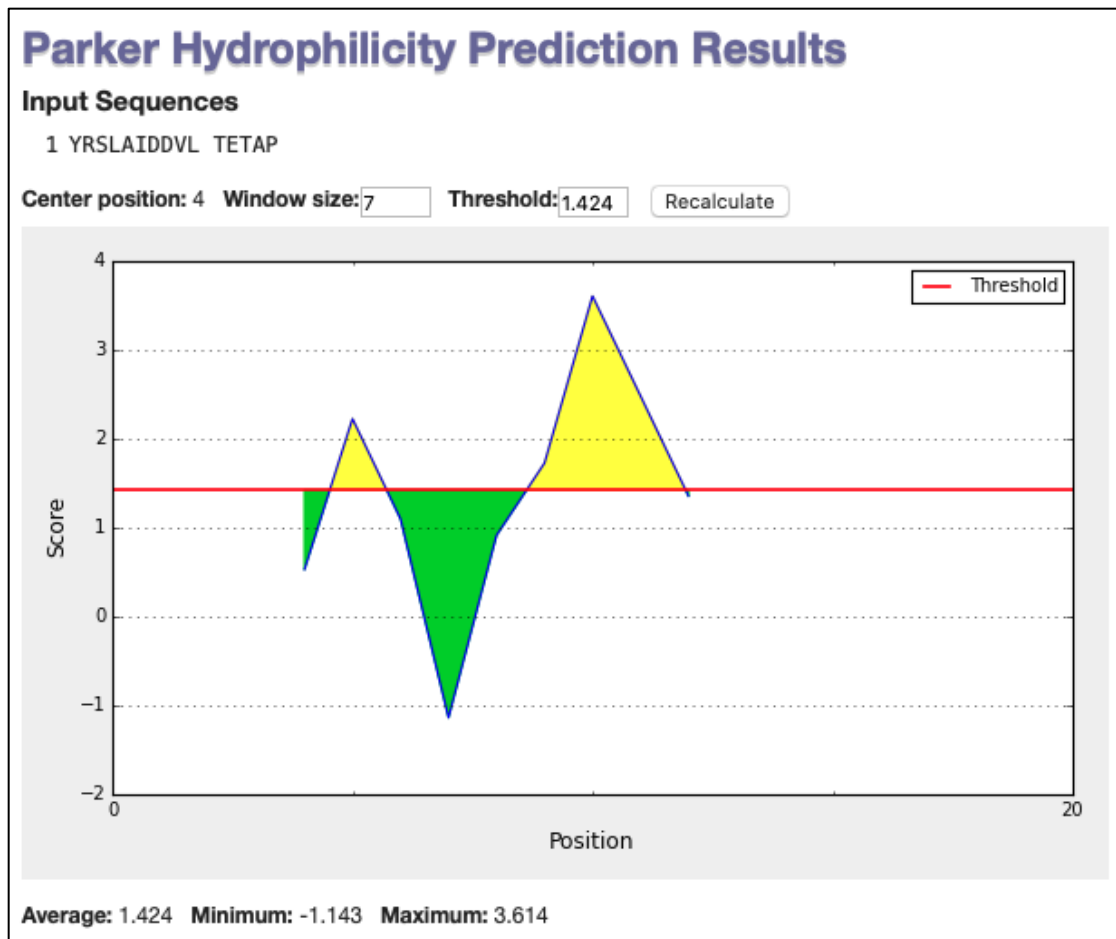


Figure 3.11 Example of Parker Hydrophilicity prediction result for the peptide YRSLAIDVLTETAP.

- The antigenicity score of each selected peptide section was confirmed by using the Kolaskar and Tongaonkar antigenicity scale prediction tool <http://tools.iedb.org/bcell/> (Kolaskar and Tongaonkar, 1990) (**Figure 3.12**).

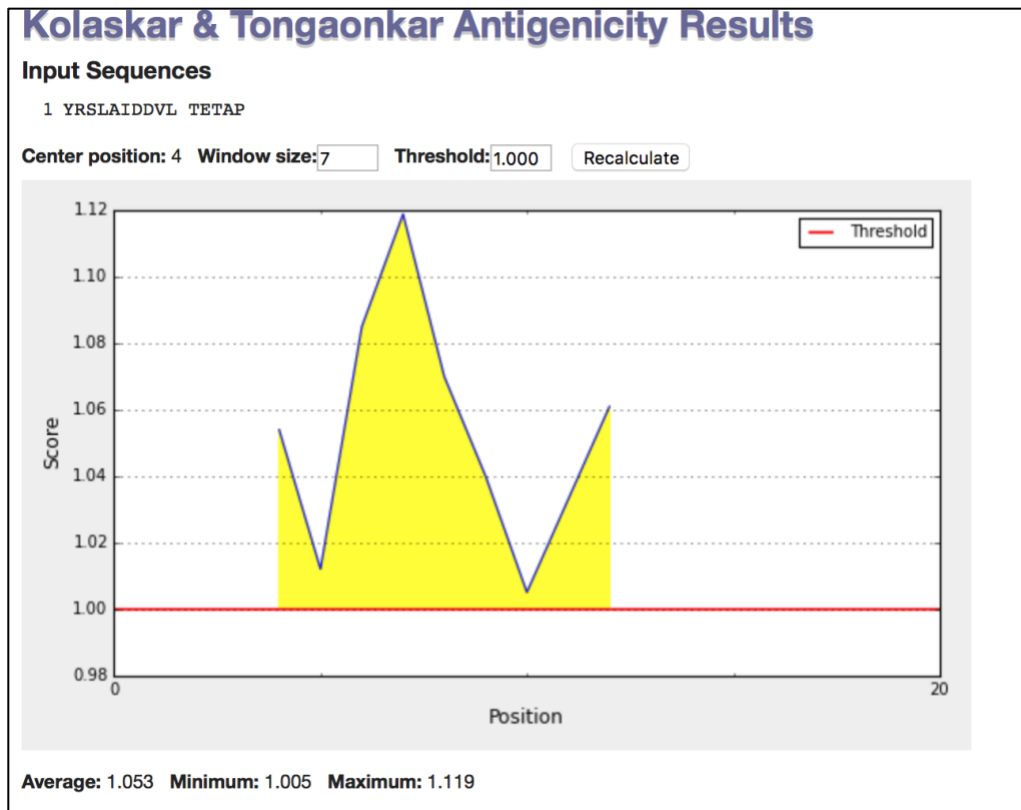


Figure 3.12 Example of Kolaskar & Tongaonkar antigenicity scale prediction tool result for the peptide YRSLADDVLTETAP.

#### 3.6.5.5 Fifth analysis: Final BLAST analysis of the individual peptide sections selected from the 15 preliminary protein candidates.

A final step included a BLAST analysis on the final peptide section candidates selected from all previous steps to confirm the specificity of their homology to *T. trichiura* and confirm that the cutoff values established initially were still valid (Figure 3.13).



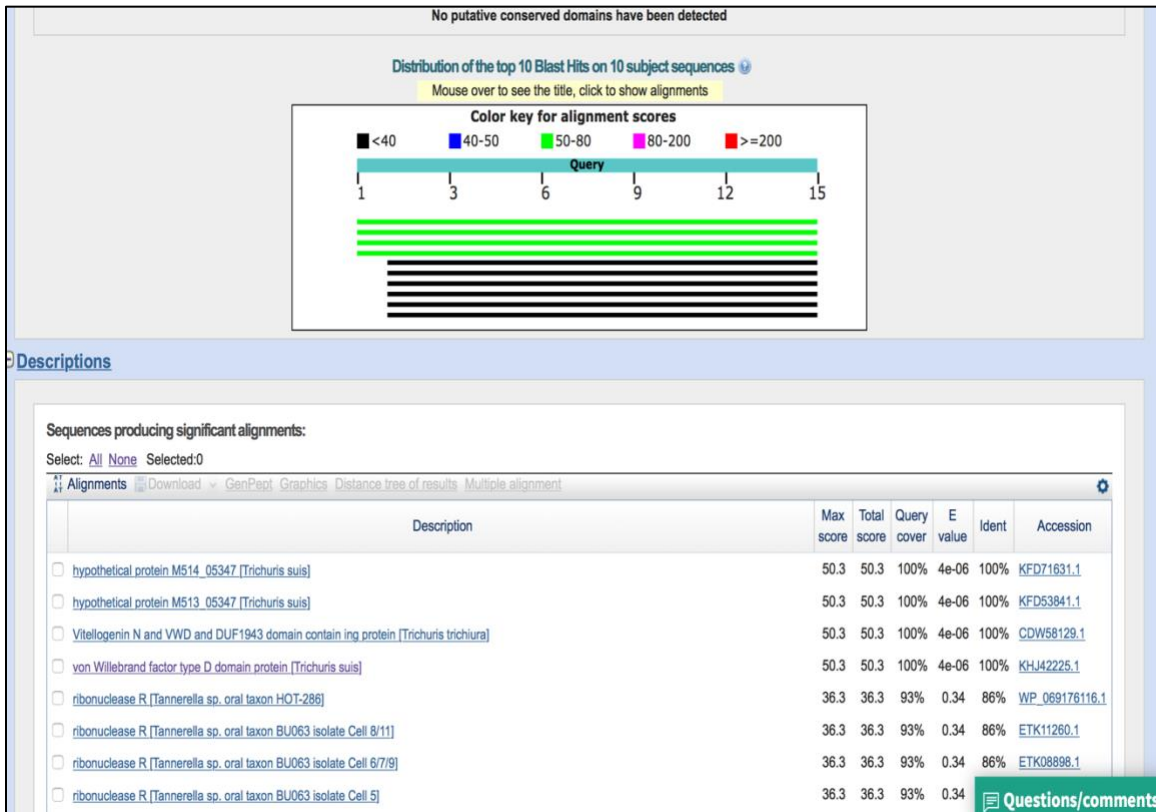


Figure 3.13 Example of final blast analysis for the peptide YRSLAIDDLVLTETAP.

The peptide sections that meet the above five bioinformatic comprehensive analysis were selected as final peptide candidates.

### 3.7 Design and evaluation of *T. trichiura* derived synthetic peptides for diagnosis

#### 3.7.1 Selection and design of final peptide candidates for ELISA

A total of four synthetic peptides were designed based on the amino acid sequences deduced from the candidate proteins present in the AE and EE, and that were potentially recognized by saliva and serum antibodies from *C. sabaesus* naturally infected with *T. trichiura*.

Peptides were synthesized by CellTein LLC DBA LifeTein LLC, Somerset, NJ (<https://www.lifetein.com>). The manufacturer quantified the purity and identity of the peptides using High-Performance Liquid Chromatography (HPLC) confirmed by mass spectrometry. The peptides were supplied as a lyophilized product. Each peptide was dissolved in a suitable solvent

(following the manufacturer's instructions) (Table 3.2) at a final concentration of 2.25 mg/mL and stored in 200  $\mu$ L aliquots at  $-80^{\circ}$  C.

### 3.7.2 Synthetic peptides

The final candidate proteins from which the peptides were designed were: Vitellogenin N and VWD and DUF1943 domain containing protein, CBM 14 domain containing protein, Kunitz BPTI domain containing protein, Poly-cysteine and histidine tailed protein isoform 2.

**Table 3.2 Final candidate proteins and respective peptide selection.**

Peptide	Solvent	Protein	Amino acid sequence	amino acid length
1	PBS	Vitellogenin N and VWD and DUF1943	YRSLAIDDVLTETAP	15
2	PBS	CBM 14	SAPTTVTTQLSPVDCVTL	18
3	Distilled water	Kunitz BPTI	QERCVATLPASVICRLP	17
4	Isopropanol and distilled water.	Poly-cysteine and histidine tailed protein isoform 2	TECVKPPAHDCPAFG	15

### 3.7.3 Indirect ELISA for testing the applicability of designed peptides

Microtiter plates (96 well; MAXISORP, NUNC-IMMUNO plates, Thermo Fisher Scientific) were coated with 10  $\mu$ g of each designed synthetic peptide diluted in 0.05 M  $\text{Na}_2\text{CO}_3$ ,  $\text{NaHCO}_3$ , pH 9.5-9.6 coating buffer in a final volume of 100  $\mu$ L per well to evaluate the applicability of the in-house ELISA as described in section 3.5.1.

## 4 RESULTS

### 4.1 Efficacy of treatment analysis and egg to worm correlation in captive *C. sabaesus*

Although AGMs are found widely in Africa there is little data on their internal parasites in their natural habitats (Blersch *et al.*, 2019) and also in captivity in other regions: Barbados (Mutani *et al.*, 2003), Korea (Lee *et al.*, 2010), China (Li *et al.*, 2015) and Brazil (Barbosa *et al.*, 2020). We found a high prevalence of *T. trichiura* (15/26; 56%), strongylids (13/26; 50%) and *Strongyloides* spp. (3/26; 12%) (Figure 4.1 and

Table 4.1), which is similar to the situations reported elsewhere.

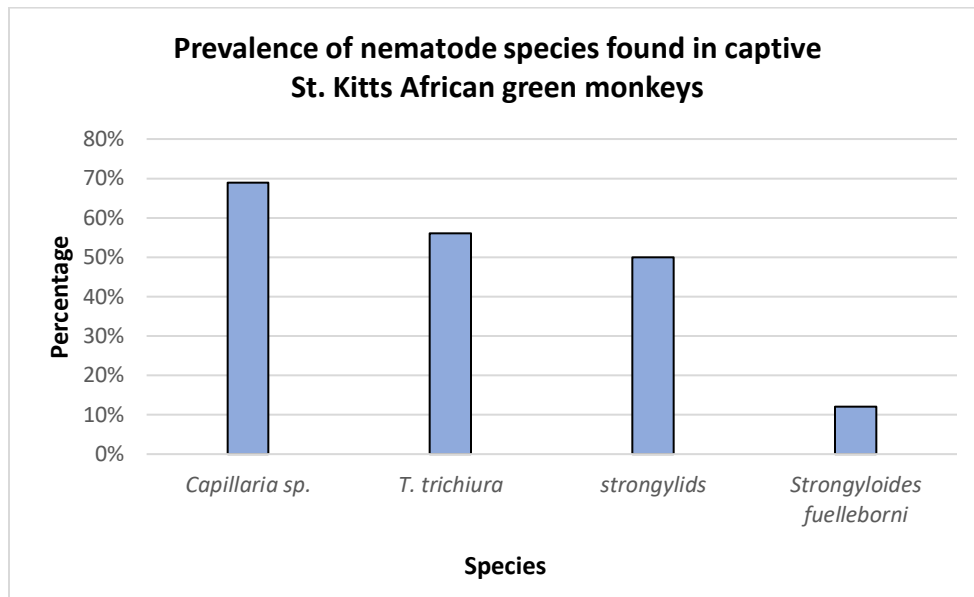


Figure 4.1 Prevalence of nematode species found in captive St. Kitts African green monkeys.

Our finding that *Capillaria* sp. were the most prevalent (18/26; 69%) is of note as the eggs of this genus have not previously been reported in feces of AGMs.

Table 4.1 Outcome of the praziquantel and albendazole treatment regimen (PRAL) on fecal eggs identified 2 to 24 months later and visual identification of adult *Trichuris trichiura* in the large intestine at necropsy.

Animal number	Months post initial PRAL treatment	<i>Capillaria</i> sp.	<i>T. trichiura</i>	strongylids	<i>S. fuelleborni</i>	<i>T. trichiura</i> observed in the large intestine at necropsy
1	2	-	+	+	-	NA
2	2	+	+	+	+	NA
3	2	+	-	-	-	NA
4	2	-	+	+	-	NA
5	2	+	+	-	-	NA
6	2	+	+	+	-	NA
7	2	+	-	+	-	NA
8	2	-	-	-	-	NA
9	2	+	+	+	-	NA
10	2	+	+	+	-	NA
11	2	+	-	-	-	NA
12	2	-	-	-	-	-
13	4	+	-	-	-	+
14	4	-	+	-	+	+
15	4	+	+	+	-	+
16	4	+	+	-	-	+
17	4	-	-	+	-	-
18	5	+	+	+	-	+
19	5	-	-	-	-	-
20	10	-	+	-	-	+
21	12	+	-	-	+	-
22	15	+	-	+	-	-
23	15	+	+	-	-	+
24	15	+	+	+	-	+
25	22	+	-	-	-	-
26	24	+	+	+	-	+
Totals		18/26	15/26	13/26	3/26	
Prevalence		69%	56%	50%	12%	

The efficacy of the PRAL treatment was limited. Only two (2/12; 17%) monkeys that received the traditional PRAL treatment were negative for nematode eggs in FECs performed two months later (Table 4.1). Four to five months post-treatment, only 1 (14%) of the seven animals studied was free of nematode eggs, while none (0/7) of the monkeys studied 10 to 24 months post initial treatment were free of eggs despite PRAL dosing for ongoing control every 3 - 5 months and prior to necropsy (Table 4.1). No difference was observed in animals that spent time in social enclosures. While *T. trichiura* were not found in the large intestines of the one animal necropsied at 2 months post-treatment, nine of the 14 (64%) monkeys necropsied at 4 to 24 months post initial treatment were infected, four of these as soon as 4 months post-treatment (Table 4.1). It is of note that of the nine monkeys that had adult *T. trichiura* in the large intestine, one was negative for eggs by FEC (animal 13). This appeared to be due to a single-sex infection as only two female *T. trichiura* were found in the large intestine of this monkey.

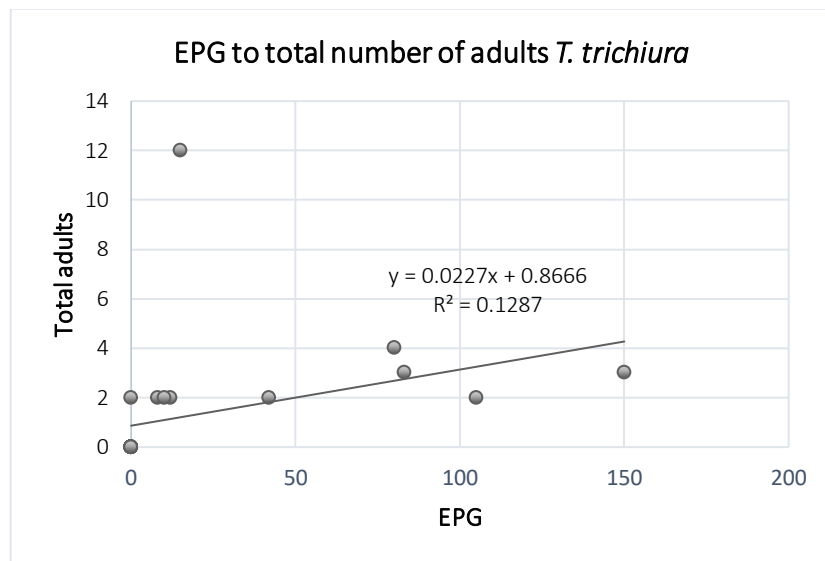


Figure 4.2 Lack of correlation between eggs per gram of feces (EPG) and total adult *T. trichiura* counts from the 26 *C. sabaeus*.

There was no correlation observed when *T. trichiura* FEC were compared with total numbers of adults ( $R^2 = 0.1287$ ) (Figure 4.2) or numbers of adult females ( $R^2=0.354$ ) (Figure 4.3). This finding provides further evidence that FECs can vary considerably and that an absence of eggs in feces is not reliable evidence of an absence of infection.

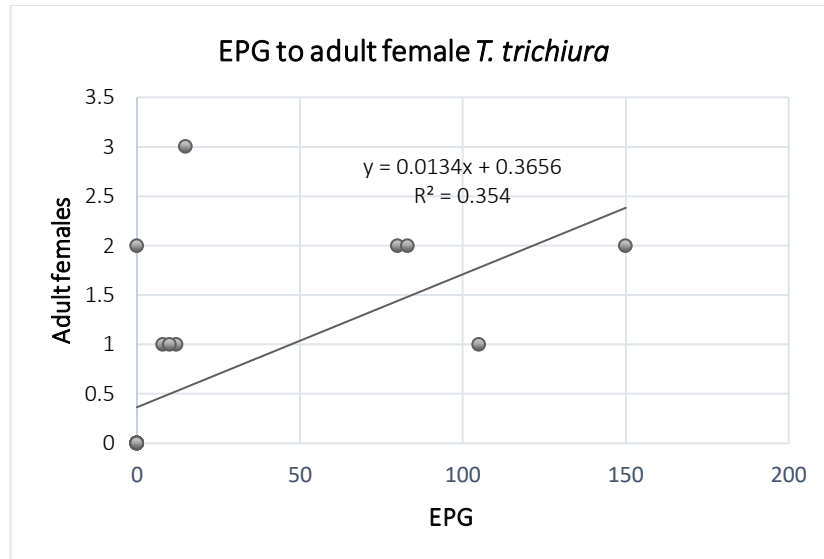


Figure 4.3 Lack of correlation between eggs per gram of feces (EPG) and total female *T. trichiura* counts from the 26 *C. sabaeus*.

Overall, the IVAL treatment regimen together with the husbandry measures in place in our study were relatively successful at controlling nematode infections in captive AGMs. Following a single IVAL treatment, 60% (6/10) of the infected AGMs were negative for nematodes 6 to 8 months later as confirmed by FEC and at necropsy (Table 4.2 A). A second IVAL treatment given to the 4 AGMs with persistent *T. trichiura* infections 3 months after the first treatment, resulted in the elimination of the *T. trichiura*, 3 to 5 months later as evidenced by negative FECs and necropsy findings (Table 4.2 B). Although apparently cleared of *Capillaria* sp. following the first IVAL treatment, three of these four AGMs had *Capillaria* sp. eggs in their feces at necropsy 3 to 5 months after a second treatment.

Table 4.2 Fecal egg count (FEC) results and adult *Trichuris trichiura* found at necropsy in animals treated with ivermectin and albendazole (IVAL).

A. Animals negative by FEC 3 months after treatment with IVAL were not treated again.

Animal number	Pretreatment FEC				FEC 3 months after one IVAL treatment				FEC 6 to 8 months after one IVAL treatment				<i>T. trichiura</i> at necropsy 6 to 8 months after one IVAL
	<i>Capillaria</i>	<i>T. trichiura</i>	strongylids	<i>S. fuelleborni</i>	<i>Capillaria</i>	<i>T. trichiura</i>	strongylids	<i>S. fuelleborni</i>	<i>Capillaria</i>	<i>T. trichiura</i>	strongylids	<i>S. fuelleborni</i>	
1	-	+	+	-	-	-	-	-	-	-	-	-	-
4	-	+	+	-	-	-	-	-	-	-	-	-	-
6	+	+	+	-	-	-	-	-	-	-	-	-	-
7	+	-	+	-	-	-	-	-	-	+	-	-	+
8	-	-	-	-	-	-	-	-	-	-	-	-	-
10	+	+	+	-	-	-	-	-	-	-	-	-	-
11	+	-	-	-	-	-	-	-	-	-	-	-	-

B. Animals positive by FEC 3 months after treatment with IVAL were treated again with IVAL

Animal number	Pretreatment FEC				FEC 3 months after first IVAL treatment				FEC 3 months after second IVAL treatment				<i>T. trichiura</i> at necropsy 3 months after second IVAL
	<i>Capillaria</i>	<i>T. trichiura</i>	strongylids	<i>S. fuelleborni</i>	<i>Capillaria</i>	<i>T. trichiura</i>	strongylids	<i>S. fuelleborni</i>	<i>Capillaria</i>	<i>T. trichiura</i>	strongylids	<i>S. fuelleborni</i>	
2	+	+	+	+	-	+	-	-	+	-	-	-	-
3	+	-	-	-	-	+	-	-	-	-	-	-	-
5	+	+	-	-	-	+	-	-	+	-	-	-	-
9	+	+	+	-	-	+	-	-	+	-	-	-	-
<b>TOTAL</b>	8/11 (73%)	7/11 (64%)	7/11 (64%)	1/11 (9%)									

## 4.2 *Trichuris trichiura* egg extract proteome reveals potential diagnostic target and immunomodulators

Our results are the first report of the proteome of soluble egg extracts of *T. trichiura* from AGMs (*C. sabaesus*) and describe the potential immunomodulators and antigens recognized by sera and saliva of naturally infected animals.

### 4.2.1 Proteomic characterization of the *T. trichiura* egg extract (EE)

With the spectrometric data obtained using ProteinPilot™ software v4.5 we identified 246 proteins. The unique peptide sequence transcript identification code obtained from the spectrometric data and their respective accession number from WormBase (<https://parasite.wormbase.org>) enabled us to characterize 231 of the 246 proteins found: 212 had significant homologies with known *T. trichiura* adult stage proteins and 19 were novel uncharacterized proteins with unknown ontology.

### 4.2.2 Gene ontology (GO)

When the proteins were categorized according to their molecular function described in the Gene Ontology (GO) database (UNIPROT; <https://www.uniprot.org>), 168 were found to have known functions. The different functional groups and biological processes of the most representative proteins of our analysis (with 10 or more distinct peptides) are shown in **Table 4.3** and **Figure 4.4**. Only a single annotation was assigned to a given protein. Functional annotation of the identified proteins was assigned using GO, which revealed functionally diverse molecules of the common protein families or groups: energy and metabolism; cytoskeleton, motility, and muscle; proteolysis; signaling; stress and detoxification; transcription and translation; and lipid binding and transport (**Table 4.3**). Their specific molecular functions range from molecules involved in ATP, actin, carbohydrate, chitin, lipid, and magnesium ion binding, as well as molecules that take part in oxidoreductase, aminopeptidase, glycogen phosphorylase and metallopeptidase activity (**Table 4.3**). Others include lipid transporter, motor, and protein disulfide isomerase



activity, together with structural constituents of the ribosome or proteins associated with the elongation phase of protein synthesis. Proteins with kinase and intracellular cholesterol transport functions were also identified (**Table 4.3**).

Table 4.3 Main proteins identified in the EE proteome (10 or more distinct peptides) organized by functional annotation.

Only a single annotation was assigned to a given protein.

Functional annotation	Molecular function**	Acc. No. Wormbase	% Cov.	Peptides* (95%)	MW (kDa)	Signal peptide	Biological process**
<b>Energy and metabolism</b>							
Alpha-1,4 glucan phosphorylase	Glycogen phosphorylase activity	A0A077YWK8	20.29	14	101.447	-	carbohydrate metabolic process
ECH domain containing protein	Catalytic activity	A0A077Z1N9	44.83	17	31.202	-	metabolic process
Enolase	Magnesium ion binding	A0A077YX57	44.49	27	49.513	-	glycolytic process
Glyceraldehyde-3-phosphate dehydrogenase	Oxidoreductase	A0A077ZHV3	56.10	66	37.536	-	glycolytic process
Malic enzyme	Oxidoreductase	A0A077Z5U2	28.04	13	62.847	-	Unknown
Phosphoenolpyruvate carboxykinase GTP	Kinase	A0A077Z7M0	29.04	20	70.975	-	gluconeogenesis
Triosephosphate isomerase	Isomerase	A0A077ZC84	57.26	10	27.399	-	gluconeogenesis
<b>Cytoskeleton, motility, and muscle</b>							
Actin	ATP binding	A0A077ZE37	55.59	35	41.838	-	unknown
Actin 5C	ATP binding	A0A077YWW9	53.66	29	41.036	-	unknown
Epididymal secretory protein E1	Intracellular cholesterol transport	A0A077Z0I4	43.44	28	45.783	1 to 23	unknown
Intermediate filament protein IFA 1	Unknown function	A0A077Z6U0	23.39	14	70.711	-	unknown
Moesin-ezrin-radixin 1	Actin binding	A0A077ZIT0	25.97	12	55.989	-	unknown
Paramyosin	Motor activity	A0A077Z8E1	38.61	30	101.488	-	unknown
Tropomyosin	Unknown function	A0A077ZIM1	41.20	38	87.298	-	unknown
<b>Proteolysis</b>							
Cytosol aminopeptidase	Aminopeptidase activity	A0A077Z3I7	23.80	10	54.409	-	unknown
Peptidase M13 and Peptidase M13 N domain containing protein	Metalloendopeptidase activity	A0A077ZJE5	24.05	14	81.361	-	unknown
<b>Signaling</b>							
78 kDa glucose regulated protein	ATP binding	A0A077Z8G8	22.58	12	72.784	1 to 18	unknown
CBM 14 domain containing protein	Chitin binding	A0A077Z111	46.72	38	95.908	-	chitin metabolic function
CBM 14 domain containing protein	Chitin binding	A0A077Z8B3	28.37	18	78.597	-	chitin metabolic process
Galectin	Carbohydrate binding	A0A077YZM7	50.72	27	31.967	-	unknown
Galectin	Carbohydrate binding	A0A077ZG03	39.64	25	32.25	-	unknown

---

**Stress and detoxification**

Chaperonin protein heat shock protein 60	ATP binding	A0A077ZIE8	28.00	11	62.806	-	protein folding
Heat shock protein 70	L-malate dehydrogenase activity	A0A077Z8E4	20.07	21	130.299	-	stress response
Heat shock protein 90	ATP binding	A0A077Z1F6	17.08	12	82.924	-	protein folding
Protein disulfide-isomerase	Protein disulfide isomerase activity	A0A077ZJZ3	35.03	14	55.125	1 to 18	cell redox homeostasis
Protein disulfide-isomerase	Protein disulfide isomerase activity	A0A077ZLF1	35.95	15	55.73	1 to 16	cell redox homeostasis
Superoxide dismutase [Cu-Zn]	Oxidoreductase	A0A077Z345	69.86	12	15.274	-	unknown

**Transcription and Translation**

40S ribosomal protein SA	Structural constituent of ribosome	A0A077YZD4	42.57	13	34.141	-	ribosomal small subunit assembly, translation
Elongation factor 1-alpha	Elongation factor	A0A077YYL7	33.48	12	51.086	-	protein biosynthesis
Mediator of RNA polymerase II transcription subunit 22	Protein disulfide isomerase activity	A0A077Z2H0	69.06	17	15.485	1 to 19	cell redox homeostasis
Ribosomal L18p and L18 c domain containing protein	Structural constituent of ribosome	A0A077ZPB6	42.67	13	35.744	-	translation

**Lipid binding and transport**

Vitellogenin N and VWD and DUF1943 domain containing protein	Lipid transporter activity	A0A077ZE83	56.35	205	198.527	1 to 19	unknown
Uncharacterized protein	Lipid binding	A0A077ZMT5	14.14	20	84.314	-	unknown

**Others**

DUF290 domain containing protein	Unknown function	A0A077Z8H2	43.67	20	17.876	1 to 19	Unknown
Poly-cysteine and histidine tailed protein isoform 2	Unknown function	A0A077Z5Q5	50.79	109	50.494	-	Unknown
Protein asteroid	Unknown function	A0A077Z2C7	63.64	34	30.674	1 to 23	Unknown
Transthyretin-like protein 46	Unknown function	A0A077Z9N4	42.57	12	16.458	1 to 18	Unknown
Uncharacterized protein	Unknown function	A0A077YXT2	16.08	10	69.581	1 to 18	unknown
Uncharacterized protein	Unknown function	A0A077YX18	20.42	10	32.73	1 to 18	unknown
Uncharacterized protein	Unknown function	A0A077Z544	48.83	19	33.553	1 to 23	unknown

\*The number of distinct peptides having at least 95% confidence.

\*\*Molecular function and biological process was obtained from the Gene Ontology (GO) database <https://www.uniprot.org>.

The most abundant category for the biological process assigned to the egg proteins were protein folding, translation, gluconeogenesis, and glycolytic process all equally represented (13%), followed by cell redox homeostasis (12%), chitin metabolic function (12%), and to a lesser extent metabolic processes, carbohydrate metabolic processes, protein biosynthesis and stress responses (Figure 4.4).

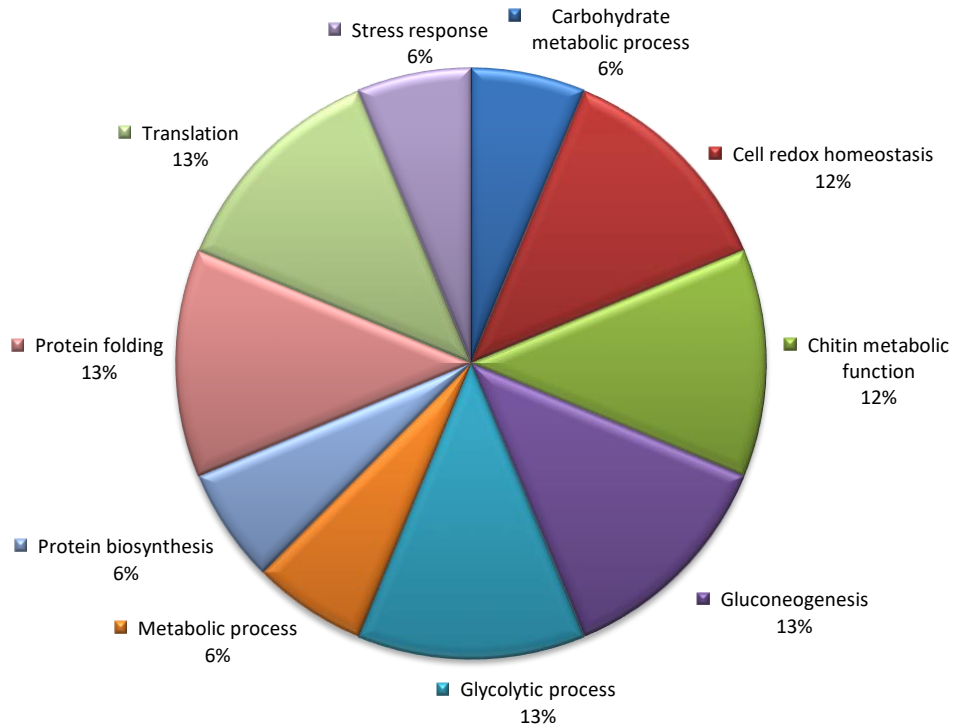


Figure 4.4 Main biological processes of the identified proteins in the non-embryonated egg extract proteome of *T. trichiura* according to information obtained from the Gene Ontology (GO) database.

<https://www.uniprot.org>

#### 4.2.3 1-DE and immunoblot analysis of *T. trichiura* EE and FE

To identify the species-specific parasite antigens, 1-DE SDS-PAGE and Western blots were performed on the egg extract (EE) and the female extract (FE) with serum and saliva from naturally infected AGMs.

For the EE, the possible identity of the antigens revealed in Western blots (Figure 4.5), Lane 1 and 1.1) was investigated by matching the molecular weights of the bands seen with those of proteins identified in the EE proteome and are presented in Table 4.4. In addition, the same

specific areas on SDS-PAGE gels (1G and 2G, **Figure 4.5** Lane 2) corresponding to the bands in the Western blots were excised and used for confirmatory proteomic analysis by LC-MS/MS and presented in **Table 4.5**.

The immune complexes identified by Western blot with the EE as antigen ranged from 37 to 200 kDa with the most immunogenic in two distinct bands, band 1W ( $\approx$  170 kDa) and band 2W ( $\approx$  37 kDa) (**Figure 4.5**, Lane 1 and 1.1).

For the FE, the comparative study for the specific immune-complexes identified by Western blot (**Figure 4.5**, lane 3 and 3.1) and areas matched on SDS-PAGE gels (**Figure 4.5**, Lane 4) were also excised and analyzed by LC-MS/MS and presented in **Table 4.6**. With the FE as antigen these ranged from 33 to 70 kDa with the most immunogenic in two distinct bands, band 3W ( $\approx$  60 -70 kDa) (**Figure 4.5**, lane 4) and band 4W ( $\approx$  37 kDa) (**Figure 4.5**, lane 3 and 3.1).

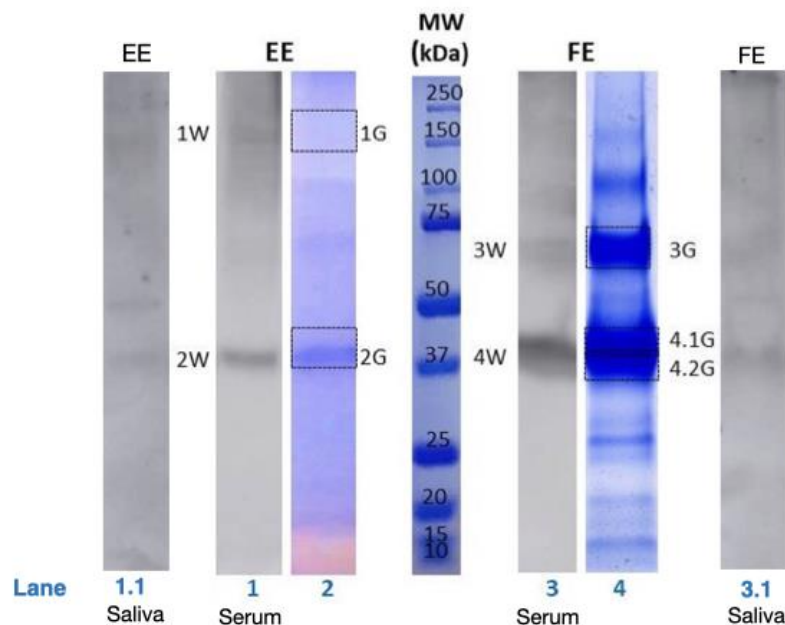


**Figure 4.5** Major immunogenic proteins detected in *T. trichiura* extracts.

Western blot showing AGMs sera and saliva antibodies response to *T. trichiura* egg extract (EE) (lane 1 and 1.1) and female extract (FE) (lane 3 and 3.1) (10  $\mu$ g/lane). Saliva or serum samples diluted 1:10 or 1:500, respectively. Secondary antibody (peroxidase-labeled goat anti-primate IgG (1:5000) or IgA (1:1000)).

Bands 1W-2W and 3W-4W indicate the regions containing antigens recognized most strongly by sera and salivary antibodies in EE and FE, respectively. Corresponding SDS-PAGE of EE (lane 2) and FE (lane 4), stained with Coomassie Brilliant Blue R-250 and excised areas of each, 1G-2G and 3G-4.1G-4.2G, containing the most immunogenic peptides for proteomic analysis. Molecular weight in kDa is lane labeled as MW.

**Table 4.4 Potential identity of the EE proteins targeted by serum and salivary antibodies based on the MW data of the EE proteome.**

Accession number	Annotation	MW (kDa)	Peptides* (95%)
<b>Band 1W (≈ 170 kDa)</b>			
A0A077ZE83	Vitellogenin N and VWD and DUF1943 domain containing protein	198.527	205
A0A077Z8E4	Heat shock protein 70	130.299	21
<b>Band 2W (≈ 37 kDa)</b>			
A0A077Z5Q5	Poly-cysteine and histidine tailed protein isoform 2	50.494	109
A0A077ZHV3	Glyceraldehyde-3-phosphate dehydrogenase	37.536	66
A0A077ZE37	Actin	41.838	35
A0A077YWW9	Actin 5C	41.036	29
A0A077YX57	Enolase	49.513	27
A0A077Z0I4	Epididymal secretory protein E1	45.783	28
A0A077Z8B3	CBM 14 domain containing protein	78.597	18

\*The number of distinct peptides having at least 95% confidence.

Based on corresponding molecular weights in the EE proteome, band 1W contained vitellogenin N and VWD and DUF1943 domain containing protein (VgNVD) with 205 distinct peptides and heat shock protein 70 (HSP-70) with 21 distinct peptides (**Table 4.4**). Confirmatory LC-MS/MS of the corresponding Coomassie-stained band confirmed that VgNVD, with 241 distinct peptides, was the most representative protein within the 1W area (**Table 4.5**).

Analysis of band 2W identified poly-cysteine and histidine-tailed protein isoform 2 (PCHTP-2), glyceraldehyde-3-phosphate dehydrogenase (GAPDH), actin, actin 5C, enolase, epididymal secretory protein E1, and CBM 14 domain containing protein (CBM14) (**Table 4.5**) and confirmatory analysis with LC-MS/MS also indicating there were other proteins present such as phosphoglycerate kinase, the dolichyl-diphosphooligosaccharide-protein glycosyltransferase 48 kDa subunit, adenosylhomocysteinase, tubulointerstitial nephritis antigen, calponin domain

containing protein, 3 ketoacyl coenzyme A thiolase, elongation factor 1-alpha and serpin domain containing protein (**Table 4.5**) while actin 5C and epididymal secretory protein E1 were not confirmed.

**Table 4.5 Protein identities, in decreasing abundance, in immunodominant bands 1W and 2W in Western blots with EE as antigen. Proteins were identified by LC-MS/MS of corresponding areas in SDS-PAGE gels, 1G and 2G.**

Accession number	Annotation	MW (kDa)	Peptides* (95%)
<b>Area 1G (≈ 150-200 kDa)</b>			
A0A077ZE83	Vitellogenin N and VWD and DUF1943 domain containing protein	198.527	241
A0A077Z8E4	Heat shock protein 70	130.299	3
<b>Area 2G (≈ 37-45 kDa)</b>			
A0A077Z5Q5	Poly-cysteine and histidine tailed protein isoform 2	50.940	66
A0A077Z8B3	CBM 14 domain containing protein	78.597	24
A0A077YX57	Enolase	49.513	18
A0A077ZHV3	Glyceraldehyde-3-phosphate dehydrogenase	37.536	15
A0A077ZE37	Actin	41.838	14
A0A077Z3K7	Phosphoglycerate kinase	44.724	12
A0A077Z8X2	Dolichyl- diphosphooligosaccharide-protein glycosyltransferase 48 kDa subunit	48.787	12
A0A077ZF21	Adenosylhomocysteinase	47.827	10
A0A077Z3H9	Tubulointerstitial nephritis antigen	50.458	9
A0A077YXR0	Calponin domain containing protein	40.694	7
A0A077ZJA3	3 ketoacyl coenzyme A thiolase	43.402	6
A0A077YYL7	Elongation factor 1-alpha	51.086	6
A0A077Z1Z4	Serpin domain containing protein	43.328	6

\*The number of distinct peptides having at least 95% confidence.

Regarding the comparative proteomic analysis of reactive areas displayed in FE Western blot, the analysis of the band 3G (≈ 60 -70 kDa) (**Figure 4.5**, lane 4), which corresponded to band 3W, revealed again PCHTP-2 as one of the proteins identified with the highest number of matching peptides. This protein was also identified in bands, 4.1G and 4.2G (**Table 4.6**). The proteomic results of both sections of the band 4W showed some proteins shared between the EE and FE, such as PCHTP-2, Actin and GAPDH, suggesting they are likely to be the major ones in both samples. This finding is not surprising, since most of the EE antigens are also present in FE (eggs contained in the uterus).

**Table 4.6 Protein identities, in decreasing abundance within FE excised gel areas (3G, 4.1G, 4.2G) with suitable MW matching Western blot band areas 3W and 4W.**

Accession number	Annotation	MW (kDa)	Peptides* (95%)
<b>Area 3G (≈ 60-70 kDa)</b>			
A0A077ZIM1	Tropomyosin	87.298	19
A0A077ZIM7	Papilin	80.804	6
A0A077ZEY0	Calsequestrin	49.211	5
A0A077YX57	Enolase	40.513	5
A0A077Z9R9	Kunitz BPTI domain containing protein	103.388	2
<b>Area 4.1G (≈ 37-45 kDa)</b>			
A0A077Z5Q5	Poly-cysteine and histidine tailed protein isoform 2	50.494	65
A0A077ZE37	Actin	41.838	7
A0A077ZHV3	Glyceraldehyde-3-phosphate dehydrogenase	37.536	5
A0A077ZEY0	Calsequestrin	49.211	5
<b>Area 4.2G (≈ 33-37 kDa)</b>			
A0A077Z0I4	Epididymal secretory protein E1	45.783	8
A0A077Z0N1	Actin-depolymerizing factor 2, isoform c	35.411	4
A0A077Z5Q5	Poly-cysteine and histidine tailed protein isoform 2	50.494	4

\*The number of distinct peptides having at least 95% confidence.

In comparing the Western blots with EE and FE as antigen, highly reactive bands were seen in both with a molecular weight of around 37 kDa (2W and 4W, **Figure 4.5**, lane 1 and 3). There were intensely staining protein bands in the corresponding SDS-PAGE gels. The other two prominent bands seen in the Western blots of the EE and FE antigens, 1W and 3W, were of different molecular weights and thus seemed to be stage-specific to the different life stages (**Figure 4.5**). Antigenic band 1W was barely detected in the corresponding SDS-PAGE indicating a low concentration of protein, while band 3W corresponded to a prominent band on the corresponding SDS-PAGE gel indicating a high concentration (3G) (**Figure 4.5**, Lane 4). Although the 2W and 4W major antigenic bands of the EE and FE, respectively, both had a molecular weight of 37 kDa and shared several proteins (PCHTP-2, Actin and GAPDH), there were also specific proteins which appeared in only the egg or adult female stage. Dolichyl-diphosphooligosaccharide-protein glycosyltransferase 48kDa subunit, CBM14 domain containing protein, adenosylhomocysteinase, tubulointerstitial nephritis antigen, calponin domain containing protein, 3 ketoacyl coenzyme A thiolase, elongation factor 1-alpha and serpin domain containing protein



appeared as typical of EE (**Table 4.5**). Meanwhile, Calsequestrin, Epididymal secretory protein E1, Actin-depolymerizing factor 2-isoform c and Kunitz Bovine basic pancreatic trypsin inhibitor (BPTI) domain containing protein (KBDCP) were only present in FE (**Table 4.6**).

### 4.3 Identification of immunogenic proteins of diagnostic value

#### 4.3.1 Specificity Immunoblot analysis

To identify patterns of parasite antigenic responses across different species, Western blots were performed on extracts of other helminths, nematodes (*Primasubulura* sp., *Anisakis simplex*, *Aspiculuris tetraptera*) and trematodes (*Fasciola hepatica*, *Dicrocoelium dendriticum* and *Gnathosoma hispidium*) with serum from naturally infected AGMs.

The immune complexes identified by Western blot with the *Primasubulura* sp., *A. simplex* and *A. tetraptera* as antigen ranged from 37 to 250 kDa with the most immunogenic band ( $\approx$  50 kDa) for *Primasubulura* sp. and *A. simplex*, and ( $\approx$  150 kDa) *A. tetraptera* (**Figure 4.6**). *Fasciola hepatica* immune-complex identified was a pronounced single band ( $\approx$  100 kDa) while *D. dendriticum* immune-complexes were mildly reactive (**Figure 4.6**). *Gnathosoma hispidium* immune complexes presented the widest range from 15 to 100 kDa with the most immunogenic distinct bands at ( $\approx$  15 kDa,  $\approx$  25 kDa,  $\approx$  50 kDa,  $\approx$  75 kDa,  $\approx$  100 kDa) (**Figure 4.6**).

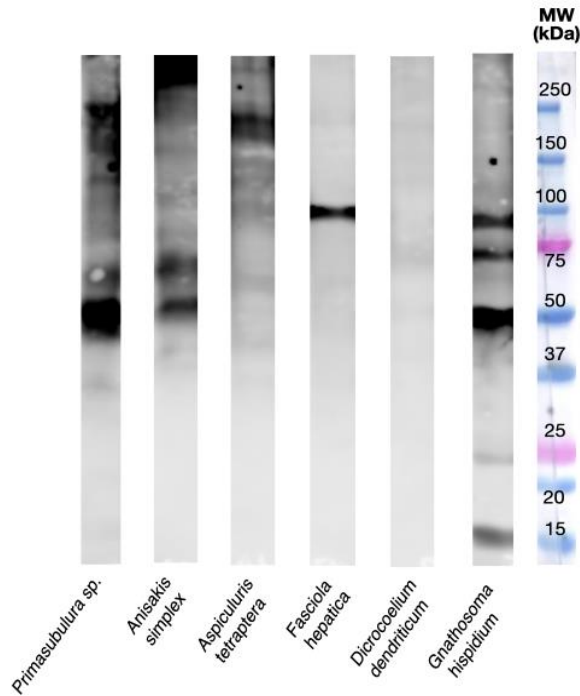


**Figure 4.6 Western blot showing AGMs sera antibodies in nematodes and trematodes extracts.**

**Molecular weight in kDa.** Western blot showing AGMs sera antibodies response in nematodes and trematodes extracts (10 µg/lane). Serum samples diluted 1:500, secondary antibody (peroxidase-labeled goat anti-primate IgG (1:5000)).

#### 4.3.2 2-DE SDS-PAGE electrophoresis and Western-Blot with serum antigenic profile

To confirm the most reactive immune complexes MW zones 2-DE SDS-PAGE and Western blot were performed on EE with serum from naturally infected AGMs. The possible MW identity of the antigens revealed in Western blots (**Figure 4.7**, zone 1 (Z1), 2 (Z2) and 3 (Z3)) was investigated by matching the molecular weights of the zones observed in the EE 2-DE SDS-PAGE (**Figure 4.7**).

The immune-complexes identified by Western blot with the EE as antigen ranged from 50 to 200 kDa with the most immunogenic zones, zone 1 (Z1) (≈ 50 - 150 kDa; pI 5-7), zone 2 (Z2) (≈ 50 kDa; pI 7-8) and zone 3 (Z3) (≈ 50 - 200 kDa; pI 8-10) (**Figure 4.7**).

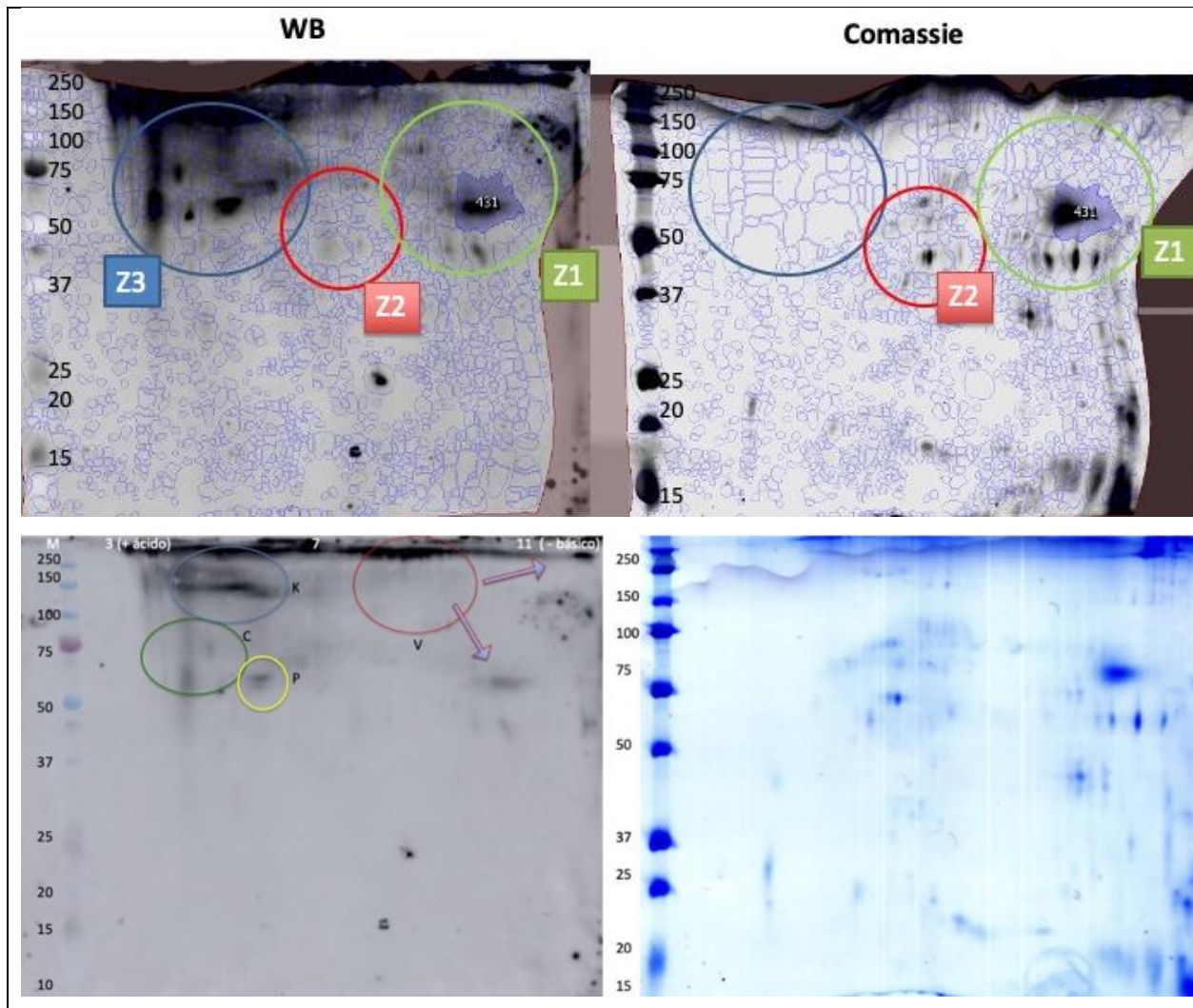


Figure 4.7 2-DE SDS-PAGE electrophoresis and Western-Blot with serum. Antigenic profile detected in *T. trichiura* egg extracts (EE).

Western blot showing AGMs sera antibody response to *T. trichiura* egg extract (EE). Egg Extract 10  $\mu\text{g}$  for Coomassie staining, and 30  $\mu\text{g}$  for 2-DE Immunoblotting. Serum was diluted 1:500 and secondary antibody (peroxidase-labeled goat anti-primate) IgG diluted 1:5000.

Zones 1, 2 and 3 indicate the regions containing antigens recognized most strongly by sera antibodies in EE. Corresponding SDS-PAGE of EE stained with Coomassie Brilliant Blue R-250. Molecular weight in kDa.

#### 4.4 Selection and evaluation of applicability of designed synthetic peptides

#### 4.4.1 Final protein candidates and derived peptide selection

##### 4.4.1.1 Vitellogenin N and VWD and DUF1943 domain containing protein

Vitellogenin N and VWD and DUF1943 domain containing protein [Acc AOA077ZE83]						
Peptides	Location and Length of aa residues	Antigenicity Score	Percentage of homology with <i>T. trichiura</i>	E -value <i>T. trichiura</i>	Percentage homology to other nematode	E - value other nematode
YRSLAIDDLTETAP*	15 aa @ 1608-1622	1.119	100 %	4e-06	100 % <i>T. suis</i>	4e-06
QFISPCPRCHQLP	13 aa @ 254-266	1.162	100 %	1e-05	77 % <i>T. suis</i>	0.17

\*Selected peptide highlighted

Selected peptide section: YRSLAIDDLTETAP, 15 aa, from 1608 - 1622

Accession number UniProtKB: [AOA077ZE83](#)

Gene: TTRE\_0000643201

MW: 196.58 kDa

Theoretical pI: 8.61

Molecular function: Lipid transporter activity

Enables the directed movement of lipids into, out of or within a cell and/or between cells.

Biological process: unknown

Subcellular location: unknown

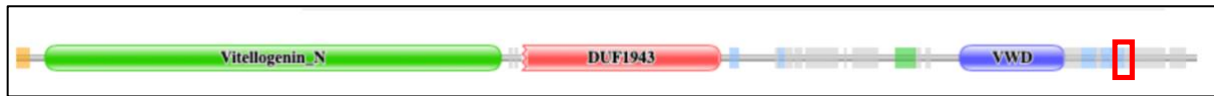
Signal peptide: 1 – 19

Chain: 20 – 1709

Family & Domains:

1. Vitellogenin domain: 42 – 702 (661 aa)
2. Domain of unknown function (DUF) DUF1943: 742 – 1026 (285 aa)
3. Von Willebrand factor type D domain (VWFD): 1358 – 1513 (156 aa)

Pfam model: <http://pfam.xfam.org/protein/A0A077ZE83> accessed April 9, 2021



Signal peptide in orange, domains labeled in color, gray areas are disordered areas, light blue areas are low complexity areas and small green area is the coiled coil. Selected peptide section outlined in red: **YRSLAIDDLVTETAP**, 15 aa, from 1608 – 1622.

#### Vitellinogen domain:

Vitellinogens are post-translationally glycosylated and phosphorylated in the endoplasmic reticulum and Golgi complex before being secreted to be taken up by oocytes. In the ovary, vitellinogens bind to specific Vtgr receptors on oocyte membranes to become internalized by endocytosis, where they are cleaved into yolk proteins by cathepsin D (<http://www.ebi.ac.uk/interpro/>, accessed April 14, 2021).

#### Domain of unknown function (DUF) DUF1943:

This domain adopts a structure consisting of several large open beta-sheets and their exact function has not been determined (<http://www.ebi.ac.uk/interpro/>, accessed April 14, 2021).

#### Von Willebrand factor, type D domain

Von Willebrand factor (VWF) is a large, multidomain blood glycoprotein synthesized in endothelial cells and megakaryocytes, that is required for normal hemostasis. VWF mediates the adhesion of platelets to sites of vascular damage by binding to specific platelet membrane glycoproteins and to constituents of exposed connective tissue. It is also essential for the transport of the blood clotting factor VIII (<http://www.ebi.ac.uk/interpro/>, accessed April 14, 2021).

**FASTA** sequence: signal peptide and selected peptide in bold

```
MGLKVVILTLAFALYAAGRHQQRLKLLRDTVNYQNVQESYFRINQKYKFKYNGQVKIGV
PDHSNQNSMTRFTA E VTLV KRSEEHFIRVNNIRLGKQLGNSKDQDEMASFELEPVEIK
QSDLKILELPVEFTYAEGVQDLV FQQDDEEWS ENLKRGIINLFQIKLQSTDRTSMEEEQ
SALNRIDTESKTNVGTAYRTREKTVEGECDTMYTVSAIDDDDDNSERGSRMLVTKAIDM
```

KSCQRRPEVWWNFQFISPCPRCHQLPRSGERSVESSTTIRYQIRGKRDKFLIERVELSND  
HVIAQQNADESAVVVKIKASLKLVSSESNDGSSEMSNFPATGQRVSDLIYSTRDDEHFD  
RFYAEGDQHYNDRLFSRRQKQDKSAALAEIIMKMMRHMKDTADEKANRYFYKAVQLMRY  
MSESEIRSTNEHHFGRQQSGMLTPEERERARNIMPNLLAQAGTSSFRQLADKIANGEIN  
PLKAAIVITTMMDTPRVSKEIITELMRLDESQTVQRNEQLRRAILLTAGSMRTMCAPQR  
HQRQQRQESQNRDDIRTDNSNHQRCDSEIKQRFVRTIADRLAASDRWEDQVILIRALGNA  
GLDVSISELESIIRNQDRRNPAAIRLEAILALRHIKDSLQKTKNILLSAAANRMESSAV  
RMAAIQMLLQQNPDRMTIDQIGVIINHDPNRRVASFAYKLIRRLADSNQPCYEENKQKLO  
TVAKSVRRRNQLPHSDMIFESVYDREKKTGFDFIMPMYDMDDIVPKFMRAGINMVERG  
ERNRNLFALEIGTSSLSNISELLPDIEQNQRGGNTEIKMKLRRMAEETRRNGNRGSRQQ  
QQQRQQQRQTAWMSMKFRNQDIMLLTFNEDRLKQLTQQNRGAESLLLLIAKMASNRQG  
SISIDEATLLRETUVKIPTAIGSQLSIRRKAPAFSAHGQASIGRNIPIQADIRARISTT  
ISMVTDVSSRTPISTNGIYLIKNIKATVPVDMTISLDHRQEDELKIQMRNHEGYKDLLK  
LESRPVIYYMRSQNPLAEAEKTVVAEKNVRMESFKRCMRGPLFGSEICMRGVITTPMCN  
HNKLLHYMAPWFGPNKVITISAYMRRTEENENENENSQVGLTIRSDSMQNKLELEYETSS  
RSLIPTKVDAKLQRQGHGQRQEICINMKTQGGKENDQRSEQTRRSSDININWGTQCNDEN  
YIKARIETASRRNVIWEQRQSNAIQEDNEERDQKQIGYGVSSSEETAGYKIQIHRNVPEW  
AVDKAEDIIRMLTSMNYWSTEIENKRQRYDSAERNRQRDEQSRAGEVRIQAIMRNEDKAD  
VKIQTPRKTIRMNNVYIPTLLRKETYRRSNFMRLMNLGMGNKHKAGTCQIRQNSITTFDG  
AIYRIPFSSCYTILARDSEEDPKFAIMARRSREQPDKKVVKLMTSDHEIELIPERGGGIE  
VKVDGQRWDDQQSKHHRAMRIRKRENEVTVDLKRPNVDVHYDGNITIRVSDKYHGRQTG  
MCGNLNADSSDEFKSNQKNRDDIWETFNEMTIRTDDCQHPQRQEQQDSQQFDSYDSDSD  
SNSYDSWEMARQHRSDSISYDDEEESMFSDSQQQQRRDQERNQH**HYRSLAIDDVLTET**  
**APVRRNKVIDSRGRKCISMRPIESCPEHGYTARGEKEEKEVPYTCLKANDELYHKIGRMQ**  
RQGTTPMDLSNSEMSFTRKETVPRKCISIV

### 3D structure databases:

1. **SWISS model EXPASY:**

LIPOVITELLIN (LV-1N, LV-1C) 1ish.1.A (Identity: 17.21) and LIPOVITELLIN (LV-2) 1ish.1.B  
(Identity: 13.36) (<https://swissmodel.expasy.org/interactive/NTnrVq/templates/>).

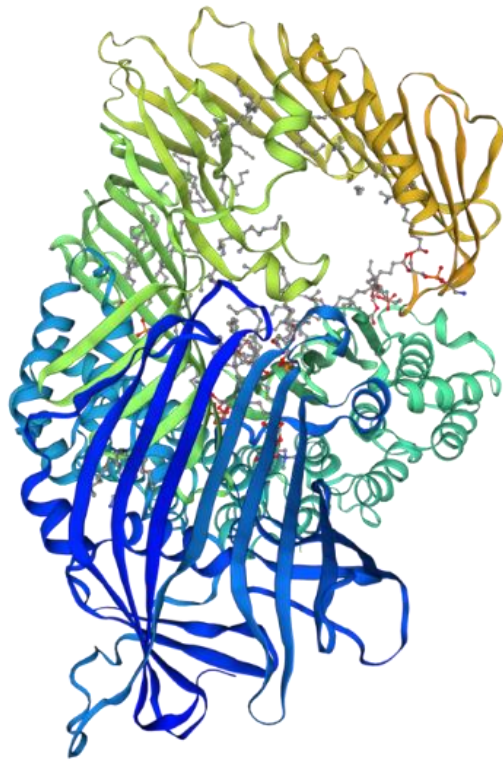


Figure 4.8 3D model Vitellogenin N and VWD and DUF1943 domain containing protein

\*Model based on known protein identities



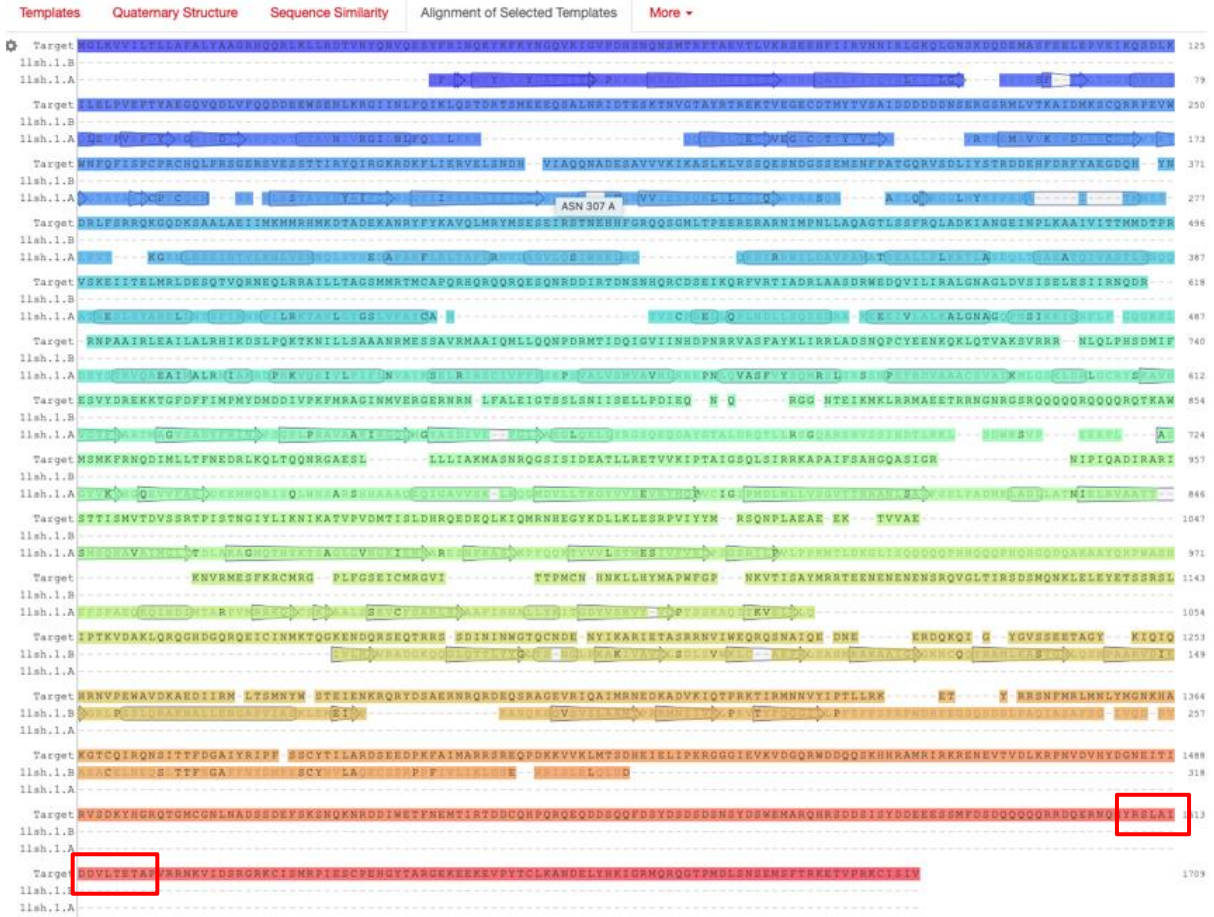


Figure 4.9 Alignment of known protein identities.  
 Selected peptide outlined in red: YRSLAIDDLVLTETAP, 15 aa, from 1608 – 1622.



#### 4.4.1.2 CBM 14 domain containing protein

CBM 14 domain containing protein [Acc AOA077Z8B3]						
Peptides	Location and Length of aa residues	Antigenicity Score	Percentage of homology with <i>T. trichiura</i>	E -value <i>T. trichiura</i>	Percentage of homology to other nematode	E - value other nematode
SAPTTVTTQLSPVDCVTL	18 aa @ 230-247	1.196	100 %	9e-09	78% <i>T. suis</i>	8e-04
RVTVTSCELQFSLRHF	16 aa @392-407	1.126	100 %	7e-08	56% <i>Acidobacteria bacterium</i>	13

\*Selected peptide highlighted

Our selected peptide section: SAPTTVTTQLSPVDCVTL, 18 aa, from 230 - 247

Accession number UniProtKB: [AOA077Z8B3](#)

Gene: TTRE\_0000321001

MW: 78.597 kDa Theoretical pI: 5.20

Molecular function: chitin binding

Interacting selectively and non-covalently with chitin, a linear polysaccharide consisting of beta-(1 - > 4)- linked N-acetyl-D-glucosamine residues.

Biological process: chitin metabolic process

Subcellular location: extracellular region

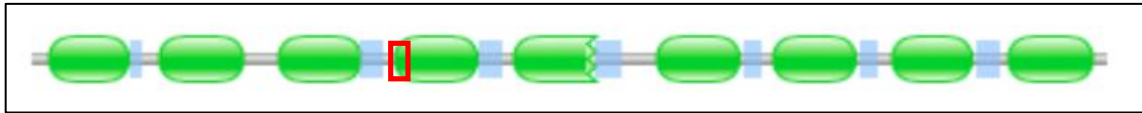
PTM/Processing: none

Family & Domains: 9 Chitin binding Peritrophin-A domains

1. CBM 14 domain: 10 – 67 chitin-binding type 2.
2. CBM 14 domain: 84 – 144 chitin-binding type 2.
3. CBM 14 domain: 164 – 223 chitin-binding type 2.
4. CBM 14 domain: 241 – 300 chitin-binding type 2.
5. CBM 14 domain: 322 - 381 chitin-binding type 2.
6. CBM 14 domain: 418 – 477 chitin-binding type 2.
7. CBM 14 domain: 496 – 555 chitin-binding type 2.
8. CBM 14 domain: 576 – 633 chitin-binding type 2.
9. CBM 14 domain: 653 – 713 chitin-binding type 2.

**Pfam model:** showing the 9 CBM 14 domains in green and low complexity areas in light blue.

<http://pfam.xfam.org/protein/AOA077Z8B3> accessed April 14, 2021



Selected peptide outlined in red **SAPTTVTTQLSPVDCVTL**, 18 aa, from 230 – 247

### Chitin binding Peritrophin-A domains:

These domains are found in chitin binding proteins particularly peritrophic matrix proteins of insects and animal chitinases. It is an extracellular domain that contains six conserved cysteines (motif) that potentially form three disulfide bridges (<http://www.ebi.ac.uk/interpro/>, accessed April 14, 2021)

**FASTA** sequence: selected peptide in bold

```
MGSMKLIDFLEKCAHIPDGNYPISPCSHHYLACSGGRGIIRVCPSGLIYNPVRNRC DNKA
DVATCGVSTTTTTPLSDITKQQTFCGSLLPDYPLQANSCLQQYFTCDANSVGVVRTC
PNDLYFDSVNRVCNFFDNIA SCSGVTAPQTTVTSTLGPTLPPVEFDCSKRKDGFYPNPAR
QCSSIIYACTAGEARRLFCGSLAYDIVTRACQSPDN TFACTGRTPVTSAPTTVTTQLS
PVDCVTLPNGLYPNPEDACSRIFACSDGIADRFVCPGELYFSDTQSCQRFS DVFACTG
VTTTTTTTTSASTTTTPQSDVGFDC TSLADGLYPNPNEICSTFYFICSGSVARRQNCPSG
LYDPEIQRCNSFGNIFVCTGTRPTTTTTTRVTVTSC ELQFSLRHFE CNMPKLSAPDLD
CTNLANGLYPNPRSQCSPIYFYCTNGFAYERRCLDDLFFNPELKICDRYSDIFECTGTRS
TPTTPTPTTPQSDVPFNCA YLPNGNYPNPSQQCSNMFFTC SNGKATIRTCPQETYFDPE
LRLCLKFSDVPACSGTQR TTTTATTTTALSDVTT PFFQCGNMPNGNYPLGSCENVYVSCV
DGNPSRRECPLNLFYDYTINECDYIYRIPGCGGQR TTTVLSDVT VTTTTTPAPGFDCSRLA
DGKYPNPDNVCYSDFYVYV CAGGRTSRMYCPAGLIYDPNAQECRFRRHAKPCKKSSLGSL
```

### 3D structure databases:

#### 1. SWISS model EXPASY:

Carbohydrate-binding module family 14 protein, 4z4a.1.A (Identity: 37.50), dust mite allergen, 4z4a.1.B (Identity: 19.57), chitotriosidase-1, 5hbf.1.A (Identity: 22.92).

(<https://swissmodel.expasy.org/interactive/F5LQzS/templates/>).

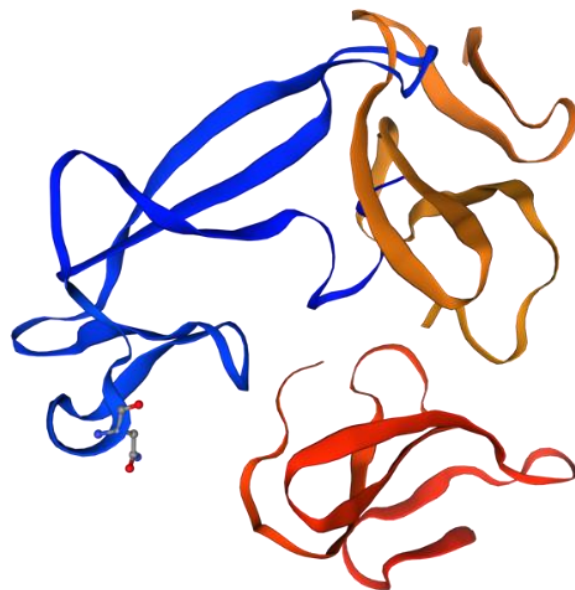


Figure 4.10 3D model CBM 14 domain containing protein model.

\*Model based on known protein identities



Figure 4.11 Alignment of known protein identities.

Selected peptide outlined in red: SAPTTVTTQLSPVDCVTL, 18 aa, from 230 – 247.

#### 4.4.1.3 Kunitz BPTI domain containing protein

Kunitz BPTI domain containing protein [Acc A0A077Z9R9]						
Peptides	Location and Length of aa residues	Antigenicity Score	Percentage of homology with <i>T. trichiura</i>	E-value <i>T. trichiura</i>	Percentage of homology to other nematode	E-value other nematode
QERCVATLPASVICRLP	17 aa @ 816-832	1.191	100%	1e-08	94% <i>T. suis</i>	1e-07
QQRCIATLPAIAFTL	15 aa @ 489-503	1.135	100%	2e-06	90% <i>T. suis</i>	5.5

\*Selected peptide highlighted

Our selected peptide section: QERCVATLPASVICRLP, 17 aa, from 816 – 832.

Accession number UniProtKB: [A0A077Z9R9](#)

Gene: TTRE\_0000541401

MW: 100.184 kDa

Theoretical pI: 5.91

**Molecular function:** chitin binding and serine endopeptidase inhibitor activity

Interacting selectively and non-covalently with chitin, a linear polysaccharide consisting of beta-(1 - > 4)- linked N-acetyl-D-glucosamine residues.

Stops, prevents, or reduces the activity of serine-type endopeptidases, enzymes that catalyze the hydrolysis of nonterminal peptide bonds in a polypeptide chain; a serine residue and a histidine residue are at the active center of the enzyme.

**Biological process:** chitin metabolic process

**Subcellular location:** extracellular region or secreted

**PTM/Processing:**

**Signal peptide:** 1 - 29.

**Chain:** 30 – 909.

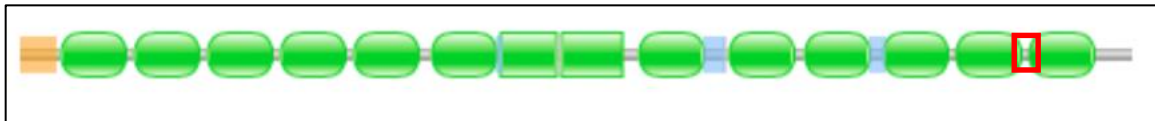
**Family & Domains:**

1. BPTI/Kunitz inhibitor domain: 36-86
2. BPTI/Kunitz inhibitor domain: 96-146

3. Chitin-binding type-2: 102-167
4. BPTI/Kunitz inhibitor domain: 156-206
5. BPTI/Kunitz inhibitor domain: 216-266
6. BPTI/Kunitz inhibitor domain: 276-326
7. Chitin-binding type-2: 282-350
8. BPTI/Kunitz inhibitor domain: 339-389
9. BPTI/Kunitz inhibitor domain: 385-439
10. BPTI/Kunitz inhibitor domain: 446-492
11. BPTI/Kunitz inhibitor domain: 509-559
12. BPTI/Kunitz inhibitor domain: 583-633
13. BPTI/Kunitz inhibitor domain: 645-695
14. BPTI/Kunitz inhibitor domain: 710-760
15. Chitin-binding type-2: 716-780
16. BPTI/Kunitz inhibitor domain: 769-819
17. BPTI/Kunitz inhibitor domain: 829-879

**Pfam model:** <http://pfam.xfam.org/protein/A0A077Z9R9> accessed April 14, 2021

Showing the signal peptide in orange, the different domains in green and low complexity areas in light blue.



Selected peptide outlined in red **QERCVATLPASVICRLP**, 17 aa, from 816 – 832.

#### **Bovine pancreatic trypsin inhibitor (BPTI)/Kunitz inhibitor domain:**

They inhibit proteases and their structure is a disulfide rich alpha + beta fold. The fold is constrained by 3 disulfide bonds. The pancreatic trypsin inhibitor (Kunitz) family is one of the numerous families of serine proteinase inhibitors (<http://www.ebi.ac.uk/interpro/>, accessed April 14, 2021).

FASTA sequence: signal peptide and selected peptide in bold

**MKPHSQASGVAVRMKITVILFLFGATFASRRKSPCNLTVDGGPCKAQFTKYYYNKESKK**  
CEPFVYGGCQGNRRNRFDTLEECTAKCAEQKKQEDSCKLPAETGPKASFTRYVYVWDQKK  
CAPFTYGGCKGNANNYESIAECEEEKGVRNKDKNPCELPAETGPCMASFIRFYNNKETKK  
CETFTYGGCQGNENNFFETLEECEAKCSDQKKQQNPCKMGDPGPCRAVFLRYYSWDWKK  
CLKFTYGGCEGNANNFESLAQCEATCVDKKNKDNPCELPAEPGPKASFLRYYNKESKK  
CETFTYGGCEGNENSFETLKECEARCVKNKKRKRQETPCELPADTGPKMNMIRYYDYG  
SKKCKTFTYGGCHGNENNFESMEKCEATCEEGEEKEEEEQGPCRAAFTKYYYNKDTKQCE  
TFIYGGCRGNANNFETKAESPVEPPIDVGPPTSHRKWFFDTVKKVCRTFVYGGCKGNGN  
RFDTKEECQQRCIATLPAIAFTLQEENPCKLPADPGPCMASFIKHYYDWSKQCLEFTYG  
GCEGNANNFETIEECQKSCPGEQEKEEEEEEEEEEQGGNPCELPAKKGPCRAAFTKY  
YNKDTKQCETFIYGGCKGNANNFETIEECQKSCPEKEEQGGNPCELPAKKGPCRAAFTK  
YYYNKDTKQCETFIYGGCKGNANNFETIEECQESCPGEEEEEEEEQGGNPCELPAKKGPCR  
AAFTKYYYNKDTKQCETFIYGGCKGNANNFETKAECESRCSVEKDGDVCSMPKDSGPCKA  
SHRKWFFDAVKKVCRTFVYGGCKGNGNRFDTKEEC**QERC**VATLPASVICRLPYAMGSCSS  
NLRFFFDFFETKQCRSFTYTGCEGNANNFISAYACYEKCGKRIYGNVEWCAVLIRWERQK  
ASYFQSLKF

### 3D structure databases:

1. **SWISS model EXPASY:** 9 sections of Kunitz-type protease inhibitor 1 (5h7v.1.a) selected to build model (<https://swissmodel.expasy.org>).

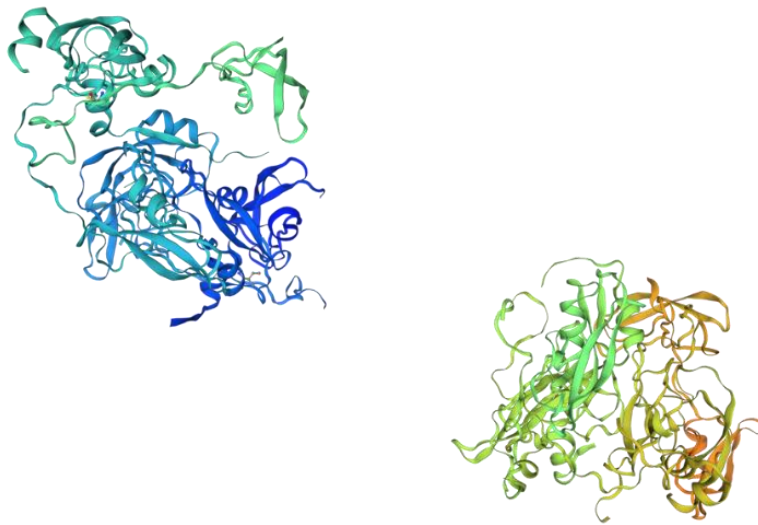


Figure 4.12 3D model Kunitz BPTI domain containing protein.

\*Model based on known protein identities



Figure 4.13 Alignment of known protein identities.

Selected peptide outlined in red: QERC VATLPASVICRLP, 17 aa, from 816 – 832

#### 4.4.1.4 Poly-cysteine and histidine tailed protein isoform 2

Poly-cysteine and histidine tailed protein isoform 2 [Acc A0A077Z5Q5]						
Peptides	Location and Length of aa residues	Antigenicity Score	Percentage of homology with <i>T. trichiura</i>	E-value <i>T. trichiura</i>	Percentage of homology to other nematode	E-value other nematode
<b>TECVKPPAHDCPAFG</b>	15 aa @214-228	1.146	100%	5e-07	100% <i>T. suis</i>	5e-07
LWFPLKDIVKHVEDHCHV	18 aa @ 237-254	1.158	100%	2e-11	89% <i>T. suis</i>	3e-09

\*Selected peptide highlighted

Our selected peptide section: **TECVKPPAHDCPAFG**, 15 aa, from 214 – 228

Accession number UniProtKB: [A0A0077Z5Q5](#)

Gene: TTRE\_0000228401

MW: 50.494 kDa

Theoretical pI: 7.09

Molecular function: unknown

Biological process: unknown

Subcellular location: unknown

PTM/Processing: none

Family & Domains: unknown

Pfam model: unknown

**FASTA sequence:** selected peptide in bold

```
MVDDGGGTSSDETVPFAWPIVNRDNDQWSPSTPTQPAPLPLISIPMGYALADHHDHCPA
WKDWRPWTDCLWYPPQNMKYKIAHACGMHAERNLTGVMELPGEAKPPPMCGHCSFKFRRCR
RRDNAKDCYPLDGEVDVCHDHGQICTLPKPLHLGCGYAFINEKCLKQCFTRPDTPSYVRLG
YRKMFIKPKKHCIEKNGMCKCCCGDYEPNESGTECVKPPAHDCPAFGPPGEWSECLWFP
LKDIVKHVEDHCHVHPEADGYRPPVTPPGIHIPEKCGYCSFRVKCMKRDKKDGCFELKL
GKKSCGHDDCPTSDICTMDKINGSCVFPKRLKEKLWDDFTAKSKEKHMPHWKRDGYAKL
LMQLPYSNCKEVGGKCKCCCHPYHPNEDGSKCVVKEYCKRVHELHDHDDHHHHHHAHHHS
SSSEDKDHHHKDHAHKEHHHR
```



3D structure databases: created April 15<sup>th</sup>, 2021.

1. **SWISS model EXPASY:** P43 (homolog protein from *T. muris*) (Bancroft *et al.*, 2019), 6qix.1.A, identity 83.33% (<https://swissmodel.expasy.org>).

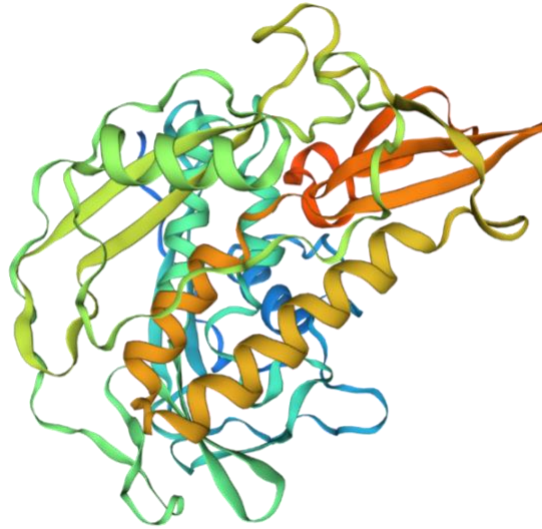
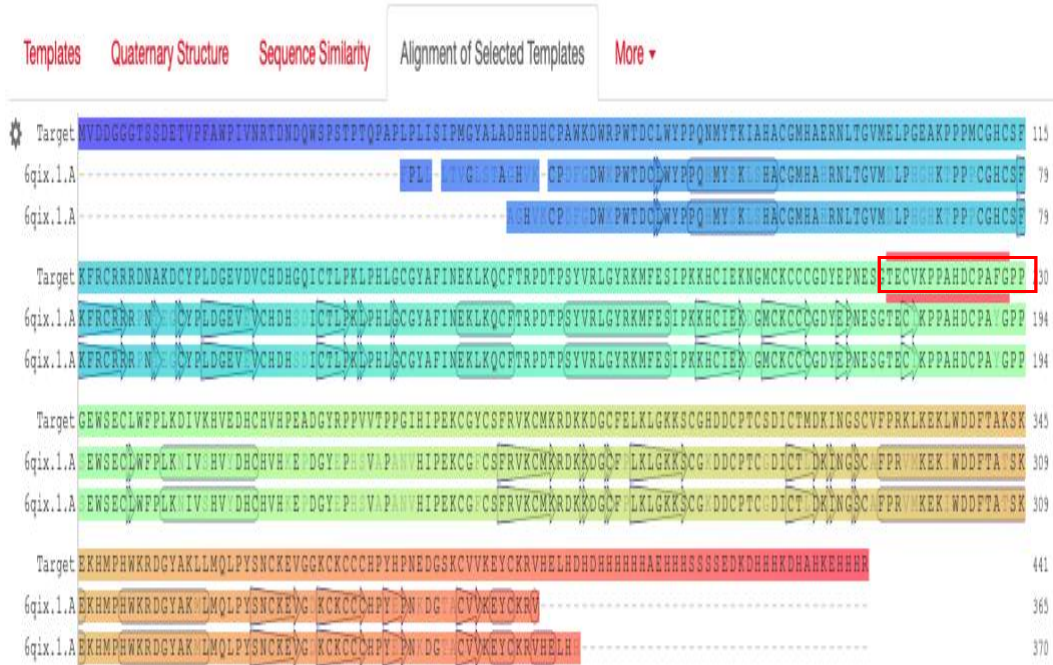


Figure 4.14 3D model Poly-cysteine and histidine tailed protein isoform 2.

\*Model based on known protein identities



**Figure 4.15 Alignment of known protein identities.**  
Selected peptide outlined in red: TECVKPPAHDCPAFG, 15 aa, from 214 – 228

#### 4.4.2 Synthetic peptides diagnostic feasibility evaluation through Indirect ELISA

The diagnostic feasibility of the selected peptides derived from the four final protein candidates VgNVD (YRSLAIDVLTETAP), KBDCP (QERCVATLPASVICRLP), CBM14 (SAPTTVTTQLSPVDCVTL), and PCHTP-2 (TECVKPPAHDCPAFG) was evaluated with 19 serum and 19 saliva samples from *T. trichiura* naturally infected AGMs and 6 negative human sample controls. The experiments were performed according to section 3.7.3. **Figure 4.16** and **Figure 4.17** show the indirect ELISA results from each individual saliva sample against each of the four peptides, and **Figure 4.18** and **Figure 4.19** show the results from each individual serum sample against each of the four peptides.

In both, the saliva and serum samples, the peptides that elicited the strongest recognition by antibodies were the KBDCP (QERCVATLPASVICRLP) an FE stage specific protein of low abundance, and the VgNVD (YRSLAIDVLTETAP) an EE stage specific protein.

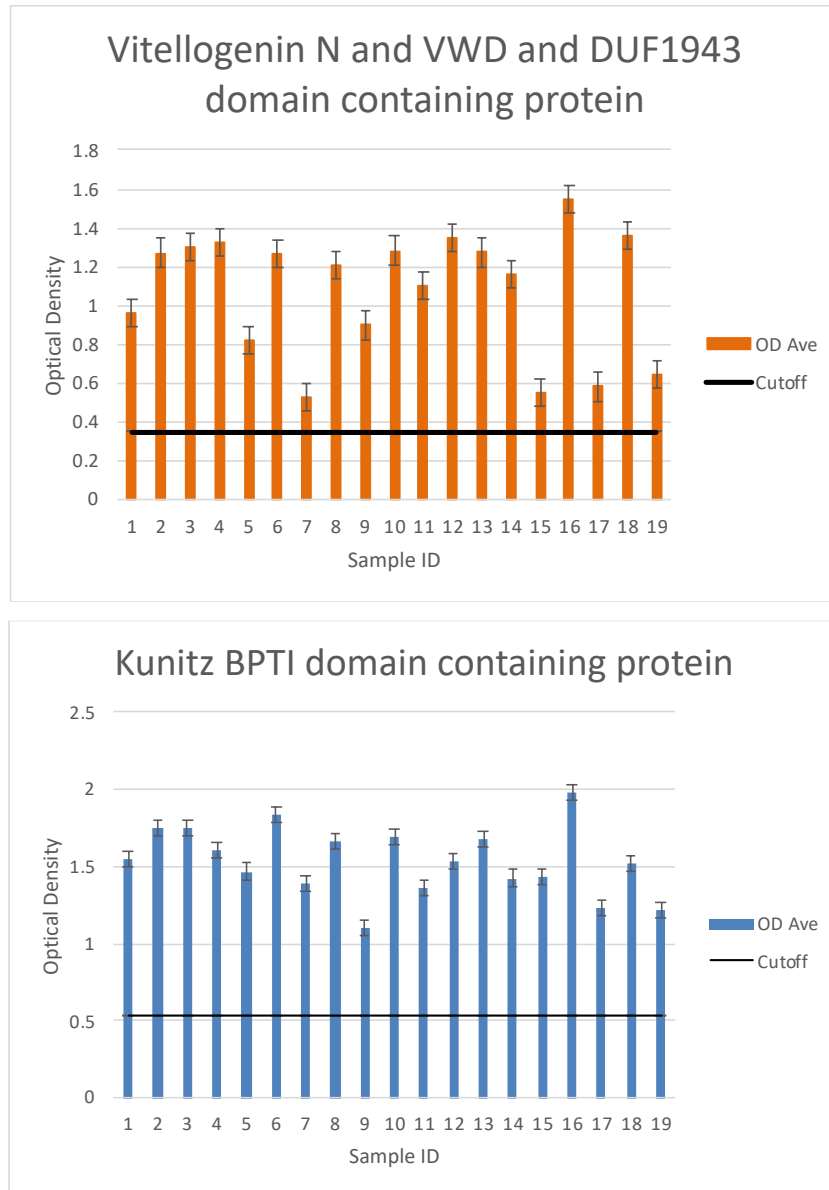


**Figure 4.16** Optical densities from 19 saliva samples from *Trichuris trichiura* infected AGMs analyzed with indirect ELISA against peptides VgNVD (YRSLAIDDVLTETAP), KBDCP (QERCVATLPASVICRLP). Each saliva sample was analyzed in duplicate. The cutoff was established as the mean OD of the negative controls plus 3 SDs.

The egg protein CBM14 peptide (SAPTTVTTQLSPVDCVTL), and the most abundant protein in all developmental stages of the parasite PCHTP-2 peptide (TECVKPPAHDCPAFG) presented the weakest signals (optical density, OD). Overall, the saliva samples showed strongest optical density values and lower cutoff values than the serum samples.

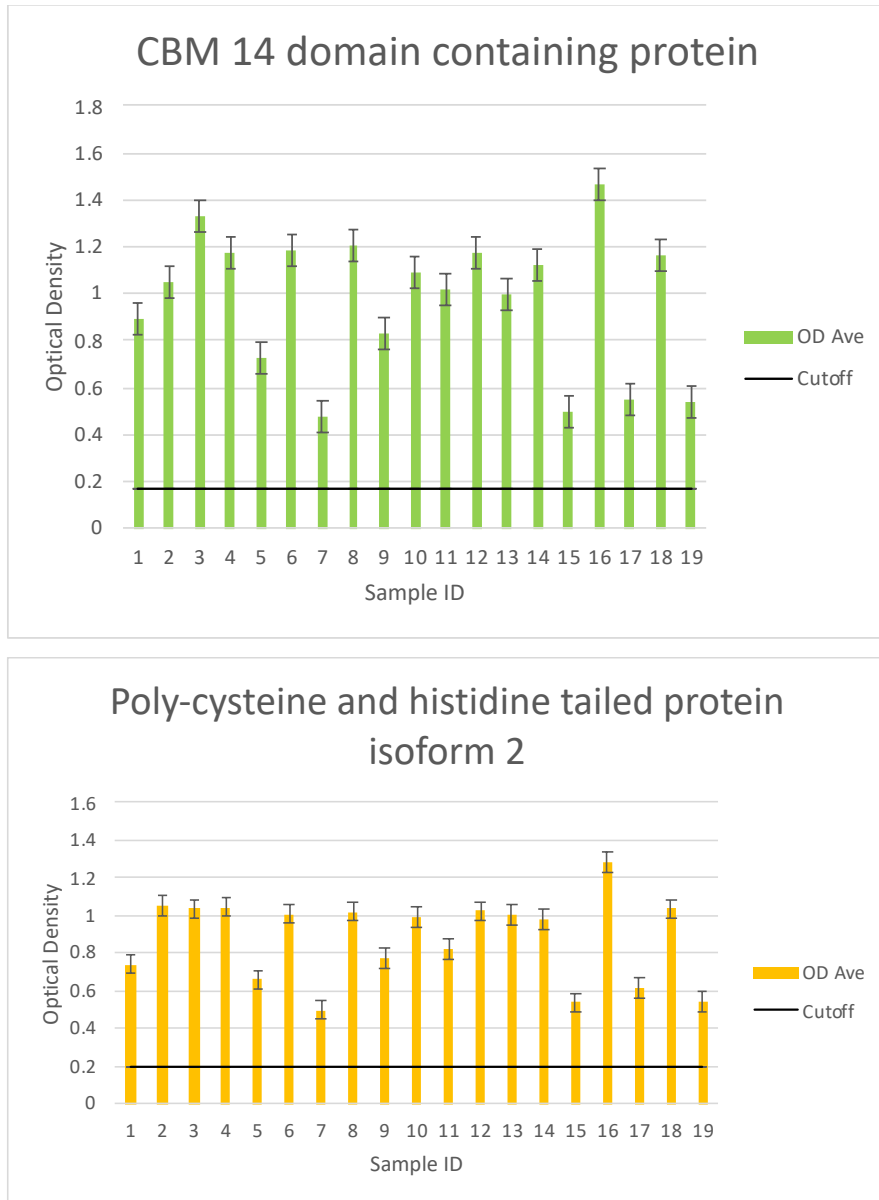
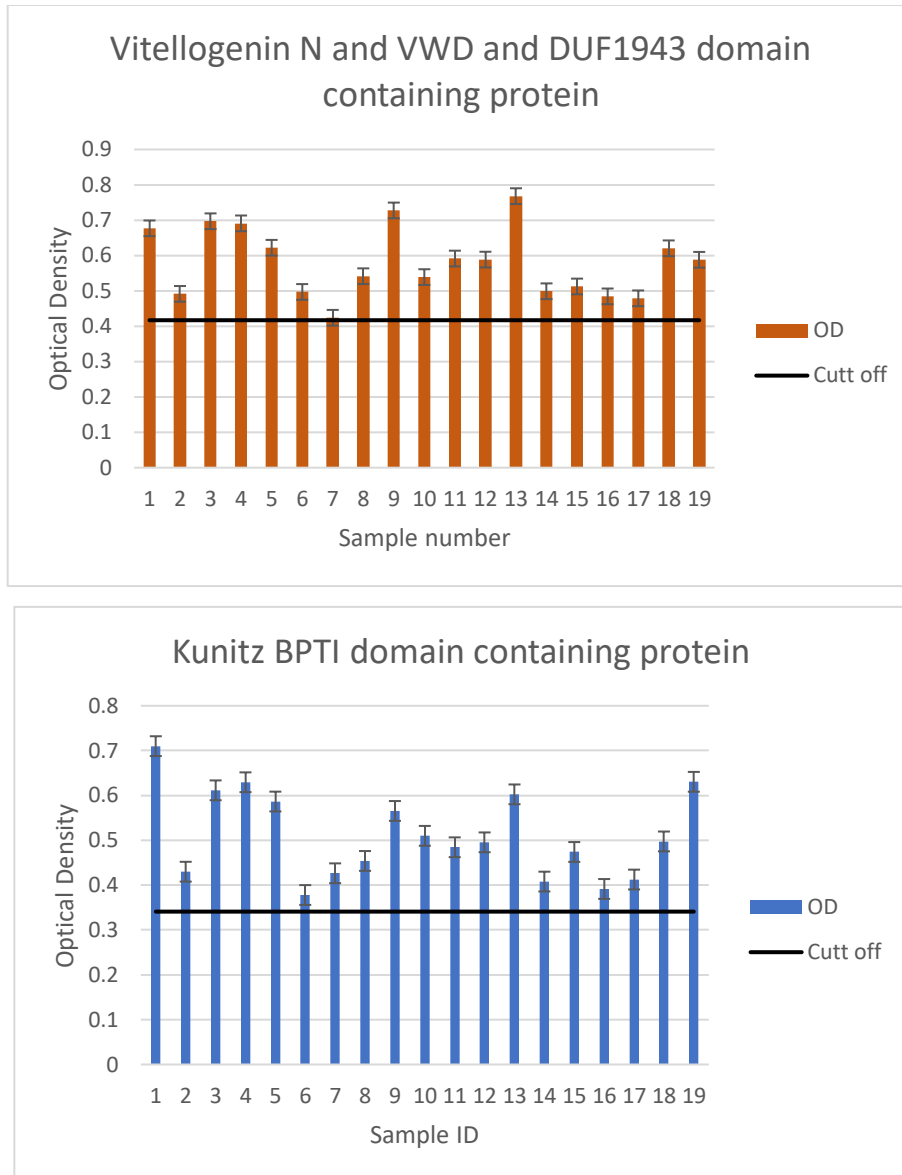


Figure 4.17 Optical densities from 19 saliva samples from *Trichuris trichiura* infected AGMs analyzed with indirect ELISA against peptides CBM14 (SAPTTVTTQLSPVDCVTL), and PCHTP-2 (TECVKPPAHDCPAFG). Each saliva sample was analyzed in duplicate. The cutoff was established as the mean OD of the negative controls plus 3 SDs.

The peptides of *T. trichiura* tested by indirect ELISA against 19 *T. trichiura* positive serum samples showed similar results as the saliva samples with an overall weaker antibody recognition.



**Figure 4.18** Optical densities from 19 serum samples from *Trichuris trichiura* infected AGMs analyzed with indirect ELISA against peptides VgNVD (YRSLAIDDVLTETAP), KBDCP (QERCVALPASVICRLP). Each serum sample was analyzed in duplicate. The cutoff was established as the mean OD of the negative controls plus 3 SDs.

The egg protein peptide CBM14 (SAPTTVTTQLSPVDCVTL), and the abundant protein PCHTP-2 peptide (TECVKPPAHDCPAFG) candidates presented the overall weakest signals (optical density, OD).

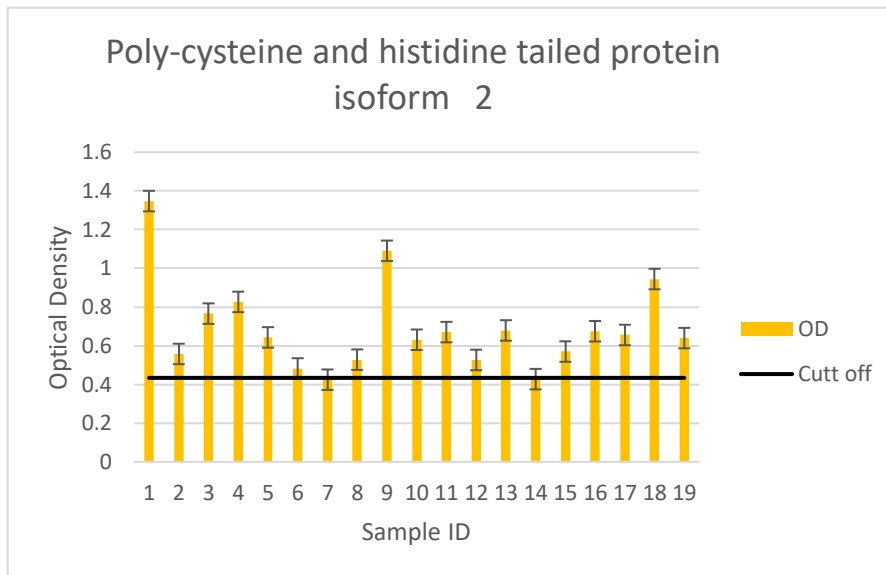
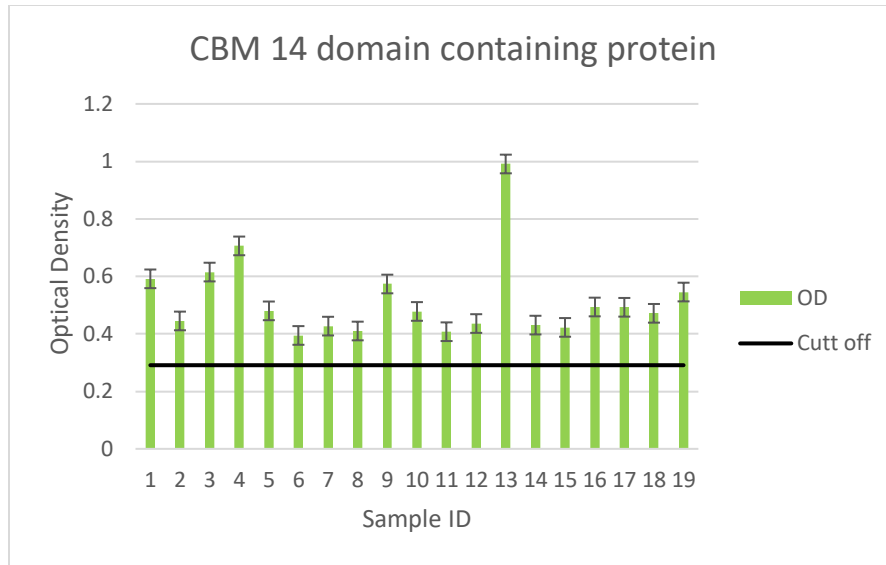


Figure 4.19 Optical densities from 19 serum samples from *Trichuris trichiura* infected AGMs analyzed with CBM14 (SAPTTVTTQLSPVDCVTL) and PCHTP-2 (TECVKPPAHDCPAFG).

Each serum sample was analyzed in duplicate. The cutoff was established as the mean OD of the negative controls plus 3 SDs.

Unfortunately, since all positive samples resulted in positive results and all the negative samples resulted in negative results, it was not possible to provide further clarification regarding the specificity and sensitivity analysis.

#### 4.5 *Trichuris trichiura* Scanning Electron Microscopy (SEM) images

The head reveals a small slit-like mouth opening with the oral stylet protruding outward (arrow). The stylet appears pointy and slim. The thin anterior portion surrounding the month opening does not display a specific cuticular pattern and immediately after a striated cuticular pattern is observed (Figure 4.20, (A)). The tick posterior end of the female displays a striated cuticular pattern with transverse grooves that taper at the anal opening (arrow) (Figure 4.20, (B)).

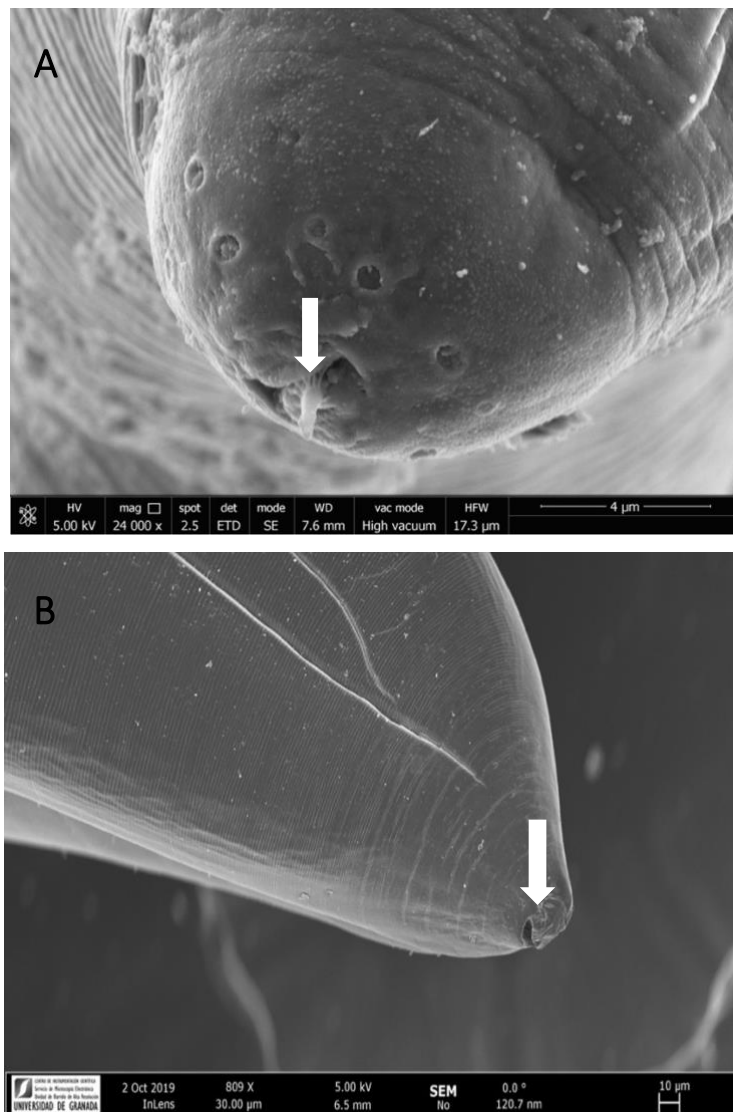


Figure 4.20 Adult female *Trichuris trichiura* anterior and posterior.

(A) Adult *Trichuris trichiura* anterior showing stylet (arrow) protruding from mouth opening. (B) Adult *Trichuris trichiura* posterior showing anal opening (arrow).

Figure 4.21(A) and (B) display the difference between a fully developed adult female vulva opening surrounded by an elevated rim-like structure deeply indented with a spinose cuticular appearance and a larval stage, possibly L2, with less defined anatomical structures.

The posterior extremity of males is equipped with a spicule enclosed in a spinose, retractile, cuticular sheath as observed in Figure 4.22 (C).

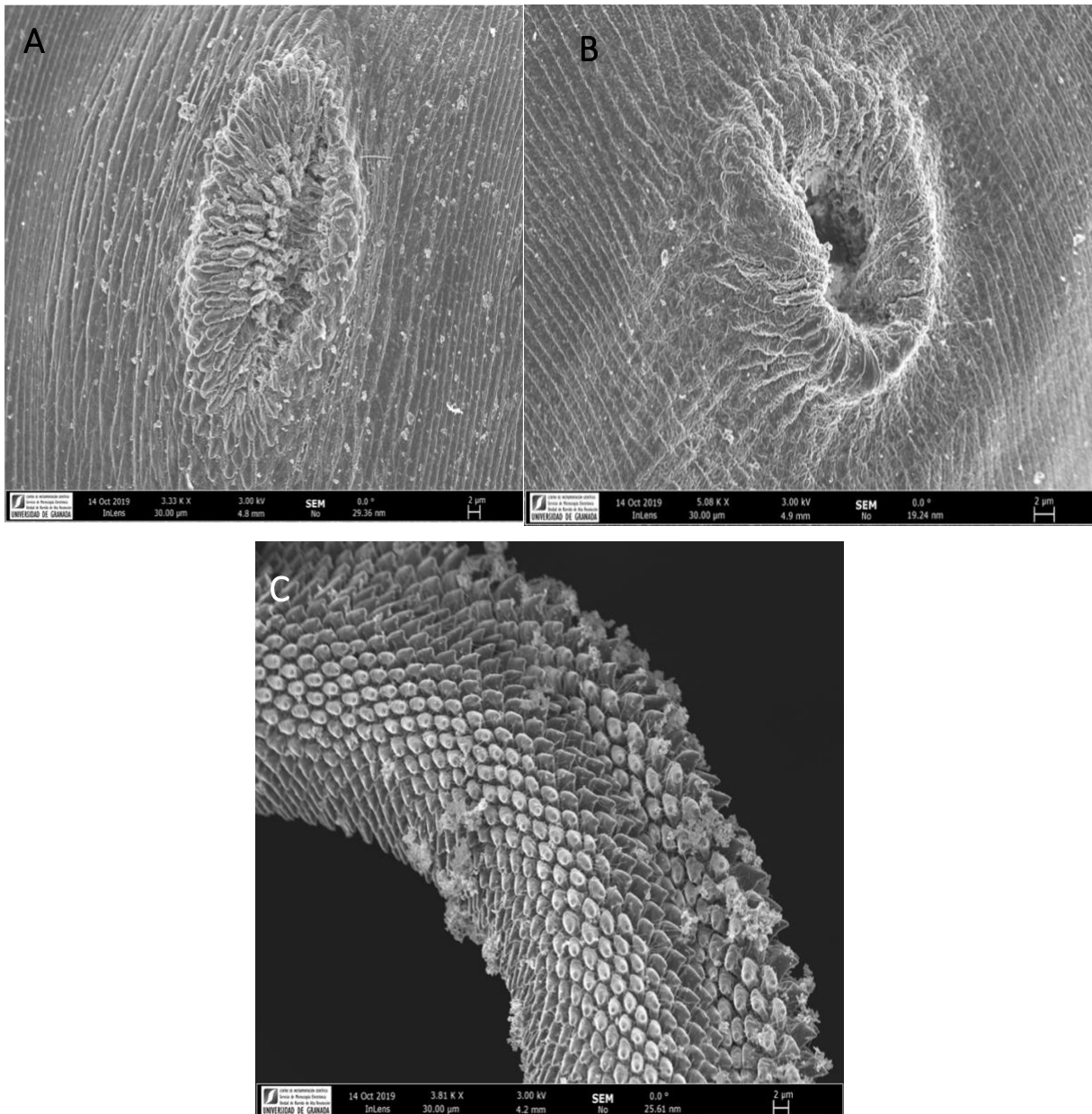


Figure 4.21 Adult *Trichuris trichiura* female and male reproductive structures.

(A) Adult *Trichuris trichiura* female vulva opening. (B) Larval stage *Trichuris trichiura* female vulva opening. (C) Adult *Trichuris trichiura* male spicule structure.



## 4.6 Histopathology

The histopathology analysis from full thickness cecum samples from 33 AGMs did not reveal abnormal morphological or structural changes suggestive of *Trichuris* infection. No other parasites were observed. See **Figure 4.22**.

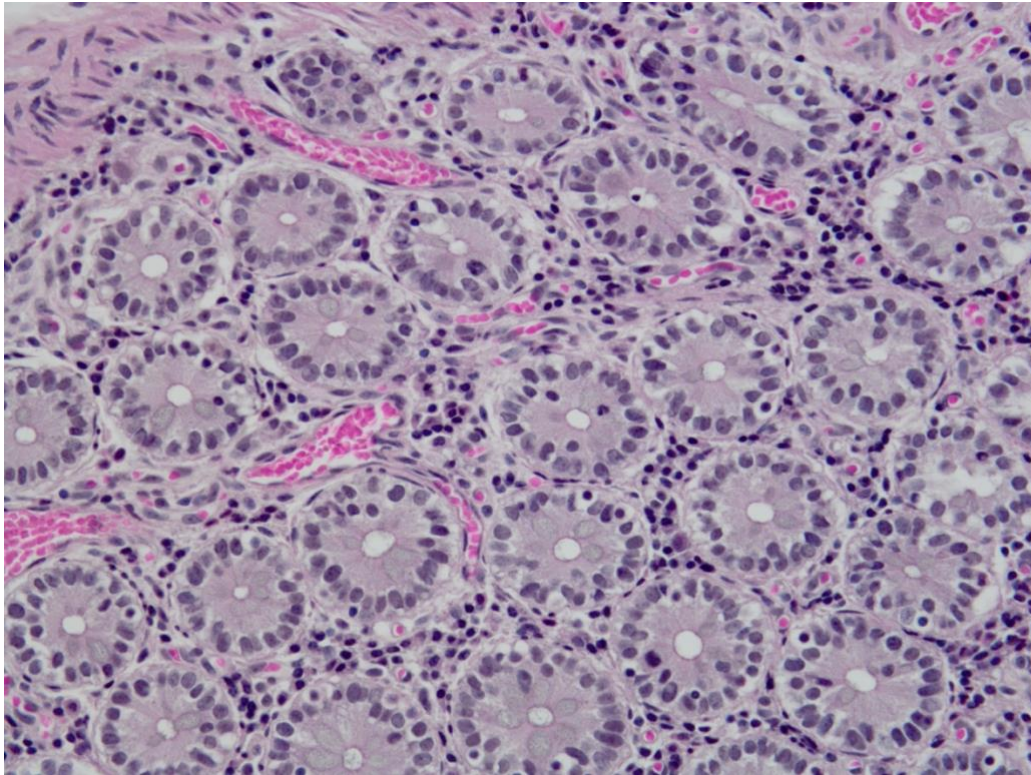


**Figure 4.22** Crypts of Lieberkühn within normal limits.

The 5  $\mu$ m AGM cecum sections stained with hematoxylin-and-eosin (H&E) and examined with an Olympus DP73 microscope (40X) (Tokyo, Japan).

## 5 Discussion

### 5.1 Control of nematode infections in captive *Chlorocebus sabaesus*

#### 5.1.1 Nematode species present in captive *Chlorocebus sabaesus*

Our study has shown a wide variety of nematodes can be found in captive AGMs on St. Kitts. Many of these have also been described in people on the island and many are regarded as zoonotic. *Trichuris trichiura* was present in 58% of the AGMs and is very common in people worldwide and also on St. Kitts (58% prevalence in 1991; Rawlins *et al.*, 1993). Strongylids species were present in 50% of the AGMs, and hookworm infections were prevalent in St. Kitts in the early 20th century (21.2 %; Annual Reports, Rockefeller Foundation, 1924), but through intensive anthelmintic administration, sanitation, and health education the hookworm disease is no longer a public health problem (Tikasingh *et al.*, 2011). *Strongyloides fuelleborni* was present in 12% of the AGMs and has not been reported in St. Kitts AGMs, further molecular studies are indicated to confirm that the AGMs on the island remain infected with *S. fuelleborni* introduced with the original animals from Africa.

We were unable to determine the *Capillaria* species present, as eggs do not have species-specific morphologies. To date only one species has been described in AGMs. *Capillaria hepatica* (syn. *Carlodium hepaticum*) was found at necropsy in the liver of one animal (*C. aethiops*) in South Africa (Fripp *et al.*, 1974). Although *C. hepatica* occurs worldwide, local experience suggests this nematode is not present on St. Kitts as the adult nematodes or associated lesions have never been observed in AGM's liver necropsied on the island, and human hepatic capillariasis has not been reported (Berger, 2020). Similarly, *Capillaria brocheri* (syn. *Aonchotheca brocheri*) (Justine *et al.*, 1988) and *Aonchotheca annulosa* Dujardin, 1845 (nematoda, Capillariidae) (Umur *et al.*, 2012) are the only other species described in NHPs, but they have also not been found in necropsies of AGMs on St. Kitts. Intestinal capillariasis by *Capillaria philippinensis* (syn. *Paracapillaria philippinensis*) has not been described in people from the island (Berger, 2020). Infections, then, might have only been acquired after the animals were introduced onto St. Kitts over 200 years ago.

Whipworms were the most common nematodes found in AGMs in previous reports (Munene *et al.*, 1998; Muriuki *et al.*, 1998; Mutani *et al.*, 2003; Gillespie *et al.*, 2004., Legesse *et*

*al.*, 2004; Petrášová *et al.*, 2010; Gaetano *et al.*, 2014; Kooriyama *et al.*, 2012; Amenu *et al.*, 2015; Li *et al.*, 2015; Wren *et al.*, 2015; Dalimi *et al.*, 2016; Valenta *et al.*, 2017; Teklemariam *et al.*, 2018; Barbosa *et al.*, 2020), and were the second most prevalent in our study. *Trichuris trichiura* is the species generally thought to be present in AGMs and this has been confirmed to be the species infecting *C. sabaesus* on St. Kitts (Hawash *et al.*, 2016; Yao *et al.*, 2018). While most infections in NHPs are subclinical, non-responsive to treatment diarrhea and inappetence, have been reported in fatal *Trichuris* infections with hemorrhagic typhlitis and ileal intussusception found at necropsy (Hennessy *et al.*, 1994; Emikpe *et al.*, 20002; Eo *et al.*, 2018). Recently, chronic whipworm infections have been reported to exacerbate egg-induced hepatopathology in nonhuman primates caused by *Schistosoma mansoni* (Le *et al.*, 2020) and have been associated with behavioral shifts (Chapman *et al.*, 2016); the affected AGMs had reduced rates of movement and socialization. Infections in people can cause clinical signs including diarrhea, abdominal pain, and in severe cases rectal prolapse (Stephenson *et al.*, 2000).

Strongylids such as *Oesophagostomum* spp. and *Trichostrongylus* spp., and the hookworms are the second most common nematodes found in most previous AGMs reports (McGrew *et al.*, 1989; Muriuki *et al.*, 1998; Mutani *et al.*, 2003; Gillespie *et al.*, 2004., Legesse *et al.*, 2004; Petrášová *et al.*, 2010; Kooriyama *et al.*, 2012; Amenu *et al.*, 2015; Wren *et al.*, 2015; Dalimi *et al.*, 2016; Valenta *et al.*, 2017; Teklemariam *et al.*, 2018; Blersch *et al.*, 2019). Although they were the third most prevalent in our study they were not reported in previous studies on St. Kitts (Cameron, 1930; Ritchie *et al.*, 1967; Hawash *et al.*, 2016; Yao *et al.*, 2018, Gallagher *et al.* 2019). The morphology of the different strongylid eggs does not enable species-level identification; however, we were able to use egg morphology to re-examine the samples and confirm that hookworms (Ancylostomatiodea) and *Trichostrongylus* spp. were present in all AGMs (Hasegawa, 2009; Modrý *et al.*, 2015; Blersch *et al.*, 2019).

Adult hookworms reside in the small intestine and *Trichostrongylus* spp. in the stomach and small intestine, but molecular analysis is needed to determine the species. Hookworms (*Necator* spp. or *Ancylostoma* spp.) are zoonotic (Hasegawa *et al.*, 2014) and can cause severe anemia. *Trichostrongylus* occurs primarily in ruminants (Acha *et al.*, 2003) and strongylid species are routinely detected in ruminants on St. Kitts, which has large populations of free-roaming

sheep, goats, and cattle. Humans can be infected, albeit infrequently, and AGMs are likely infected when exposed to larvae while foraging on lands where ruminants have grazed. Infections in NHPs are mostly asymptomatic, but in people with acute trichostrongyliasis there can be transitory eosinophilia and digestive disorders (Acha *et al.*, 2003).

*Strongyloides* spp. have been reported in AGMs from St. Kitts (Ritchie *et al.*, 1967; Gallagher *et al.*, 2019) but, although they are the third most common nematode reported in previous AGMs studies (McGrew *et al.*, 1989; Munene *et al.*, 1998; Muriuki *et al.*, 1998; Mutani *et al.*, 2003; Gillespie *et al.*, 2004; Petrášová *et al.*, 2010; Gaetano *et al.*, 2014; Kooriyama *et al.*, 2012; Amenu *et al.*, 2015; Li *et al.*, 2015; Wren *et al.*, 2015; Dalimi *et al.*, 2016; Valenta *et al.*, 2017 and Teklemariam *et al.*, 2018), they were the least prevalent in our study. Nonhuman primates can be infected with the major zoonotic species of the genus, *S. stercoralis* and *S. fuelleborni* (Kouassi *et al.*, 2015), but we only identified the latter, which is found mainly in tropical regions of Africa and Asia (White *et al.*, 2019). Mild infections with *S. fuelleborni* are mostly asymptomatic and self-limiting with occasional diarrhea in immunocompetent animals, but massive infections in young or immunocompromised animals can cause bronchopneumonia, pulmonary hemorrhage, intense diarrhea, anorexia, emaciation and reduce growth (Acha *et al.*, 2003; Cogswell, 2007).

While two different genera of strongylid species were identified in our AGMs, further molecular studies are warranted to confirm if AGMs are hosts to more than one strongylid species and to determine the species of *Capillaria*.

### 5.1.2 Treatment and control outcomes

Our data further emphasize the importance of establishing the most effective treatment regimen for captive monkeys to prevent zoonotic nematodes from spreading to animal handlers and other people that might come into contact with AGMs feces and contaminated soil. Establishing the most effective and least invasive treatments will help in ensuring optimal health and minimal stress in captive monkey populations.

Our findings that captive *C. sabaesus* on St. Kitts had high infection rates with a variety of nematodes post-PRAL treatment regimen indicates this is not an effective treatment regimen.

Praziquantel is mainly effective against cestodes and trematodes (Utzinger and Keiser 2004; Geary *et al.*, 2010). Although St. Kitts was endemic for human schistosomiasis in the 20th century, with AGMs also infected with *S. mansoni* (Cameron, 1928), the disease was eliminated from the island in the 1960s (Hewitt and Willingham, 2019) and cestode and trematode infections are now very rare on the island (Berger, 2020). Therefore, the use of praziquantel on the AGMs of St. Kitts appears unnecessary unless guided by a specific diagnosis. On the contrary, benzimidazoles such as albendazole, are used for the control of helminthiasis such as *Ascaris lumbricoides*, *T. trichiura*, and hookworms (Geary *et al.*, 2010) and also for *Capillaria* sp. (Cross, 1992). As three of these nematodes were found in our AGMs, (*Capillaria*, *Trichuris*, strongylids) the drug appears indicated for treatment.

Although albendazole has ovicidal and larvicidal activity by binding to intercellular tubulin (Dayan *et al.*, 2003), repeated consecutive doses of the drug are needed to achieve optimal efficacy in people (Geary *et al.*, 2010) and in AGMs (Kagira *et al.*, 2011). The PRAL treatment regimen based on existing recommendations (Junge, 2015; nonhuman primate formulary, 2018) that we used consisted of two doses of albendazole, but these were not consecutive which most likely explains the poor results of the regimen. The use of three consecutive doses of albendazole in the IVAL treatment, however, proved better efficacy with 64% of the *C. sabaesus* having a negative FEC for all parasites three months post-treatment; the four animals remaining positive by FEC had only *T. trichiura*.

Macrocyclic lactones such as ivermectin are potent and safe against adult and larval nematodes by inhibiting their motion and feeding (Martin *et al.*, 1997). The disadvantage is that when only a single dose is given, the inhibition can be temporary and may only reduce the fecundity of the female decreasing the egg output (Kagira *et al.*, 2011; Wang *et al.*, 2008), instead of triggering their death or expulsion. This can potentially lead to the recovering parasites continuing to produce eggs (Petersen *et al.*, 1996), a situation that can result in false negative results if the post-treatment monitoring times are short and fall below the parasite prepatent period (Reichard *et al.*, 2017). The three consecutive daily doses in our IVAL treatment protocol would seem to prevent the above problem and have resulted in more effective expulsion of nematodes. Although it has been shown there is no potentiation synergism between ivermectin

and albendazole (Entrocasso *et al.*, 2008), when used together, the drugs have shown to have better efficacy against nematodes (Olsen, 2007; Geary *et al.*, 2010).

Although we generally observed good results with the IVAL regimen there were apparent treatment failures that warrant further comment. Four AGMs had *T. trichiura* eggs three months after one treatment with IVAL but became negative after a second treatment. Although there are many possible explanations, we think it most likely the IVAL treatment was carried out during the prepatent period of *T. trichiura*, which might be as long as 16 weeks (Hansen *et al.*, 2016). It is also possible the animals became infected while in captivity, which is the most likely explanation for the one AGM that was negative for *T. trichiura* before, and 3 months after, the first IVAL treatment but was positive for adults and eggs at necropsy 8 months later.

*T. trichiura* eggs can remain inactive on surfaces for years (Bundy and Cooper, 1989) and have been found on fruits and vegetables (Kłapeć *et al.*, 2012). Although the AGMs cages in our study were cleaned and disinfected regularly, eggs are difficult to inactivate (Bundy and Cooper, 1989). It is of note that six of these seven animals that were negative by FEC three months after the one IVAL treatment were still negative six to eight months post-treatment. This indicates the hygiene measures in place were mostly effective at preventing reinfection, which is difficult as *T. trichiura* eggs can survive temperatures of 50 °C and – 9 °C for 5 days and 100% humidity for a week (Bundy and Cooper, 1989). They also resist short wave radiation (180 – 315 nm) (Nolf, 1932) and the eggshell only dissolves in 10% sodium hypochlorite after 25 hours of immersion (Wharton and Jenkins, 1978). Of the husbandry practices used in our study, it would appear that the steam cleaning (>82 °C) could yield better control of reinfection.

The fruits and vegetables fed to our AGMs may have been a source of reinfection as they were only washed if evidently soiled. However, it is known that nematode eggs can be present on fruits and vegetables even after excess soil is removed (Kłapeć *et al.*, 2019). Although water has been shown to be a source of infection with a variety of nematode eggs (Noda *et al.*, 2009), the smallest nematode eggs found in our study are larger (20-30 µm wide) than the 5 µm filters used in the water supply for our study animals. Although the water was also treated with UV light, a recent meta-analysis concluded that this is not very efficient for controlling parasites (Hazell *et al.*, 2019). Finally, cockroaches and flies can be mechanical transmitters of nematode eggs (El-Sherbini

and El-Sherbini, 2011) a challenge to control fully in the partially open environment at the SKBRF facilities.

All of the eight AGMs that were positive for *Capillaria* sp. eggs before IVAL treatment were negative at 3 months post-treatment. However, four AGMs (50%) subsequently became positive, all despite a second IVAL treatment. As the morphology of *Capillaria* sp. eggs cannot be used for speciation and no *Capillaria* were reported in the necropsy findings we could not determine the specie/s infecting our AGMs. Without knowledge of the infecting specie/s life cycle/s it is not possible to determine if these AGMs that became positive had been in the prepatent period during treatment, were autoinfected, reinfected, or had false-negative test results previously.

The presence of single-sex infections and the lack of correlation between egg output and total nematode or female counts at necropsy highlights that fecal egg counts have an overall low diagnostic sensitivity. Inaccurate estimations can be obtained when worm loads are calculated based on egg counts (Kannangara, 1975), contributing to the lack of adequate and active diagnosis of infections.

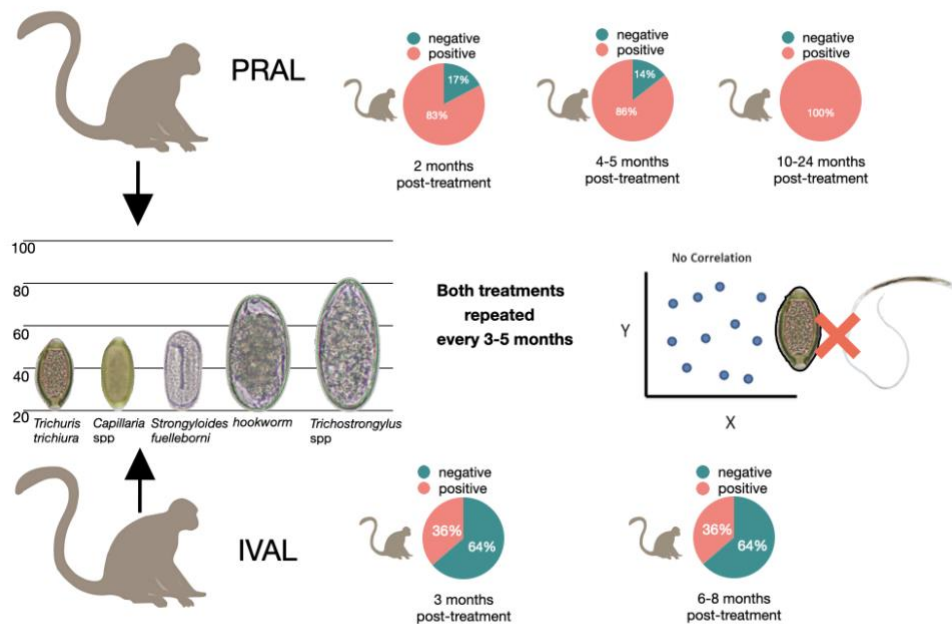


Figure 5.1 Graphical representation of treatment results evaluated in captive AGM

## 5.2 *Trichuris trichiura* immunogenic proteins of diagnostic value

### 5.2.1 Diagnostic challenges to overcome

Recent reports confirm that most cases of *T. trichiura* infections remain undiagnosed (Jourdan *et al.*, 2018), and chronic infections can remain undetected for years (Else *et al.*, 2020). This is because diagnosis of infections is based on the detection of eggs through coprological analyses that do not predict true parasite loads or real-time infection status. Early diagnosis of trichuriasis and diagnostic methods that do not rely on inconsistent clinical signs or fecal analysis are crucial to detect the infections following accidental ingestion and during the prolonged prepatent period of the parasite. At present, there are only limited data on *T. trichiura* antigens that can be used in serological diagnostic tests and the purpose of this study is to present the first description of the *T. trichiura* egg proteome and the immunodominant proteins present in both EE and FE. We also consider that the method described for *T. trichiura* egg isolation would be suitable for isolating large amounts of eggs from a more sterile and practical environment than the feces and, although the in-uteri eggs are not yet embryonated, they do present somatic and excretory/secretory proteins of the eggshell and those of dividing embryonic cells. We are demonstrating that their immunoproteomic analysis provides valuable information that warrants further study.

### 5.2.2 *Trichuris trichiura* genome and other helminths provide insights into the egg proteome.

In *T. trichiura*, the parasite-host interactions are poorly understood and are highly influenced by the parasite's life cycle. Limited information on stage-specific antigens, immune evasion strategies and immunomodulatory effects have been described in animal models of *T. muris* and *T. suis* (Leroux *et al.*, 2018; Shears *et al.*, 2018; Bancroft *et al.* 2019). Foth and collaborators (Foth *et al.*, 2014) described the whole-genome of the human-infective adult *T. trichiura* and we can now compare the *T. trichiura* egg proteome to their findings; they also identified numerous genes that are differentially expressed in a sex- or stage-specific manner. The most abundant transcripts found in this extensive study included proteins we have now definitively identified in the EE proteome, such as two WAP domain containing SLPI-like proteins, protease



inhibitors such as cystatin-domain containing protein and nematode cuticle collagen N-terminal domain containing proteins and chitin binding domain containing proteins such as CBM14 domain containing proteins.

Furthermore, with more or less representation, but of particular interest within the context of the present work, we have found *Trichuris* egg proteins with known immunomodulatory properties such as macrophage migration inhibitory factor homolog (MIF), previously identified in *T. trichiura* adult (Santos *et al.*, 2013), and 14-3-3 protein which has also been identified in several developmental stages of other nematodes, *Trichinella britovi* (Grzelak *et al.*, 2018) and *Trichinella spiralis* (Yang *et al.*, 2016) and trematodes, *Schistosoma japonicum* (Luo *et al.*, 2009). Both proteins are considered as enhancers of humoral and cellular immune responses (da Silva *et al.*, 2018). Although their function and biological process in *T. trichiura* remains unknown we are confirming the presence in the EE proteome and highlighting their potential role in the initial stages of the parasite-host interaction.

#### 5.2.2.1 EE proteome proteins with the largest numbers of distinct peptides

*Lipid transporter and major secreted protein with unknown function.* Interestingly, two of the proteins identified with the largest numbers of distinct peptides in the EE proteome presented in our work, VgNVD and PCHTP-2, were also among the top 25 most abundant transcripts found by Foth and collaborators (Foth *et al.*, 2014). Vitellogenins are a lipid transfer proteins, they play a significant role in embryonic development and are extensively conserved amongst nematodes (Chen *et al.*, 1997). They provide the growing embryo with amino acids (Vercauteren *et al.*, 2003), therefore VgNVD being the most abundant protein in the EE proteome represents an important antigenic target that can be consistently identified in eggs and adult females. The detection of PCHTP-2 in the EE proteome as the second most frequently detected protein is in accordance with Shears and collaborators (2018) who found it to be the most abundant protein in the *T. muris* adult secretome. Even though a specific function has not been assigned yet for *T. trichiura*, Bancroft and collaborators (2019) identified PCHTP-2 as the most abundant protein in cecal mucus from chronically infected mice with *T. muris* and confirmed its expression in all developmental stages

confirming PCHTP-2 as the major secreted protein of the whipworm despite not presenting signal peptide.

*Energy and metabolism.* One of the most represented groups of proteins we found in the egg proteome were those related to energy and metabolism and included proteins associated with glycolysis (enolase and glyceraldehyde-3-phosphate dehydrogenase (GADPH), gluconeogenesis (triosephosphate isomerase and phosphoenolpyruvate carboxykinase GTP) and other metabolic enzymes such as alpha-1,4 glucan phosphorylase and malic enzyme. This fact is consistent with previous studies in which these metabolic enzymes were described on the surface of the helminths, nematodes, and trematodes, found to participate in oxidative processes, parasite invasion and migration processes within the host (Sotillo *et al.*, 2008; Bernal *et al.*, 2006; Dea-Ayuela *et al.*, 2005; Pérez-Sánchez *et al.*, 2008; Sotillo *et al.*, 2011; Sotillo *et al.*, 2012).

*Muscle, motility, and cytoskeleton.* The ensuing functional group with the largest number of representatives was related to the cytoskeleton, muscle, and motility. Actin, tropomyosin, paramyosin, intermediate filament protein IFA 1 and epididymal secretory protein E1 were found with a high number of distinct peptides. These proteins are essential to enhance the motility of nematodes and have also been recorded in many helminthic proteomes: somatic extract of adults of *T. spiralis* (Yang *et al.*, 2015), *T. britovi* (Grzelak *et al.*, 2018), *Syphacia muris* (Sotillo *et al.*, 2012), and *Echinostoma caproni* (Sotillo *et al.*, 2010); and in egg secretions of *Schistosoma mansoni* (Cass *et al.*, 2007). Specifically, intermediate filament protein IFA1 has been studied in *Caenorhabditis elegans*, demonstrating that in nematodes and potentially similar for *T. trichiura*, they allow epidermal elongation in the larval stages to grow into adults (Woo *et al.*, 2004).

*Survival: antioxidants and chaperones.* We also found proteins essential for the survival of the nematode within its host, in the hostile conditions of the cecum, during stress and for detoxifying processes including antioxidants and chaperones. The Cu/Zn superoxide dismutase (Cu/Zn-SOD) was found in the EE proteome and has also been identified on *Trichuris ovis* homogenates (Sanchez-Moreno *et al.*, 1992), the adult surface and larval extracts (secreted and somatic) of *Toxocara canis* (da Silva *et al.*, 2018), in the somatic extract of adults of *Fasciola hepatica*, and the *S. mansoni* egg secretome (Cass *et al.*, 2007; Kim *et al.*, 2000). This essential

enzyme antagonizes the host's inflammatory responses by regulating the free radical balance and reactive oxygen species in cells protecting helminths against cell death (Cardoso *et al.*, 2004). Heat shock proteins (HSP90, HSP70, HSP60) are inducible conserved proteins widely described in parasite proteomes and secretomes, and we have confirmed their presence in the EE proteome. They act as molecular chaperones which fold, assemble and translocate other proteins to ensure the survival of the parasite by defending it against stressful situations being important in stress tolerance (Higón *et al.*, 2008). Small heat shock proteins HSP20 and HSP20 domain containing protein were also identified in EE proteome, which are known to aid parasite survival under hostile conditions such as heat or nutritional stress (Pérez-Morales *et al.*, 2015).

*Signaling.* Within the proteins implicated in signaling pathways, we identified galectin in the EE proteome, a type of lectin found in different extracts of nematodes such as adults and larvae of *T. canis* (da Silva *et al.*, 2018) and extract of infective larvae (L3) of *Haemonchus contortus* (Turner *et al.*, 2008) with a role in immune signaling pathways. Nematode galectins are believed to be immunological mediators with implications in survival and interaction with the host (Young *et al.*, 2002) and modulate a range of immune responses, including the cellular immune response, inflammatory processes, and immune regulation (Shi *et al.*, 2018) all essential for prolonged survival of *T. trichiura* in the host.

#### **5.2.2.2 Antigenic profile of *T. trichiura* EE and FE extracts and identification of the top immunodominant proteins**

Previous studies have used an immunoproteomic approach to determine the antigenic proteins of helminths at different developmental stages (larvae and adults) (International Helminth Genomes Consortium, 2018) and the serological responses to soluble protein extracts of *Ascaris lumbricoides* (Acevedo *et al.*, 2013), *Trichinella britovi* (Grzelak *et al.*, 2018), *Schistosoma japonicum* (Wang *et al.*, 2013) and *Taenia solium* (Santiváñez *et al.*, 2010).

Parasitic worms, like *T. trichiura* have a remarkable ability to modulate the host immune response through several mechanisms; specific parasite-derived proteins can modulate immune

functions playing an essential role in the parasite-host interaction (International Helminth Genomes Consortium, 2018). Excretion/secretion proteins from larvae and adults of the porcine whipworm, *T. suis*, closely related to the human *T. trichiura*, were investigated by Leroux et al. (Leroux *et al.* 2018), who identified a subset of proteins that promote specific anti-inflammatory functions and immunomodulatory properties. Here we present the combination of proteomic techniques, such as one dimensional gel electrophoresis and tandem mass spectrometry as a comprehensive approach to identify *T. trichiura* proteins of immunodiagnostic value.

**Vitellogenin N and VWD and DUF1943 domain containing protein.** Our findings of VgNVD being a major protein in the EE proteome and having immunogenic value in our naturally infected monkeys is significant as Shears and collaborators (Shears *et al.*, 2018) identified VgNVD in extracellular vesicles (EVs) of *T. muris* as a potential immunogenic candidate. Antigenic homologs of VgNVD have been identified in free-living nematodes such as *C. elegans*, and adult parasites secretomes of *Ascaris suum*, *Nippostrongylus brasiliensis*, *Heligmosomoides polygyrus* and *Litomosoides sigmodontis* (Mei *et al.*, 1997; Moreno *et al.*, 2011; Armstrong *et al.* 2014; Chehayeb *et al.*, 2014; Sotillo *et al.*, 2014; Ibáñez-Shimabukuro *et al.*, 2019) and also in *H. polygyrus* eggs (Hewitson *et al.*, 2013) which confirms the significance of our results in the context of current efforts to identify potential diagnostic, vaccine or drug targets. The VgNVD was not a distinct immune complex of interest identified in the FE alone when compared to other nematode banding patterns, therefore its presence in the FE was not identified.

**Heat shock protein 70.** HSP70 and heat shock proteins, in general, have caught the attention of researchers for acting typically as immunodominant antigens eliciting strong humoral responses as major targets of host immune responses, suggesting them out as possible candidates for antiparasitic, allergic and autoimmune diseases treatments (Mayer *et al.*, 2005; Mansilla *et al.*, 2014). Our findings that HSP70 is present in the EE in low abundance is in contrast to other work where the HSP70 is amongst the most highly abundant protein identified in egg secretions of *S. mansoni* and *H. polygyrus* (Cass *et al.*, 2007; Hewitson *et al.*, 2013) [17,62]. HSP70 is also heavily represented in *E. caproni*, *F. hepatica*, *H. polygyrus*, *Schistosoma bovis*, *T. trichiura*, *T. britovi*, and *Zygodotyle lunata* adult worms extract (Santos *et al.*, 2013; Grzelak *et al.*, 2018); Sotillo *et al.*, 2011;

Sotillo *et al.*, 2010; De la Torre-Escudero *et al.*, 2011; Hewitson *et al.*, 2011) which highlights that for the EE this can be a less abundant target. However, the contrasting finding of low prevalence may be due to the NE stage of the *Trichuris* eggs use in the study. Further studies are warranted to establish this comparison. Others have reported on their immunogenicity linked to stimulation of IgG and IgM responses (Dea-Ayuela *et al.*, 2005; Schmitt *et al.*, 2007; Tsan *et al.*, 2009), and they have been suggested as possible vaccine targets (Wang *et al.*, 2009).

**Poly-cysteine and histidine tailed protein isoform 2.** PCHTP-2 was the second most abundant in the EE and also present in the FE. This protein was identified as a strong immunogen of *Trichinella pseudospiralis* adult secretome (Wang *et al.*, 2017). Another protein of the same family, poly-cysteine and histidine-tailed metalloprotein, implicated in metal storage and/or transport, was the first member of the nematode poly-cysteine protein family described in *T. spiralis* (Radoslavov *et al.*, 2010). Since these proteins are unique for parasites of the Superfamily Trichinelloidea, their potential applications in diagnostics and treatment could be exploited in the future (Radoslavov *et al.*, 2010) and we show here that in the case of *T. trichiura* PCHTP-2 has a strong presence. Recent work by Bancroft (Bancroft *et al.*, 2019) hypothesized that the unique structural features of the homolog protein allows binding to IL-13, which is considered the key effector cytokine responsible for *T. muris* expulsion, able to inhibit IL-13 function both *in vitro* and *in vivo*. Our finding that PCHTP-2 is equally abundant in EE and FE as well as a strong immunogen in our naturally infected AGMs is significant as we can confirm that this protein has a strong presence in both life cycle stages and in accordance with Bancroft (Bancroft *et al.*, 2019) in the *T. muris* model. Our results are in agreement with presenting PCHTP-2 as a *Trichuris*-derived immunomodulatory molecule that could serve as a key target for the development of immunodiagnosics, vaccination or drug based therapeutics.

**Enolase and glyceraldehyde-3-phosphate dehydrogenase.** We identified certain glycolytic enzymes such as enolase and GAPDH, as immunoactive components of the *T. trichiura* EE and FE. Both of them are present on the surface of helminths interacting with the host surface as is the case of the delicate interaction between *T. trichiura* and the enteric cells of the cecum. Furthermore, enolase plays a vital role in the degradation of the intracellular matrix through the

activation of plasminogen facilitating the invasion, migration, and fixation in the host (Foth *et al.*, 2014; Cass *et al.*, 2007; Bernal *et al.*, 2006; Sotillo *et al.*, 2012) all essential mechanisms to ensure *T. trichiura* prolonged survival. In *T. spiralis* (Dea-Ayuela *et al.*, 2005) and *T. britovi* (Grzelak *et al.*, 2018), this enzyme has been confirmed as immunodominant, suggesting that it may assist in tissue migration of the larvae a critical task that *T. trichiura* must accomplish shortly after the hatching from the egg. Enolase and heat shock proteins have also been classified as exosome markers (Shears *et al.*, 2018; Buck *et al.*, 2014) in accordance with our findings of enolase lacking signal peptide. Likewise, GAPDH has been previously linked to fibronectin, laminin, entactin, and collagen binding (Gozalbo *et al.*, 1998) and Cass and collaborators (Cass *et al.*, 2007) suggested that in the case of *S. mansoni* this protein could be involved in the attachment of the eggs to host tissues or aid the passage of live eggs across host tissues to the external environment. Our results suggest GAPDH as having a relative abundance in both EE and FE that could align with Cass (Cass *et al.*, 2007) findings and warrant further study.

**Kunitz BPTI domain containing protein.** With lower abundance but strong immunogenicity presence in the FE, we identified KBDCP, a protease inhibitor protein part of the WAP domain-containing proteins strongly expressed in the anterior region of adult whipworms and likely secreted based on the presence of signal peptide (Foth *et al.*, 2014). Protease inhibitors are involved in protecting the nematodes from host proteinases; they modulate their activity and protect them from degradation. Also, they assist parasite survival by facilitating feeding and manipulating the host response to the parasite (Knox, 2007). Kunitz BPTI domain containing proteins are also the most abundant protease inhibitors across all nematodes species (International Helminth Genomes Consortium, 2018)

**Carbohydrate-binding module 14 domain containing protein.** Present only in the EE, we identified CBM14, a chitin binding domain protein associated with the formation of the eggshells or a related function due to the characteristic presence of chitin in the trichuris eggshell (Wharton and Jenkins, 1978; Foth *et al.*, 2014). Eggshell chitin synthesis starts at fertilization (Johnston *et al.*, 2010) and transcripts for proteins with chitin-binding domains have been described as upregulated in the female whipworm (Foth *et al.*, 2014) confirming the relevance of this finding.

### 5.2.2.3 Diagnostic applicability of the synthetic peptides designed from FE and EE

The advantage in utilizing the smaller amino acid sequences chosen for the design of the synthetic peptides is that these sequence regions can be carefully selected and are specific for *T. trichiura* with a predicted antigenicity. In contrast to utilizing whole proteins of larger size, the possibility of having crossed reactions is more significant due to the presence of common epitopes amongst them. In recent years, there exists a higher tendency to use synthetic peptides derived from key proteins to diagnose other parasitic diseases (List *et al.*, 2010; Intapan *et al.*, 2013).

Furthermore, the development of serological diagnosis is hampered by the limited availability of antigen. The antigen extracts need to be prepared from live worms. Access to worms from humans is scarce, and limited populations of NHP offer the possibility of harvesting parasites as an alternative source of parasitic material. Here we show the advantage of using the captive wild-caught population of the St. Kitts Biomedical Research Foundation & Virscio as disease and disease-free animal model. Varying methods of antigen preparation makes inter-laboratory standardization difficult. Therefore, the use of synthetic peptides as a diagnostic antigen is a good alternative. The peptide ELISA for detecting of IgG4-specific antibodies improved the diagnostic value for neurocysticercosis (Intapan *et al.*, 2008) and fascioliasis (Intapan *et al.*, 2005; Tantrawatpan *et al.*, 2007). Also, for filariasis (Pandiaraja *et al.*, 2010), cestodes such as *Echinococcus granulosus* (González-Sapienza *et al.*, 2000) and trematodes such as *S. mansoni* (Noya *et al.*, 2003; Oliveira *et al.*, 2006). Immunodiagnostic methods have expanded with time and now still remain one of the most robust tools for diagnostic of parasitic diseases.

Based on the sequences of our final four protein candidates characterized in our laboratory with the best immunogenic potential using saliva and serum from naturally infected nonhuman primates, four peptides were synthesized. The amino acid regions selected had no homology with other nematodes. To evaluate their diagnostic capacity, the indirect ELISA assays were performed with serum and saliva from naturally infected nonhuman primates and negative human controls. All the naturally infected positive samples were positive, and all the negative human samples were negative with all four peptide candidates. Therefore, it was not possible to infer further results regarding the sensitivity or the specificity data. Kunitz BPTI domain containing protein and VgNVD

showed the highest reactivity, while PCHTP-2 and CBM14 showed the lowest reactivity with saliva and serum. Saliva samples results, however, were more consistent across all peptides.

Efforts were made to acquire true negative samples from nonhuman primates after treatment, confirmed at necropsy and by histology of the cecum due to the prevalence of trichuriasis being so high on the island. Unfortunately, the positive biological samples had lost their diagnostic value when the disease-free biological samples were identified. Future studies with human positive and negative samples as well as nonhuman primate positive and true negative samples are warranted to further study the diagnostic potential of the four novel diagnostic peptides for *T. trichiura* identified in our work.



## 6 Conclusions

1. A wide range of nematode parasites can be found in captive AGMs on St. Kitts and effective anthelmintic protocols are needed to ensure these animals remain healthy in captivity.
2. All the nematodes identified in the AGMs on St. Kitts are potentially zoonotic and thus AGMs represent a threat to the health of people on the island.
3. In the absence of significant cestode and trematode infections, the IVAL treatment protocol would appear to be effective in controlling nematode infections in captive AGMs as long as sound husbandry practices are in place. In particular, thorough washing of fruits and vegetables, and insect pest control which all help prevent reinfections that can impact optimal health and behavior of study animals.
4. It is important to note that regular FECs will not detect all *T. trichiura* infections. There is no correlation between egg counts and total nematode or female counts at necropsy; therefore, full advantage should be taken of necropsied animals for parasite detection and surveillance.
5. The *T. trichiura* life cycle inside the host starts with the egg hatching and the release of the larva. This period of time remains as an undiagnosed stage. The proteins described in this doctoral thesis are directly exposed to the immune system during this undiagnosed time and, as we demonstrate, can elicit anti-*Trichuris* antibodies by the host, which may have diagnosis applicability.
6. Our study is the first effort to identify the proteome of the NE *T. trichiura* eggs as a novel source of potential diagnostic targets and provides details which might serve for improved diagnostics, identification of immunomodulators, and facilitate treatment and control of this neglected disease.
7. As the infective developmental stage of the nematode, the eggs signal the host interface with their shell surface antigens and the subsequent release of larvae and associated fluids as the first stimuli to the host's immune system. Later in infections, the NE eggs released by the females into the cecum and their secretomes would also be expected to stimulate the hosts' immune system. The NE egg proteome revealed common families of proteins which are known to play roles in energy and metabolism; cytoskeleton, muscle, and

motility; proteolysis; signaling; the stress response and detoxification; transcription and translation; and lipid binding and transport.

8. This initial list of *T. trichiura* egg proteins (proteome and antigenic profile) can be used in future research into the immunobiology and pathogenesis of human trichuriasis and the treatment of human intestinal immune-related diseases.
9. The designed synthetic peptides and confirmatory indirect ELISA results are promising and showed that the novel amino acid sequences chosen represent important candidates for future assay development and refinement with either positive human samples or true negative nonhuman primate samples.

## 7 Appendices

### 7.1 Appendix I. Karnovsky's fixative protocol

Karnovsky's fixative 3% Glutaraldehyde, 2% Formalin in 0.1M PO<sub>4</sub> buffer, pH 7.2

Materials:

1. 3, 2 mL vials of 8% glutaraldehyde
2. Distilled water
3. 3.2 mL of 10% formalin solution
4. 0.1 M Phosphate buffer pH 7.4 (Prepare ahead):
  1. 20.209 g of Sodium Phosphate dibasic (mw: 268 g/mol)
  2. 3.3994 g of Sodium Phosphate monobasic (mw: 138 g/mol)
  3. Add distilled water to 1L
  4. Adjust pH with HCl or NaOH

Protocol:

1. Take the one vial of 8% glutaraldehyde (2 mL)
2. Add 0.67 mL of distilled water to make 2.67 mL of 6% glutaraldehyde.
3. Take 1.068 mL 10% formalin and dilute in 1.602 mL of Na<sub>2</sub>HPO<sub>4</sub> Buffer to make 4% formalin solution.
4. Add 6% glutaraldehyde sol to 4% formalin solution 1:1 as needed.
5. Keep solutions separate until needed, any leftover mix can be saved at 4 °C for 1 month in a dark container.

## 7.2 Appendix II. Double centrifugation with Sheather's sugar flotation solution

### Materials:

1. Two small plastic containers
2. Cheesecloth square (4 layers)
3. Tongue depressor
4. 20 mL test tube; ensure that the top of the test tube is not cracked.
5. Bamboo sticks
6. Cover slip
7. Slide
8. Swing bucket centrifuge

### Protocol:

1. Label the test tube and slide with your sample numbers.
2. Weigh 1 gram of sample in the plastic container.
3. Use up to 15 mL of tap water to mix your sample. Be sure to mix it well to create a homogenous sample.
4. Set the cheesecloth over the second container and strain the sample. Use a small amount of water to rinse the first container.
5. Squeeze the cheesecloth to remove as much sample as possible.
6. Transfer the sample to the test tube. Use a small amount of water to rinse the container to recover all the sample. The total quantity of water should not exceed 20 mL (max capacity of the test tube).
7. Centrifuge at 500 x *g* for 5 minutes.
8. Decant the supernatant.
9. Add approximately 5 mL Sheather's sugar solution (1/4 of the test tube) and stir until the pellet has dissolved using a bamboo stick.
10. Place the test tube in the centrifuge and fill with Sheather's sugar solution – avoid creating bubbles. Continue to fill until there is a reverse meniscus on the surface.
11. Place a coverslip on the test tube and press down gently to create a seal.

12. Centrifuge again  $500 \times g$  for 5 minutes.
13. Allow the sample to sit 10 minutes for the eggs to rise to the cover slip. There is no maximum time period set. However, the cover slip must be removed and read prior to crystallization of the sugar (3-6 hrs).
14. Gently remove the coverslip from the test tube and place it on a microscope slide, at an angle initially to avoid trapping bubbles of air.
15. Complete the analysis of the slide using a light microscope 10x magnification.

### 7.3 Appendix III. Standard Operating Procedure for saliva collection

Purpose:

This SOP describes the procedure for collecting saliva from *C. sabaesus*.

Materials:

1. Extra-small chemical free braided cotton rolls (2)
2. 3 mL syringe (1)
3. Individually labeled zip top bags (1 per study subject)
4. Ice packs
5. Cooler
6. 15 mL Falcon tubes
7. Refrigerated Centrifuge
8. Micropipette
9. Micropipette tips
10. Eppendorf 2mL tubes
11. Eppendorf storage box
12. Eppendorf labels

Protocol:

1. Collection must be during the morning hours when circadian cycle changes in the salivary glands ensure optimal salivary flow and composition.
2. Record study subject number, time, and date of sample collection.
3. First, place 1 cotton roll under the upper lip on either side of the labial frenum.
4. Second, place 1 cotton roll under the lower lip on either side of the labial frenum.
5. Leave the cotton rolls in for a maximum of 5 min.
6. Assess the salivary flow by checking how full the cotton roll is after 2 to 3 min.
7. If cotton rolls are not filling up, meaning that salivary flow is low, gently massage them against the attached gingiva, aiming for the coronal-cervical junction and the gumline and

the rest of the mucobuccal folds avoiding the area of the 3<sup>rd</sup> molar where Stensen's duct from the parotid gland opens.

8. For the last minute, gently rub the cotton rolls against the hard and soft palates as well as the top of the tongue.
9. Gently remove the cotton rolls to avoid sloughing the mucosal lining and place them in the 3 mL syringes. Reconnect the plunger.
10. Place the labeled syringe in the prelabeled zip top bag and place it on ice or at 4 °C immediately.
11. Process the saliva within 2-3 hrs of collection.
12. Take the plunger off the syringe and place it, plunger end upwards, into a 15 mL falcon tube.
13. Centrifuge at 1500 x *g* at 4 °C for 20 min.
14. Remove the syringe containing the now dry cotton rolls and discard in biohazard bin.
15. Using a micropipette estimate the total amount of saliva collected.
16. Transfer the saliva into a pre labeled 2 mL Eppendorf tube and record the quantity as well as any other observations on consistency or color.
17. Add equal amounts of saliva conservation mix (1:1) (**Appendix IV**).
18. Freeze at -20 °C (for short term use up to 2 weeks) or -80 °C.
19. Avoid multiple freeze-thaw cycles.

## 7.4 Appendix IV. Saliva conservation mix

Saliva conservation mix (2x)

Materials

1. cOmplete™ Protease Inhibitor Cocktail Tablet, EDTA -free- (Roche ®) (2 tablets)
2. ProClin® (Sigma – Aldrich®) (100 µL)
3. PBS sterile (20 mL)
4. One 50 mL Falcon tube
5. Vortex
6. 100 µL Pipette and tips
7. 20 mL Pipette aid

Protocol:

1. Mix 2 tablets of protease inhibitor (cOmplete™ Protease Inhibitor Cocktail Tablet, EDTA - free - Roche ®) in 20 mL of PBS.
2. Add 100 µL of ProClin® (Sigma - Aldrich®).
3. Mix by vortexing until tablets have dissolved completely.
4. Store frozen -20° C until ready to use.
5. Defrost at 4 C°
6. Add to saliva samples 1:1



## 7.5 Appendix V. List of brand names and commercial addresses used

1. BMJ-III, Jiangsu, China
2. Olympus DP73 microscope, Tokyo, Japan
3. Roche<sup>®</sup>, Mannheim, Germany
4. Sigma-Aldrich<sup>®</sup>, MO, USA
5. Dremel<sup>®</sup>, Mount Prospect, IL, USA
6. Misonix, NY, USA
7. Bio-Rad<sup>®</sup> CA, USA
8. Balzer Union, Balzers, Liechtenstein
9. Zeiss Auriga, Oberkochen, Germany
10. BD Microlance<sup>™</sup>, Fraga, Huesca, Spain
11. Spartan Chemical Company Inc, Ohio, USA
12. Virox<sup>®</sup> Technologies Inc. Ontario, Canada
13. Envigo<sup>®</sup> Teklad 8773 primate biscuits, Indiana, USA
14. Lixit<sup>®</sup> water valves, California, USA
15. Neologic solutions<sup>©</sup>, South Carolina, USA
16. Sanitron<sup>©</sup> ultraviolet water purifiers, Atlantic Ultraviolet Corporation<sup>®</sup>, New York, USA
17. Avidity Science<sup>©</sup>, Wisconsin, USA
18. Droncit<sup>®</sup>, Kansas, USA
19. Valbazen<sup>®</sup>, Michigan, USA
20. Bioiniche Pharma USA LLC, IL, USA
21. AnaSed<sup>®</sup> Akorn, Inc., IL, USA.
22. Richmond<sup>™</sup>, NC, USA
23. BD Luer-Lok tip, NJ, USA
24. Falcon<sup>™</sup>, NY, USA
25. Noromectin<sup>®</sup>, Newry, Co. Down, Northern Ireland
26. Thermo Fisher Scientific, MA, USA
27. Novusbio<sup>™</sup> Novus Biologicals LLC, CO, USA
28. Abcam<sup>®</sup>, Cambridge, UK

29. Amersham™ Imager 600 (GE Healthcare®, IL, USA)
30. Pharmacia Biotech AB®, Uppsala, Sweden
31. GE Healthcare®, New Jersey, USA
32. Promega, Madison, WI, USA
33. AB SCIEX®, CA, USA
34. Nikkyo Technos Co., Ltd, Tokyo, Japan
35. LC Packings, A Dionex Company, Amsterdam, Netherlands
36. Applied Biosystems®/MDS Sciex, MA USA

## 7.6 Appendix VII. IACUC approvals for African green monkey samples



**IACUC Tissue/Sample Use Approval Letter**

**Approved:** IACUC Application for Collection of Samples and Tissues

**DATE:** 1/30/2018

**TO:** Dr. Patrick Kelly

**FROM:** Ross University Institutional Animal Care and Use Committee

**Project Title:** Immunodiagnostics for *Trichuris Trichiura*

The purpose of this memo is to verify that the Ross University Institutional Animal Care and Use Committee (IACUC) reviewed and granted approval of the above described form submission.

Sincerely,

A handwritten signature in blue ink, appearing to read "Sree", with a horizontal line underneath.

**Dr. SREEKUMARI RAJEEV**

**Chair, Institutional Animal Care and Use Committee**

# AXION RESEARCH FOUNDATION

Biomedical Research on the Central Nervous System

February 26, 2018

**IACUC #: AC18175**

(Please refer this number when  
inquiring about this project)

PRINCIPAL INVESTIGATOR: Shervin Liddie, Ph.D.

RxGen Inc.  
3 Science Park, 4<sup>th</sup> Flr  
New Haven, CT 065111

TITLE OF PROJECT: *Evaluation of the safety profile of Adeno-Associated Virus (AAV) vectors following single intravenous infusion dosing in African green monkeys*

CURRENT APPROVAL PERIOD: 02/23/18 TO 02/22/19

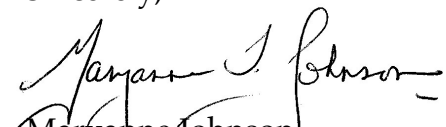
The IACUC Office granted approval for the use of animals in the project referenced above on 02/23/18. Please attach a copy of this approval to the approved protocol for your files.

According to Federal Regulations, approval of this protocol is effective for one year and approval may be renewed twice. If the project will extend past three years another new protocol application will be required for IACUC review. Prior to the expiration of initial approval and each of the two renewal periods, you will be asked to submit a short progress report if you wish approval extended for an additional year. If you do not renew approval, you will be unable to use or order any animals under this project.

The Axion Research Foundation / St. Kitts Biomedical Research Foundation, has an approved Animal Welfare Assurance number, A4384-01, from the Office of Laboratory Animal Welfare, National Institutes of Health, effective May 20, 2020.

If you have any questions, or require any additional assistance, please do not hesitate to call me.

Sincerely,

  
Maryanne Johnson  
Committee Secretary

100 Deepwood Drive  
Hamden, CT 06517-3415 USA  
203-773-9300  
FAX 203-776-2893

## 7.7 Appendix VIII. IRB approvals for human samples



## EXEMPTION CERTIFICATION

MEMO: Katalina Cruz, DDS, MSc  
PhD Candidate

FROM: Darryn Knobel, BVSc, MSc, MRCVS, PhD  
Institutional Review Board Chair

SUBJECT: Exemption Certification for Protocol No. 18-10-EX

DATE: June 14<sup>th</sup>, 2018

The Chair of the IRB determined that your project entitled: *Immunodiagnostics for Trichuris Trichiur*, meets federal criteria to qualify as an exempt study under 45 CFR 46.101(b)(4).

Because the study has been certified as exempt, you will not be required to complete continuation or final review reports. However, **it is your responsibility to notify the IRB prior to making any changes to the study.** Please note that **changes made to an exempt protocol may disqualify it from exempt status and require an expedited or full review.**

The IRB Office will hold your exemption application for six years. Before the end of the sixth year, you will be notified that your file will be closed and the application destroyed. If your project is still ongoing, you will need to contact the IRB Office upon receipt of that letter and follow the instructions for completing a new exemption application.

If you have questions or need additional information, please contact the Doris M. Castellanos at 401-1330 or [dcastellanos@rossvet.edu.kn](mailto:dcastellanos@rossvet.edu.kn).

**Darryn Knobel, BVSc MSc PhD MRCVS Dipl. ACVPM**  
**Chair, RUSVM Institutional Review Board**  
Professor of Epidemiology and Population Health  
Director, Center for Conservation Medicine and Ecosystem Health



## EXEMPTION CERTIFICATION

MEMO: Patrick Kelly, PhD  
Professor Small Animal Medicine

FROM: Darryn Knobel, BVSc, MSc, MRCVS, PhD  
Institutional Review Board Chair

SUBJECT: Exemption Certification for Protocol No. 18-11-EX

DATE: August 1<sup>st</sup>, 2018

The Chair of the IRB determined that your project entitled: *Immunodiagnosics for Trichuris Trichiur*, meets federal criteria to qualify as an exempt study under 45 CFR 46.101(b)(4).

Because the study has been certified as exempt, you will not be required to complete continuation or final review reports. However, **it is your responsibility to notify the IRB prior to making any changes to the study.** Please note that **changes made to an exempt protocol may disqualify it from exempt status and require an expedited or full review.**

The IRB Office will hold your exemption application for six years. Before the end of the sixth year, you will be notified that your file will be closed and the application destroyed. If your project is still ongoing, you will need to contact the IRB Office upon receipt of that letter and follow the instructions for completing a new exemption application.

If you have questions or need additional information, please contact the Doris M. Castellanos at 401-1330 or [dcastellanos@rossvet.edu.kn](mailto:dcastellanos@rossvet.edu.kn).

**Darryn Knobel, BVSc MSc PhD MRCVS Dipl. ACVPM**  
**Chair, RUSVM Institutional Review Board**  
**Professor of Epidemiology and Population Health**  
**Director, Center for Conservation Medicine and Ecosystem Health**



## 8 References

- Abee, C. R., Mansfield, K., Tardif, S. D. and Morris, T. (2012). Parasitic diseases of nonhuman primates. In: *Nonhuman Primates in Biomedical Research: Diseases*, 2nd ed., (pp. 243-244). London, Elsevier Academic.
- Acevedo, N., Mohr, J., Zakzuk, J., Samonig, M., Briza, P., Erler, A., Pomés A., Huber C.G., Ferreira F., Caraballo L. (2013). Proteomic and Immunochemical Characterization of Glutathione Transferase as a New Allergen of the Nematode *Ascaris lumbricoides*. *PLoS ONE*, 8(11), e78353.
- Acha, P. N., and B. Szyfres. (2003). Zoonoses and communicable diseases common to man and animals: Volume 3. Parasitoses. III. Pan American Health Organization, New York, New York.
- Amenu, K., Tesfaye, D., Tilahun, G. A., & Mekibib, B. (2015). Gastrointestinal parasites of vervet monkeys around Lake Hawassa recreational sites, southern Ethiopia. *Comparative Clinical Pathology*, 24(6), 1491-1496. <https://doi.org/10.1007/s00580-015-2105-0>
- Appleton, C., & White, B. (1990). The structure of the shell and polar plugs of the egg of the whipworm, *Trichuris trichiura* (Nematoda: Trichuridae) from the Samango monkey (*Cercopithecus albogularis*). *The Onderstepoort Journal of Veterinary Research*, 56, 219–221.
- Areekul, P., Putaporntip, C., Pattanawong, U., Sitthicharoenchai, P., & Jongwutiwes, S. (2010). *Trichuris vulpis* and *Trichuris trichiura* infections among schoolchildren of a rural community in northwestern Thailand: The possible role of dogs in disease transmission. *Asian Biomedicine*, 4(1), 49–60. <https://doi.org/10.2478/abm-2010-0006>
- Armstrong, S. D., Babayan, S. A., Lhermitte-Vallarino, N., Gray, N., Xia, D., Martin, C., Kumar, S., Taylor, D. W., Blaxter, M. L., Wastling, J. M., Makepeace, B. L. (2014). Comparative Analysis of the Secretome from a Model Filarial Nematode (*Litomosoides sigmodontis*) Reveals Maximal Diversity in Gravid Female Parasites. *Molecular and Cellular Proteomics*, 13(10):2527–44.
- Association of Primate Veterinarians (nd.) Nonhuman primate formulary in <https://www.primat vets.org/education--resources>, accessed May 4, 2020.

- Bancroft, A. J., Levy, C. W., Jowitt, T. A., Hayes, K. S., Thompson, S., Mckenzie, E. A., Ball, M. D., Dubaissi, E., France, A. P., Bellina, B., Sharpe, C., Mironov, A., Brown, S. L., Cook, P. C., MacDonald, A. S., Thornton, D. J., & Grecis, R. K. (2019). The major secreted protein of the whipworm parasite tethers to matrix and inhibits interleukin-13 function. *Nature Communications*, 10(1), 1–11. <https://doi.org/10.1038/s41467-019-09996-z>
- Barbosa, A. da S., Pinheiro, J. L., dos Santos, C. R., de Lima, C. S. C. C., Dib, L. V., Echarte, G. V., Augusto, A. M., Bastos, A. C. M. P., Antunes Uchôa, C. M., Bastos, O. M. P., Santos, F. N., Fonseca, A. B. M., & Amendoeira, M. R. R. (2020). Gastrointestinal Parasites in Captive Animals at the Rio de Janeiro Zoo. *Acta Parasitologica*, 65(1), 237–249. <https://doi.org/10.2478/s11686-019-00145-6>
- Berger, D. S. (2020). *Infectious Diseases of Saint Kitts and Nevis*. GIDEON Informatics Inc. Accessed online <https://books.google.es/books?id=lvzVDwAAQBAJ&dq>
- Bernal, D., Carpena, I., Espert, A. M., De la Rubia, J. E., Esteban, J. G., Toledo, R., Marcilla, A. (2006). Identification of proteins in excretory/secretory extracts of *Echinostoma friedi* (Trematoda) from chronic and acute infections. *Proteomics*, 6(9), 2835–43.
- Betson, M., Sjøe, M. J., & Nejsum, P. (2015). Human trichuriasis: Whipworm genetics, phylogeny, transmission and future research directions. *Current Tropical Medicine Reports*, 2(4), 209–217.
- Blersch, R., Archer, C., Suleman, E., Young, C., Kindler, D., Barrett, L., & Henzi, S. P. (2019). Gastrointestinal Parasites of Vervet Monkeys (*Chlorocebus pygerythrus*) in a High Latitude, Semi-Arid Region of South Africa. *Journal of Parasitology*, 105(4), 630–637. <https://doi.org/10.1645/19-19>
- Blum M, Chang H, Chuguransky S, Grego T, Kandasaamy S, Mitchell A, Nuka G, Paysan-Lafosse T, Qureshi M, Raj S, Richardson L, Salazar GA, Williams L, Bork P, Bridge A, Gough J, Haft DH, Letunic I, Marchler-Bauer A, Mi H, Natale DA, Necci M, Orengo CA, Pandurangan AP, Rivoire C, Sigrist CJA, Sillitoe I, Thanki N, Thomas PD, Tosatto SCE, Wu CH, Bateman A and Finn RD (2020). The InterPro protein families and domains database: 20 years on *Nucleic Acids Research*. doi: 10.1093/nar/gkaa977 <http://www.ebi.ac.uk/interpro/>

- Bogitsh, B. J., Carter, C. E., & Oeltmann, T. N. (2013). Intestinal Nematodes. In *Human Parasitology* (pp. 291–327). Elsevier. <https://doi.org/10.1016/B978-0-12-415915-0.00016-9>
- Briggs, N., Wei, J., Versteeg, L., Zhan, B., Keegan, B., Damania, A., Pollet, J., Hayes, K. S., Beaumier, C., Seid, C. A., Leong, J., Grecis, R. K., Bottazzi, M. E., Sastry, K. J., & Hotez, P. J. (2018). *Trichuris muris* whey acidic protein induces type 2 protective immunity against whipworm. *PLoS Pathogens*, 14(8), e1007273. <https://doi.org/10.1371/journal.ppat.1007273>
- Buck, A. H., Coakley, G., Simbari, F., McSorley, H. J., Quintana, J. F., Le Bihan, T., Kumar, S., Abreu-Goodger, C., Lear, M., Harcus, Y., Ceroni, A., Babayan, S. A., Blaxter, M., Ivens, A., Maizels, R. M. (2014). Exosomes secreted by nematode parasites transfer small RNAs to mammalian cells and modulate innate immunity. *Nature Communications*, 5(1), 1–12.
- Bundy, D. A. P., & Cooper, E. S. (1989). *Trichuris* and Trichuriasis in Humans. In *Advances in Parasitology*, (Vol. 28, pp. 107–173). Elsevier. [https://doi.org/10.1016/S0065-308X\(08\)60332-2](https://doi.org/10.1016/S0065-308X(08)60332-2)
- Bradford, M.M. A. (1976). Rapid and sensitive method for the quantitation of microgram quantities of protein utilizing the principle of protein-dye binding. *Analytical Biochemistry*, 72, 248–54.
- Calle, P. P. and Joslin, J. O. (2014). New world and old world monkeys. In: Fowler, M. E. & Miller, R. E. (Eds.), *Fowler's Zoo and Wild Animal Medicine*, 8th ed., (pp. 301-335). St Louis, Elsevier Saunders.
- Cameron, T. W. M. (1928). A New Definitive Host for *Schistosoma mansoni*. *Journal of Helminthology*, 6(4), 219–222. <https://doi.org/10.1017/S0022149X00002364>
- Cameron, T. W. M. (1930). The Species of *Subulura* Molin in Primates. *Journal of Helminthology*, 8(01), 49. <https://doi.org/10.1017/S0022149X00002510>
- Cantacessi, C., Mitreva, M., Jex, A. R., Young, N. D., Campbell, B. E., Hall, R. S., Doyle, M. A., Ralph, S. A., Rabelo, E. M., Ranganathan, S., Sternberg, P. W., Loukas, A., & Gasser, R. B. (2010). Massively Parallel Sequencing and Analysis of the *Necator americanus* Transcriptome. *PLoS Neglected Tropical Diseases*, 4(5). <https://doi.org/10.1371/journal.pntd.0000684>

- Cardoso, R.M.F., Silva C.H.T.P., de Araújo, A.P.U., Tanaka, T., Tanaka, M., Garratt, R.C. (2004). Structure of the cytosolic Cu, Zn superoxide dismutase from *Schistosoma mansoni*. *Acta Crystallographica Section D*, 60(9), 1569–78.
- Cavallero, S., De Liberato, C., Friedrich, K. G., Di Cave, D., Masella, V., D'Amelio, S., & Berrilli, F. (2015). Genetic heterogeneity and phylogeny of *Trichuris* spp. From captive nonhuman primates based on ribosomal DNA sequence data. *Infection, Genetics and Evolution*, 34, 450–456. <https://doi.org/10.1016/j.meegid.2015.06.009>
- Cavallero, S., Nejsum, P., Cutillas, C., Callejón, R., Doležalová, J., Modrý, D., & D'Amelio, S. (2019). Insights into the molecular systematics of *Trichuris* infecting captive primates based on mitochondrial DNA analysis. *Veterinary Parasitology*, 272, 23–30. <https://doi.org/10.1016/j.vetpar.2019.06.019>
- Callejón, R., Nadler, S., De Rojas, M., Zurita, A., Petrášová, J., & Cutillas, C. (2013). Molecular characterization and phylogeny of whipworm nematodes inferred from DNA sequences of cox1 mtDNA and 18S rDNA. *Parasitology Research*, 112(11), 3933–3949. <https://doi.org/10.1007/s00436-013-3584-z>
- Cass, C.L., Johnson J.R., Califf, L.L., Xu T., Hernandez, H.J., Stadecker, M.J., Yates J. R, Williams, D. L. (2007). Proteomic Analysis of *Schistosoma mansoni* Egg Secretions. *Molecular and Biochemical Parasitology*, 155(2), 84–93.
- CDC, (2013) Parasites – *Trichuriasis* (also known as whipworm infection) <https://www.cdc.gov/parasites/whipworm/>).
- CDC, (2016) Parasite comparative morphology tables. Accessed May 2020. <https://www.cdc.gov/dpdx/diagnosticProcedures/stool/morphcomp.html>
- Chapman, C. A., Friant, S., Godfrey, K., Liu, C., Sakar, D., Schoof, V. A. M., Sengupta, R., Twinomugisha, D., Valenta, K., & Goldberg, T. L. (2016). Social Behaviours and Networks of Vervet Monkeys Are Influenced by Gastrointestinal Parasites. *PLoS ONE*, 11(8). <https://doi.org/10.1371/journal.pone.0161113>
- Chen, J-S., Sappington T.W., Raikhel, AS. (1997) Extensive Sequence Conservation Among Insect, Nematode, and Vertebrate Vitellogenins Reveals Ancient Common Ancestry. *Journal of Molecular Evolution*, 44(4):440–51.

- Chehayeb, J.F., Robertson, A.P., Martin, R.J., Geary, T.G. (2014). Proteomic Analysis of Adult *Ascaris suum* Fluid Compartments and Secretory Products. Jex AR, editor. *PLoS Neglected Tropical Diseases*, 8(6): e2939.
- Cogswell F (2007) Parasites of nonhuman primates. In: Flynn RJ, Baker, D G., editor. *Flynn's Parasites of Laboratory Animals*. Ames, Iowa: Blackwell Pub. 693–743.
- Cooper, E. S., Bundy, D. A. P., & Henry, F. J. (1986). CHRONIC DYSENTERY, STUNTING, AND WHIPWORM INFESTATION. *The Lancet*, 328(8501), 280–281. [https://doi.org/10.1016/S0140-6736\(86\)92093-3](https://doi.org/10.1016/S0140-6736(86)92093-3)
- Cross, J. H. (1992). Intestinal capillariasis. *Clinical Microbiology Reviews*, 5(2), 120–129. <https://doi.org/10.1128/CMR.5.2.120>
- Cruz, K., Marcilla, A., Kelly, P., Vandenplas, M., Osuna, A., & Trelis, M. (2021). *Trichuris trichiura* egg extract proteome reveals potential diagnostic targets and immunomodulators. *PLOS Neglected Tropical Diseases*, 15(3), e0009221. <https://doi.org/10.1371/journal.pntd.0009221>
- Cruz, K., Corey, T. M., Vandenplas, M., Trelis, M., Osuna, A., & Kelly, P. J. (2021). Case report: Control of intestinal nematodes in captive *Chlorocebus sabaeus*. *The Onderstepoort Journal of Veterinary Research*, 88(1).
- da Silva, M. B., Urrego A., J. R., Oviedo, Y., Cooper, P. J., Pacheco, L. G. C., Pinheiro, C. S., Ferreira, F., Briza, P., Alcántara-Neves, N. M. (2018). The somatic proteins of *Toxocara canis* larvae and excretory-secretory products revealed by proteomics. *Veterinary Parasitology*, 259:25–34.
- Dalimi, A., Motamedi, G., Hablolvarid, M. H., & Abdoli, A. (2016). Alimentary tract parasites of vervet monkeys (*Cercopithecus aethiops*): A potential reservoir for human transmission. *Archives of Razi Institute*, 71, 277–281. <https://doi.org/10.22034/ari.2016.107513>
- Dayan, A. D. (2003). Albendazole, mebendazole and praziquantel. Review of non-clinical toxicity and pharmacokinetics. *Acta Tropica*, 86(2), 141–159. [https://doi.org/10.1016/S0001-706X\(03\)00031-7](https://doi.org/10.1016/S0001-706X(03)00031-7)

- Dea-Ayuela, M.A., Bolás-Fernández, F. (2005). Two-dimensional electrophoresis and mass spectrometry for the identification of species-specific *Trichinella* antigens. *Veterinary Parasitology*, 132(1), 43–9.
- De la Torre-Escudero, E., Manzano-Román, R., Valero, L., Oleaga, A., Pérez-Sánchez, R., Hernández-González, A., Siles-Lucas, M. (2011). Comparative proteomic analysis of *Fasciola hepatica* juveniles and *Schistosoma bovis schistosomula*. *Journal of Proteomics*, 74(9), 1534–44.
- Dige, A., Rasmussen, T. K., Nejsum, P., Hagemann-Madsen, R., Williams, A. R., Agnholt, J., Dahlerup, J. F., & Hvas, C. L. (2017). Mucosal and systemic immune modulation by *Trichuris trichiura* in a self-infected individual. *Parasite Immunology*, 39(1), e12394. <https://doi.org/10.1111/pim.12394>
- Dore, K. M., Gallagher, C. and Mill, C.A. (2021). Estimation of green monkey population size in St. Kitts using telemetry and home range analysis. Unpublished manuscript.
- Faulkner, H., Turner, J., Kamgno, J., Pion, S. D., Boussinesq, M., & Bradley, J. E. (2002). Age- and Infection Intensity–Dependent Cytokine and Antibody Production in Human Trichuriasis: The Importance of IgE. *The Journal of Infectious Diseases*, 185(5), 665–672. <https://doi.org/10.1086/339005>
- Gaetano, T. J., Danzy, J., Mtshali, M. S., Theron, N., Schmitt, C. A., Grobler, J. P., Freimer, N., & Turner, T. R. (2014). Mapping Correlates of Parasitism in Wild South African Vervet Monkeys (*Chlorocebus aethiops*). *South African Journal of Wildlife Research*, 44(1), 56–70. <https://doi.org/10.3957/056.044.0105>
- Gallagher, C., Beierschmitt, A., Cruz, K., Choo, J., & Ketzis, J. (2019). Should monkeys wash their hands and feet: A pilot-study on sources of zoonotic parasite exposure. *One Health*, 7, 100088. <https://doi.org/10.1016/j.onehlt.2019.100088>
- Ghai, R. R., Simons, N. D., Chapman, C. A., Omeja, P. A., Davies, T. J., Ting, N., & Goldberg, T. L. (2014). Hidden Population Structure and Cross-species Transmission of Whipworms (*Trichuris* sp.) in Humans and Nonhuman Primates in Uganda. *PLoS Neglected Tropical Diseases*, 8(10), e3256. <https://doi.org/10.1371/journal.pntd.0003256>
- Gillespie, T. R., Greiner, E. C., & Chapman, C. A. (2004). Gastrointestinal parasites of the guenons of western Uganda. *Journal of Parasitology*, 90(6), 1356–1360.

- Geary, T. G., Woo, K., McCarthy, J. S., Mackenzie, C. D., Horton, J., Prichard, R. K., de Silva, N. R., Olliaro, P. L., Lazdins-Helds, J. K., Engels, D. A., & others. (2010). Unresolved issues in anthelmintic pharmacology for helminthiasis of humans. *International Journal for Parasitology*, 40(1), 1–13.
- Gomez-Samblas, M., García-Rodríguez, J. J., Trelis, M., Bernal, D., Lopez-Jaramillo, F. J., Santoyo-Gonzalez, F., Vilchez, S., Espino, A. M., Bolás-Fernández, F., & Osuna, A. (2017). Self-adjuvanting C18 lipid vinyl sulfone-PP2A vaccine: Study of the induced immunomodulation against *Trichuris muris* infection. *Open Biology*, 7(4), 170031. <https://doi.org/10.1098/rsob.170031>
- González-Sapienza, G., Lorenzo, C., & Nieto, A. (2000). Improved Immunodiagnosis of Cystic Hydatid Disease by Using a Synthetic Peptide with Higher Diagnostic Value Than That of Its Parent Protein, *Echinococcus granulosus* Antigen B. *Journal of Clinical Microbiology*, 38(11), 3979–3983.
- Grzelak, S., Moskwa, B., Bień, J. (2018). *Trichinella britovi* muscle larvae and adult worms: stage-specific and common antigens detected by two-dimensional gel electrophoresis-based immunoblotting. *Parasite and Vectors*, 11(1).
- Hewitt, R., & Willingham, A. L. (2019). Status of Schistosomiasis Elimination in the Caribbean Region. *Tropical Medicine and Infectious Disease*, 4(1). <https://doi.org/10.3390/tropicalmed4010024>
- Else, K. J., Keiser, J., Holland, C. V., Grecis, R. K., Sattelle, D. B., Fujiwara, R. T., Bueno, L. L., Asaolu, S. O., Sowemimo, O. A., & Cooper, P. J. (2020). Whipworm and roundworm infections. *Nature Reviews Disease Primers*, 6(1), 1–23. <https://doi.org/10.1038/s41572-020-0171-3>
- Entrocasso, C., Alvarez, L., Manazza, J., Lifschitz, A., Borda, B., Virkel, G., Mottier, L., & Lanusse, C. (2008). Clinical efficacy assessment of the albendazole–ivermectin combination in lambs parasitized with resistant nematodes. *Veterinary Parasitology*, 155(3), 249–256. <https://doi.org/10.1016/j.vetpar.2008.04.015>
- Emikpe, B. O., Ayoade, G. O., Ohore, O. G., Olaniyan, O. O. and Akusu, M. O. (2002). Fatal trichuriasis in a captive baboon (*Papio anubis*) in Ibadan Nigeria: A case report. *Tropical Veterinarian*. 20: 36-39.

- Eo, K.-Y., Seo, M.-G., Lee, H.-H., Jung, Y.-M., Kwak, D., & Kwon, O.-D. (2018). Severe whipworm (*Trichuris* spp.) infection in the hamadryas baboon (*Papio hamadryas*). *Journal of Veterinary Medical Science*, 17 – 0568. <https://doi.org/10.1292/jvms.17-0568>
- El-Sherbini, G. T., & El-Sherbini, E. T. (2011). The role of cockroaches and flies in mechanical transmission of medical important parasites. *Journal of Entomology and Nematology*, 3(7), 98–104.
- Evans, A.C., Marcus M.B, Manson R. J, & Steel R. (1996). Late stone-age coprolite reveals evidence of prehistoric parasitism. *South African Medical Journal*, 86 (3), 274–275.
- Fahmy, M. A. M. (1954). An investigation on the life cycle of *Trichuris muris*. *Parasitology*, 44(1–2), 50. <https://doi.org/10.1017/S003118200001876X>
- Foth, B. J., Tsai, I. J., Reid, A. J., Bancroft, A. J., Nichol, S., Tracey, A., Holroyd, N., Cotton, J. A., Stanley, E. J., Zarowiecki, M., Liu, J. Z., Huckvale, T., Cooper, P. J., Grencis, R. K., Berriman, M. (2014). Whipworm genome and dual-species transcriptome analyses provide molecular insights into an intimate host-parasite interaction. *Nature Genetics*, 46(7), 693–700.
- Fernández-Soto, P., Fernández-Medina, C., Cruz-Fernández, S., Crego-Vicente, B., Febrer-Sendra, B., García-Bernalt Diego, J., Gorgojo-Galindo, Ó., López-Abán, J., Vicente Santiago, B., & Muro Álvarez, A. (2020). Whip-LAMP: A novel LAMP assay for the detection of *Trichuris muris*-derived DNA in stool and urine samples in a murine experimental infection model. *Parasites & Vectors*, 13(1), 552. <https://doi.org/10.1186/s13071-020-04435-1>
- Fripp, P. J., & Kaschula, V. R. (1974). The presence of *Capillaria hepatica* (Bancroft, 1893) Travassos, 1915 in a vervet monkey *Cercopithecus aethiops*. *The South African Journal of Medical Sciences*, 39(2), 85.
- Gozalbo, D., Gil-Navarro, I., Azorín, I., Renau-Piqueras, J., Martínez, J.P., Gil, M.L. (1998). The Cell Wall-Associated Glyceraldehyde-3-Phosphate Dehydrogenase of *Candida albicans* Is Also a Fibronectin and Laminin Binding Protein. *Infection and Immunity*, 66(5), 2052–9.
- Hansen, E. P., Kringel, H., Williams, A. R., & Nejsum, P. (2015). Secretion of RNA-Containing Extracellular Vesicles by the Porcine Whipworm, *Trichuris suis*. *Journal of Parasitology*, 101(3), 336–340. <https://doi.org/10.1645/14-714.1>



- Hansen, E. P., Tejedor, A. M., Thamsborg, S. M., Alstrup Hansen, T. V., Dahlerup, J. F., & Nejsum, P. (2016). Faecal egg counts and expulsion dynamics of the whipworm, *Trichuris trichiura* following self-infection. *Journal of Helminthology*, 90(03), 298–302. <https://doi.org/10.1017/S0022149X1500019X>
- Hasegawa, H. (2009). Useful diagnostic references and images of protozoans, helminths, and nematodes commonly found in wild primates. *Primate Parasite Ecology*, 507–513.
- Hasegawa, H., Modrý, D., Kitagawa, M., Shutt, K. A., Todd, A., Kalousová, B., Profousová, I., & Petrželková, K. J. (2014). Humans and Great Apes Cohabiting the Forest Ecosystem in Central African Republic Harbour the Same Hookworms. *PLOS Neglected Tropical Diseases*, 8(3), e2715. <https://doi.org/10.1371/journal.pntd.0002715>
- Hawash, M. B. F., Betson, M., Al-Jubury, A., Ketzis, J., LeeWillingham, A., Bertelsen, M. F., Cooper, P.J., Littlewood, D.T.J., Zhu, X.Q. and Nejsum, P. (2016). Whipworms in humans and pigs: origins and demography. *Parasites & Vectors*, 9, 37. <https://doi.org/10.1186/s13071-016-1325-8>
- Hayes, K. S., Bancroft, A. J., Goldrick, M., Portsmouth, C., Roberts, I. S., & Grencis, R. K. (2010). Exploitation of the Intestinal Microflora by the Parasitic Nematode *Trichuris muris*. *Science*, 328(5984), 1391–1394. <https://doi.org/10.1126/science.1187703>
- Hayon, J., Weatherhead, J., Hotez, P. J., Bottazzi, M. E., & Zhan, B. (2021). Advances in vaccine development for human trichuriasis. *Parasitology*, 1–12. <https://doi.org/10.1017/S0031182021000500>
- Hazell, L., Braun, L., & Templeton, M. R. (2019). Ultraviolet sensitivity of WASH (water, sanitation, and hygiene) -related helminths: A systematic review. *PLOS Neglected Tropical Diseases*, 13(9), e0007777. <https://doi.org/10.1371/journal.pntd.0007777>
- Hennessy, A., Phippard, A. F., Harewood, W. J., Horam, C. J. and Horvath, J. S. (1994). Helminthic infestation complicated by intussusception in baboons (*Papio hamadryas*). *Laboratory Animals*, 28: 270-273.
- Hewitson, J. P., Filbey, K. J., Grainger, J. R., Dowle, A. A., Pearson, M., Murray, J., Harcus, Y., Maizels, R. M. (2011). *Heligmosomoides polygyrus* Elicits a Dominant Nonprotective Antibody

- Response Directed against Restricted Glycan and Peptide Epitopes. *Journal of Immunology*, 187(9), 4764–77.
- Hewitson, J. P., Ivens, A. C., Harcus, Y., Filbey, K. J., McSorley, H. J., Murray, J., Bridgett, S., Ashford, D., Dowle, A. A., Maizels, R. M. (2013). Secretion of Protective Antigens by Tissue-Stage Nematode Larvae Revealed by Proteomic Analysis and Vaccination-Induced Sterile Immunity. *PLoS Pathogens*, 9(8), e1003492.
- Higón, M., Monteagudo, C., Fried, B., Esteban, J. G., Toledo, R., Marcilla, A. (2008). Molecular cloning and characterization of *Echinostoma caproni* heat shock protein-70 and differential expression in the parasite derived from low- and high-compatible hosts. *Parasitology*, 135(12), 1469–77.
- Hotez PJ, Brindley PJ, Bethony JM, King CH, Pearce EJ, *et al.* (2008). Helminth infections: the great neglected tropical diseases. *The Journal of Clinical Investigation* 118:1311–1321.
- Hu, J., Bae, Y.-K., Knobel, K. M., & Barr, M. M. (2006). Casein Kinase II and Calcineurin Modulate TRPP Function and Ciliary Localization. *Molecular Biology of the Cell*, 17, 12.
- Humphries, D. L., Scott, M. E., & Vermund, S. H. (Eds.). (2021). Nutrition and Infectious Diseases: Shifting the Clinical Paradigm. *Springer International Publishing*.  
<https://doi.org/10.1007/978-3-030-56913-6>
- Ibáñez-Shimabukuro, M., Rey-Burusco, M. F., Gabrielsen, M., Franchini, G. R., Riboldi-Tunncliffe, A., Roe, A. J., Griffiths, K., Cooper, A., Córscico, B., Kennedy, M. W., & Smith, B. O. (2019). Structure and ligand binding of As-p18, an extracellular fatty acid binding protein from the eggs of a parasitic nematode. *Bioscience Reports*, 39(7).  
<https://doi.org/10.1042/BSR20191292>
- International Helminth Genomes Consortium. (2018). Comparative genomics of the major parasitic worms. *Nature Genetics*, 51(1), 163.
- Intapan, P. M., Sanpool, O., Janwan, P., Laummaunwai, P., Morakote, N., Kong, Y., & Maleewong, W. (2013). Evaluation of IgG4 Subclass Antibody Detection by Peptide-Based ELISA for the Diagnosis of Human Paragonimiasis Heterotrema. *The Korean Journal of Parasitology*, 51(6), 763–766. <https://doi.org/10.3347/kjp.2013.51.6.763>

- Intapan, P. M., Khotsri, P., Kanpittaya, J., Chotmongkol, V., Maleewong, W., & Morakote, N. (2008). *Evaluation of IgG4 and Total IgG Anti- bodies against Cysticerci and Peptide Antigens for the Diagnosis of Human Neurocysticercosis by ELISA. Asian Pacific Journal of Allergy and Immunology, 26: 237-244.*
- Intapan, P. M., Tantrawatpan, C., Maleewong, W., Wongkham, S., Wongkham, C., & Nakashima, K. (2005). Potent epitopes derived from *Fasciola gigantica* cathepsin L1 in peptide-based immunoassay for the serodiagnosis of human fascioliasis. *Diagnostic Microbiology and Infectious Disease, 53(2)*, 125–129. <https://doi.org/10.1016/j.diagmicrobio.2005.05.010>
- James, S. L., Abate, D., Abate, K. H., Abay, S. M., Abbafati, C., Abbasi, N., Abbastabar, H., Abd-Allah, F., Abdela, J., Abdelalim, A., Abdollahpour, I., Abdulkader, R. S., Abebe, Z., Abera, S. F., Abil, O. Z., Abraha, H. N., Abu-Raddad, L. J., Abu-Rmeileh, N. M. E., Accrombessi, M. M. K., Murray, C. J. L. (2018). Global, regional, and national incidence, prevalence, and years lived with disability for 354 diseases and injuries for 195 countries and territories, 1990–2017: A systematic analysis for the Global Burden of Disease Study 2017. *The Lancet, 392(10159)*, 1789–1858. [https://doi.org/10.1016/S0140-6736\(18\)32279-7](https://doi.org/10.1016/S0140-6736(18)32279-7)
- Johnston, W. L., Krizus, A., & Dennis, J. W. (2010). Eggshell Chitin and Chitin-Interacting Proteins Prevent Polyspermy in *C. elegans*. *Current Biology, 20(21)*, 1932–1937. <https://doi.org/10.1016/j.cub.2010.09.059>
- Jourdan, P. M., Lamberton, P. H. L., Fenwick, A., & Addiss, D. G. (2018). Soil-transmitted helminth infections. *The Lancet, 391(10117)*, 252–265. [https://doi.org/10.1016/S0140-6736\(17\)31930-X](https://doi.org/10.1016/S0140-6736(17)31930-X)
- Jouvin, M-H., Kinet, J-P. *Trichuris suis* ova: Testing a helminth-based therapy as an extension of the hygiene hypothesis. (2012). *Journal of Allergy and Clinical Immunology, 130(1)*, 3–10.
- Junge RE. Prosimians. In: Fowler ME, Miller RE, editors. *Zoo and wild animal medicine*. 8th edition. St. Louis (MO); 2015. Page. 311.
- Justine, J. L. (1988). [*Capillaria brochieri* n. sp. (Nematoda: Capillariinae) intestinal parasite of the chimpanzee (*Pan paniscus*) in Zaire]. *Annales De Parasitologie Humaine Et Comparee, 63(6)*, 420–438. <https://doi.org/10.1051/parasite/1988636420>

- Kagira, J. M., Mulei, I., Oluoch, G., Waititu, K., Maingi, N., & Ngotho, M. (2011). High Efficacy of Combined Albendazole and Ivermectin Treatment Against Gastrointestinal Nematodes in Vervet Monkeys and Baboons. *Scandinavian Journal of Laboratory Animal Science.*, 38(3), 187–193.
- Kaminsky, R. G., Castillo, R. V., & Flores, C. A. (2015). Growth retardation and severe anemia in children with *Trichuris* dysenteric syndrome. *Asian Pacific Journal of Tropical Biomedicine*, 5(7), 591–597. <https://doi.org/10.1016/j.apjtb.2015.05.005>
- Kannangara, D. W. W. (1975). A comparison of post-mortem analysis of helminths with faecal egg counts. *Transactions of the Royal Society of Tropical Medicine and Hygiene*, 69(4), 406–409.
- Khuroo, M. S., Khuroo, M. S., & Khuroo, N. S. (2010). *Trichuris* dysentery syndrome: A common cause of chronic iron deficiency anemia in adults in an endemic area (with videos). *Gastrointestinal Endoscopy*, 71(1), 200–204. <https://doi.org/10.1016/j.gie.2009.08.002>
- Kim, T.S., Jung, Y., Na, B-K., Kim, K.S., Chung, P.R. (2000). Molecular Cloning and Expression of Cu/Zn-Containing Superoxide Dismutase from *Fasciola hepatica*. *Infection and Immunity*, 68(7), 3941–8.
- Kłapeć, T., & Borecka, A. (2012). Contamination of vegetables, fruits and soil with geohelminths eggs on organic farms in Poland. *Annals of Agricultural and Environmental Medicine*, 19(3), 5.
- Knox, D. P. (2007). Proteinase inhibitors and helminth parasite infection. *Parasite Immunology*, 29(2), 57–71. <https://doi.org/10.1111/j.1365-3024.2006.00913.x>
- Kolaskar, A. S., & Tongaonkar, P. C. (1990). A semi-empirical method for prediction of antigenic determinants on protein antigens. *FEBS Letters*, 276(1–2), 172–174. [https://doi.org/10.1016/0014-5793\(90\)80535-q](https://doi.org/10.1016/0014-5793(90)80535-q)
- Kooriyama, T., Hasegawa, H., Shimozuru, M., Tsubota, T., Nishida, T., & Iwaki, T. (2012). Parasitology of five primates in Mahale Mountains National Park, Tanzania. *Primates*, 53(4), 365–375. <https://doi.org/10.1007/s10329-012-0311-9>

- Kouassi, R. Y. W., McGraw, S. W., Yao, P. K., Abou-Bacar, A., Brunet, J., Pesson, B., Bonfoh, B., N'goran, E. K., & Candolfi, E. (2015). Diversity and prevalence of gastrointestinal parasites in seven non-human primates of the Taï National Park, Côte d'Ivoire. *Parasite*, 22, 1. <https://doi.org/10.1051/parasite/2015001>
- Lai, H.-J., Lo, S. J., Kage-Nakadai, E., Mitani, S., & Xue, D. (2009). The Roles and Acting Mechanism of *Caenorhabditis elegans* DNase II Genes in Apoptotic DNA Degradation and Development. *PLoS ONE*, 4(10). <https://doi.org/10.1371/journal.pone.0007348>
- Le, L., Khatoon, S., Jiménez, P., Peterson, C., Kernen, R., Zhang, W., Molehin, A. J., Lazarus, S., Sudduth, J., May, J., Karmakar, S., Rojo, J. U., Ahmad, G., Torben, W., Carey, D., Wolf, R. F., Papin, J. F., & Siddiqui, A. A. (2020). Chronic whipworm infection exacerbates *Schistosoma mansoni* egg-induced hepatopathology in non-human primates. *Parasites & Vectors*, 13(1), 109. <https://doi.org/10.1186/s13071-020-3980-z>
- Lee, J.-I., Kang, S.-J., Kim, N.-A., Lee, C.-W., Ahn, K.-H., Kwon, H.-S., Park, C.-G., & Kim, S.-J. (2010). Investigation of helminths and protozoans infecting old world monkeys: Captive vervet, cynomolgus, and rhesus monkeys. *Korean Journal of Veterinary Research*, 50(4), 273-277.
- Legesse, M., & Erko, B. (2004). Zoonotic intestinal parasites in *Papio anubis* (baboon) and *Cercopithecus aethiops* (vervet) from four localities in Ethiopia. *Acta Tropica*, 90(3), 231–236. <https://doi.org/10.1016/j.actatropica.2003.12.003>
- Leroux, L. P., Nasr, M., Valanparambil, R., Tam, M., Rosa, B. A., Siciliani, E., Hill, D. E., Zarlenga, D. S., Jaramillo, M., Weinstock, J. V., Geary, T. G., Stevenson, M. M., Urban, J. F., Jr, Mitreva, M., Jardim, A. (2018). Analysis of the *Trichuris suis* excretory/secretory proteins as a function of life cycle stage and their immunomodulatory properties. *Scientific Reports*, 8, 15921.
- Li, M., Zhao, B., Li, B., Wang, Q., Niu, L., Deng, J., Gu, X., Peng, X., Wang, T., & Yang, G. (2015). Prevalence of gastrointestinal parasites in captive non-human primates of twenty-four zoological gardens in China. *Journal of Medical Primatology*, 44(3), 168–173.
- Liu, G.-H., Gasser, R. B., Su, A., Nejsum, P., Peng, L., Lin, R.-Q., Li, M.-W., Xu, M.-J., & Zhu, X.-Q. (2012). Clear Genetic Distinctiveness between Human- and Pig-Derived *Trichuris* Based

- on Analyses of Mitochondrial Datasets. *PLOS Neglected Tropical Diseases*, 6(2), e1539.  
<https://doi.org/10.1371/journal.pntd.0001539>
- Lillywhite, J. E., Bundy, D. A., Didier, J. M., Cooper, E. S., & Bianco, A. E. (1991). Humoral immune responses in human infection with the whipworm *Trichuris trichiura*. *Parasite Immunology*, 13(5), 491–507.
- Lillywhite, J. E., Cooper, E. S., Needham, C. S., Venugopal, S., Bundy, D. A., & Bianco, A. E. (1995). Identification and characterization of excreted/secreted products of *Trichuris trichiura*. *Parasite Immunology*, 17(1), 47–54.
- List, C., Qi, W., Maag, E., Gottstein, B., Müller, N., & Felger, I. (2010). Serodiagnosis of *Echinococcus* spp. Infection: Explorative Selection of Diagnostic Antigens by Peptide Microarray. *PLOS Neglected Tropical Diseases*, 4(8), e771. <https://doi.org/10.1371/journal.pntd.0000771>
- Luo, Q. L., Qiao, Z. P., Zhou, Y. D., Li, X. Y., Zhong, Z. R., Yu, Y. J., Zhang, S. H., Liu, M., Zheng, M. J., Bian, M. H., Shen, J. L. (2009). Application of signaling protein 14-3-3 and 26kDa glutathione-S-transferase to serological diagnosis of *Schistosomiasis japonica*. *Acta Tropica*, 112(2):91–6.
- Lustigman, S., Prichard, R. K., Gazzinelli, A., Grant, W. N., Boatman, B. A., McCarthy, J. S., & Basáñez, M.-G. (2012). A Research Agenda for Helminth Diseases of Humans: The Problem of Helminthiasis. *PLoS Neglected Tropical Diseases*, 6(4), e1582.  
<https://doi.org/10.1371/journal.pntd.0001582>
- Mansilla, M. J., Costa, C., Eixarch, H., Tepavcevic, V., Castillo, M., Martin, R., Lubetzki, C., Aigrot, M. S., Montalban, X., Espejo, C. (2014). Hsp70 Regulates Immune Response in Experimental Autoimmune Encephalomyelitis. *PLoS ONE*, 9(8):e105737.
- Marcilla, A., Sotillo, J., Pérez-García, A., Igual-Adell, R., Valero, M. L., Sánchez-Pino, M. M., Bernal D., Muñoz-Antolí C., Trelis M., Esteban, J. G. (2010). Proteomic analysis of *Strongyloides stercoralis* L3 larvae. *Parasitology*, 137(10), 1577–83.
- Marcilla, A., Garg, G., Bernal, D., Ranganathan, S., Forment, J., Ortiz, J., Muñoz-Antolí, C., Dominguez, M. V., Pedrola, L., Martinez-Blanch, J., Sotillo, J., Trelis, M., Toledo, R., & Esteban, J. G. (2012). The transcriptome analysis of *Strongyloides stercoralis* L3i larvae

- reveals targets for intervention in a neglected disease. *PLoS Neglected Tropical Diseases*, 6(2), e1513. <https://doi.org/10.1371/journal.pntd.0001513>
- Mardahl, M., Borup, A., & Nejsum, P. (2019). A new level of complexity in parasite-host interaction: The role of extracellular vesicles. In *Advances in Parasitology*, (Vol. 104, pp. 39–112). Elsevier. <https://doi.org/10.1016/bs.apar.2019.02.003>
- Martin, R.J., Robertson, A.P., Bjorn, H. (1997). Target sites of anthelmintics. *Parasitology* 114 (7) (Suppl.), S111–S124.
- Mayer, M.P., Bukau, B. (2005). Hsp70 chaperones: Cellular functions and molecular mechanism. *CMLS, Cellular and Molecular Life Sciences*, 62(6), 670.
- Mei, B., Kennedy, M. W., Beauchamp, J., Komuniecki, P. R., & Komuniecki, R. (1997). Secretion of a Novel, Developmentally Regulated Fatty Acid-binding Protein into the Perivitelline Fluid of the Parasitic Nematode, *Ascaris suum*\*. *Journal of Biological Chemistry*, 272(15), 9933–9941. <https://doi.org/10.1074/jbc.272.15.9933>
- McGrew, W., Tutin, C., & File, S. (1989). Intestinal parasites of two species of free-living monkeys in far western Africa, *Cercopithecus (aethiops) sabaeus* and *Erythrocebus patas*. *African Journal of Ecology*, 27, 261–262.
- McGuire, M. T. (1974). The St. Kitts vervet (*Cercopithecus aethiops*). *Journal of medical primatology*, 3, 285-297.
- Modrý D., Petrželková K.J., Kalousová B., Hasegawa H. HPI-Lab Brno; (2015). Parasites of African Great Apes Atlas of Coproscopic Diagnostics.
- Moreno, Y., Gros, P. P., Tam, M., Segura, M., Valanparambil, R., Geary, T. G., Stevenson, M. M. (2011). Proteomic Analysis of Excretory-Secretory Products of *Heligmosomoides polygyrus* Assessed with Next-Generation Sequencing Transcriptomic Information. *PLoS Neglected Tropical Diseases*, 5(10), e1370.
- Munene, E., Otsyula, M., Mbaabu, D. A. N., Mutahi, W. T., Muriuki, S. M. K., & Muchemi, G. M. (1998). Helminth and protozoan gastrointestinal tract parasites in captive and wild-trapped African non-human primates. *Veterinary Parasitology*, 78(3), 195–201. [https://doi.org/10.1016/S0304-4017\(98\)00143-5](https://doi.org/10.1016/S0304-4017(98)00143-5)

- Muriuki, S. M. K., Murugu, R. K., Munene, E., Karere, G. M., & Chai, D. C. (1998). Some gastrointestinal parasites of zoonotic (public health) importance commonly observed in old world non-human primates in Kenya. *Acta Tropica*, *71*(1), 73–82. [https://doi.org/10.1016/S0001-706X\(98\)00040-0](https://doi.org/10.1016/S0001-706X(98)00040-0)
- Mutani, A., Rhynd, K., & Brown, G. (2003). A preliminary investigation on the gastrointestinal helminths of the Barbados green monkey, *Cercopithecus aethiops sabaesus*. *Revista Do Instituto de Medicina Tropical de São Paulo*, *45*(4), 193–195. <https://doi.org/10.1590/S0036-46652003000400003>
- Mutombo, P. N., Man, N. W. Y., Nejsum, P., Ricketson, R., Gordon, C. A., Robertson, G., Clements, A. C. A., Chacón-Fonseca, N., Nissapatorn, V., Webster, J. P., & McLaws, M.-L. (2019). Diagnosis and drug resistance of human soil-transmitted helminth infections: A public health perspective. In *Advances in Parasitology*, (Vol. 104, pp. 247–326). Elsevier. <https://doi.org/10.1016/bs.apar.2019.02.004>
- National Academies Press. (2011). *Guide for the care and use of laboratory animals* (8<sup>th</sup> ed.). Washington, D.C.
- Nikolay, B., Brooker, S. J., & Pullan, R. L. (2014). Sensitivity of diagnostic tests for human soil-transmitted helminth infections: A meta-analysis in the absence of a true gold standard. *International Journal for Parasitology*, *44*(11), 765–774. <https://doi.org/10.1016/j.ijpara.2014.05.009>
- Needham, C. S., & Lillywhite, J. E. (1994). Immunoepidemiology of intestinal helminthic infections. 2. Immunological correlates with patterns of *Trichuris* infection. *Transactions of the Royal Society of Tropical Medicine and Hygiene*, *88*(3), 262–264.
- Needham, C. S., Lillywhite, J. E., Beasley, N. M., Didier, J. M., Kihamia, C. M., & Bundy, D. A. (1996). Potential for diagnosis of intestinal nematode infections through antibody detection in saliva. *Transactions of the Royal Society of Tropical Medicine and Hygiene*, *90*(5), 526–530.
- Nejsum, P., Betson, M., Bendall, R. P., Thamsborg, S. M., & Stothard, J. R. (2012). Assessing the zoonotic potential of *Ascaris suum* and *Trichuris suis*: Looking to the future from an analysis of the past. *Journal of Helminthology*, *86*(2), 148–155. <https://doi.org/10.1017/S0022149X12000193>



- Ngari, M. G., Mwangi, I. N., Njoroge, M. P., Kinyua, J., Osuna, F. A., Kimeu, B. M., Okanya, P. W., & Agola, E. L. (2020). Development and evaluation of a loop-mediated isothermal amplification (LAMP) diagnostic test for detection of whipworm, *Trichuris trichiura*, in faecal samples. *Journal of Helminthology*, 94. <https://doi.org/10.1017/S0022149X2000022X>
- Noda, S., Hoa, N. T. V., Uga, S., Thuan, L. K., Aoki, Y., & Fujimaki, Y. (2009). Parasite egg contamination of water and air in a suburban area of Hanoi, Vietnam. *Tropical Medicine and Health*, 37(2), 55–61. <https://doi.org/10.2149/tmh.2009-04>
- Nolf, L. O. (1932). Experimental studies on certain factors influencing the development and viability of the ova of the human *trichuris* as compared with those of the human *ascaris*. *American Journal of Epidemiology*, 16(1), 288–322. <https://doi.org/10.1093/oxfordjournals.aje.a117862>
- Noya, O., Patarroyo, M., Guzman, F., & de Noya, B. (2003). Immunodiagnosis of Parasitic Diseases with Synthetic Peptides. *Current Protein & Peptide Science*, 4(4), 299–308. <https://doi.org/10.2174/1389203033487153>
- Oliveira, E. J. de, Kanamura, H. Y., Takei, K., Hirata, R. D. C., Nguyen, N. Y., & Hirata, M. H. (2006). Application of synthetic peptides in development of a serologic method for laboratory diagnosis of schistosomiasis mansoni. *Memórias Do Instituto Oswaldo Cruz*, 101(suppl 1), 355–357. <https://doi.org/10.1590/S0074-02762006000900058>
- Olsen, A. (2007). Efficacy and safety of drug combinations in the treatment of schistosomiasis, soil-transmitted helminthiasis, lymphatic filariasis and onchocerciasis. *Transactions of The Royal Society of Tropical Medicine and Hygiene*, 101(8), 747–758. <https://doi.org/10.1016/j.trstmh.2007.03.006>
- Parker, J. M., Guo, D., & Hodges, R. S. (1986). New hydrophilicity scale derived from high-performance liquid chromatography peptide retention data: Correlation of predicted surface residues with antigenicity and X-ray-derived accessible sites. *Biochemistry*, 25(19), 5425–5432. <https://doi.org/10.1021/bi00367a013>
- Pandiaraja, P., Arunkumar, C., Hoti, S. L., Rao, D. N., & Kaliraj, P. (2010). Evaluation of synthetic peptides of WbSXP-1 for the diagnosis of human lymphatic filariasis. *Diagnostic Microbiology and Infectious Disease*, 68(4), 410–415. <https://doi.org/10.1016/j.diagmicrobio.2010.07.015>

- Pérez-Sánchez, R., Valero, M. L., Ramajo-Hernández, A., Siles-Lucas, M., Ramajo-Martín, V., Oleaga, A. (2008). A proteomic approach to the identification of tegumental proteins of male and female *Schistosoma bovis* worms. *Molecular and Biochemical Parasitology*, 161(2), 112–23.
- Pérez-Morales, D., Espinoza, B. The role of small heat shock proteins in parasites. (2015). *Cell Stress and Chaperones*, 20(5), 767–80.
- Petersen, M. B., Várady, M., Bjørn, H., & Nansen, P. (1996). Efficacies of different doses of ivermectin against male, female and L4 *Oesophagostomum dentatum* in pigs. *Veterinary Parasitology*, 65(1), 55–63. [https://doi.org/10.1016/0304-4017\(96\)00948-X](https://doi.org/10.1016/0304-4017(96)00948-X)
- Petrášová, J., Modrý, D., Huffman, M. A., Mapua, M. I., Bobáková, L., Mazoch, V., Singh, J., Kaur, T., & Petrželková, K. J. (2010). Gastrointestinal Parasites of Indigenous and Introduced Primate Species of Rubondo Island National Park, Tanzania. *International Journal of Primatology*, 31(5), 920–936. <https://doi.org/10.1007/s10764-010-9439-x>
- Pullan, R. L., Smith, J. L., Jasrasaria, R., Brooker, S. J. Global numbers of infection and disease burden of soil transmitted helminth infections in 2010. *Parasit Vectors*. 2014; 7:37.
- Ravasi, D. F., O’Riain, M. J., Davids, F., & Illing, N. (2012). Phylogenetic Evidence That Two Distinct *Trichuris* Genotypes Infect both Humans and Nonhuman Primates. *PLoS ONE*, 7(8), e44187. <https://doi.org/10.1371/journal.pone.0044187>
- Radoslavov, G., Jordanova, R., Teofanova, D., Georgieva, K., Hristov, P., Salomone-Stagni, M., Liebau, E., Bankov, I. (2010). A Novel Secretory Poly-Cysteine and Histidine-Tailed Metalloprotein (Ts-PCHTP) from *Trichinella spiralis* (Nematoda). *PLoS ONE*, 5(10), e13343.
- Rawlins, S. C., Tikasingh, E. S., Baboolal, S., Hector, O., Hobsons, P., Halliday, J., & Jones, T. R. (1993). Significant changes in gastrointestinal tract parasitic infections in children of St. Kitts over the 9-year period 1982-1991. *The West Indian Medical Journal*, 42(1), 18–21.
- Reichard, M. V., Thomas, J. E., Chavez-Suarez, M., Cullin, C. O., White, G. L., Wydysh, E. C., & Wolf, R. F. (2017). Pilot Study to Assess the Efficacy of Ivermectin and Fenbendazole for Treating Captive-Born Olive Baboons (*Papio anubis*) Coinfected with *Strongyloides fülleborni* and *Trichuris trichiura*. *Journal of the American Association for Laboratory Animal Science*, 56(1), 52–56.

- Ritchie, L. S., Knight, W. B., Oliver-Gonzalez, J., Frick, L. P., Morris, J. M., & Croker, W. L. (1967). *Schistosoma mansoni* Infections in *Cercopithecus sabaues* Monkeys. *The Journal of Parasitology*, 53(6), 1217. <https://doi.org/10.2307/3276683>
- Rivero, J., Callejón, R., & Cutillas, C. (2021). Complete Mitochondrial Genome of *Trichuris trichiura* from *Macaca sylvanus* and *Papio papio*. *Life*, 11(2), 126. <https://doi.org/10.3390/life11020126>
- Salaam-Blyther, T. (2011). Neglected Tropical Diseases (NTD): Background, Responses, and Issues for Congress. Congressional Research Service. CRS Report for Congress, Washington, DC. <https://fas.org/sgp/crs/misc/R41607.pdf>.
- Sanchez-Moreno, M., Garcia-Rejon, L., Salas, I., Osuna, A., & Monteoliva, M. (1992). Superoxide dismutase from *Trichuris ovis*, inhibition by benzimidazoles and pyrimidine derivatives. *Memórias do Instituto Oswaldo Cruz*, 87, 241-246. doi: 10.1590/s0074-02761992000500045
- Santos, L. N., Gallo, M. B., Silva, E. S., Figueiredo, C. A. V., Cooper, P. J., Barreto, M. L., Loureiro, S., Pontes-de-Carvalho, L. C., & Alcantara-Neves, N. M. (2013). A proteomic approach to identify proteins from *Trichuris trichiura* extract with immunomodulatory effects. *Parasite Immunology*, 35(5–6), 188–193.
- Santiváñez, S. J., Hernández-González, A., Chile, N., Oleaga, A., Arana, Y., Palma, S., Verastegui, M., González, A. E., Gilman, R., Garcia, H. H., Siles-Lucas, M. (2010). Cysticercosis Working Group in Peru. Proteomic study of activated *Taenia solium* oncospheres. *Molecular and Biochemical Parasitology*, 171(1), 32–9.
- Shears, R. K., Bancroft, A. J., Hughes, G. W., Grencis, R. K., & Thornton, D. J. (2018). Extracellular vesicles induce protective immunity against *Trichuris muris*. *Parasite Immunology*, 40(7), e12536. <https://doi.org/10.1111/pim.12536>
- Shevchenko, A., Jensen, O. N., Podtelejnikov, A. V., Sagliocco, F., Wilm, M., Vorm, O., Mortensen, P., Shevchenko, A., Boucherie, H., Mann, M. (1996). Linking genome and proteome by mass spectrometry: Large-scale identification of yeast proteins from two dimensional gels. *Proceedings of the National Academy of Sciences of the United States of America*, 93(25), 14440–5.

- Shilov, I. V., Seymour, S. L., Patel, A. A., Loboda, A., Tang, W. H., Keating, S. P., Hunter, C. L., Nuwaysir, L. M., & Schaeffer, D. A. (2007). The Paragon Algorithm, a next generation search engine that uses sequence temperature values and feature probabilities to identify peptides from tandem mass spectra. *Molecular & Cellular Proteomics*, 6(9), 1638–1655. <https://doi.org/10.1074/mcp.T600050-MCP200>
- Schmitt, E., Gehrmann, M., Brunet, M., Multhoff, G., Garrido, C. Intracellular and extracellular functions of heat shock proteins: repercussions in cancer therapy. *Journal of Leukocyte Biology*, 2007; 81(1), 15–27.
- Sotillo, J., Valero, L., Sánchez Del Pino, M. M., Fried, B., Esteban, J. G., Marcilla, A., Toledo, R. (2008). Identification of antigenic proteins from *Echinostoma caproni* (Trematoda) recognized by mouse immunoglobulins M, A and G using an immunoproteomic approach. *Parasite Immunology*, 30(5), 271–9.
- Sotillo, J., Valero, M. L., Del Pino, M. M. S., Fried, B., Esteban, J. G., Marcilla, A., Toledo, R. (2010). Excretory/secretory proteome of the adult stage of *Echinostoma caproni*. *Parasitology Research*. 107(3), 691–7.
- Sotillo, J., Valero, M. L., Del Pino, M. M. S., Fried, B., Esteban, J. G., Marcilla, A., Toledo, R. (2011). *Zygodontia schultzei*: Proteomic analysis of the adult stage. *Experimental Parasitology*. 128(2), 133–7.
- Sotillo, J., Trelis, M., Cortés, A., Valero, M. L., Del Pino, M. S., Esteban J. G., J., Marcilla, A., Toledo, R. (2012). Proteomic analysis of the pinworm *Syphacia muris* (Nematoda: Oxyuridae), a parasite of laboratory rats. *Parasitology International*, 61(4), 561–4.
- Sotillo, J., Sánchez-Flores, A., Cantacessi, C., Harcus, Y., Pickering, D., Bouchery, T., Camberis, M., Tang, S. C., Giacomini, P., Mulvenna, J., Mitreva, M., Berriman, M., LeGros, G., Maizels, R. M., Loukas, A. (2014). Secreted Proteomes of Different Developmental Stages of the Gastrointestinal Nematode *Nippostrongylus brasiliensis*. *Molecular and Cell Proteomics*, 13(10), 2736–51.
- Stephenson, L. S., Holland, C. V., Cooper, E. S. (2000) The public health significance of *Trichuris trichiura*. *Parasitology*, 121(S1), S73–S95.

- Sturrock, S. L., Yiannakoulis, N., & Sanchez, A. L. (2017). The Geography and Scale of Soil-Transmitted Helminth Infections. *Current Tropical Medicine Reports*, 4(4), 245–255. <https://doi.org/10.1007/s40475-017-0126-2>
- Stracke, K., Jex, A. R., & Traub, R. J. (2020). Zoonotic Ancylostomiasis: An Update of a Continually Neglected Zoonosis. *The American Journal of Tropical Medicine and Hygiene*, 103(1), 64–68. <https://doi.org/10.4269/ajtmh.20-0060>
- Summers, R. W., Elliott, D. E., Urban Jr, J. F., Thompson, R. A., & Weinstock, J. V. (2005). *Trichuris suis* therapy for active ulcerative colitis: A randomized controlled trial. *Gastroenterology*, 128(4), 825–832.
- Shi, W., Xue, C., Su, X. Z., Lu, F. (2018). The roles of galectins in parasitic infections. *Acta Tropica*, 177, 97–104.
- Tantrawatpan, C., Maleewong, W., Wongkham, C., Wongkham, S., Intapan, P. M., & Nakashima, K. (2007). Evaluation of immunoglobulin G4 subclass antibody in a peptide-based enzyme-linked immunosorbent assay for the serodiagnosis of human fascioliasis. *Parasitology*, 134(14), 2021–2026. <https://doi.org/10.1017/S0031182007003435>
- Tarr, D. E. K., & Scott, A. L. (2005). MSP domain proteins. *Trends in Parasitology*, 21(5), 224–231. <https://doi.org/10.1016/j.pt.2005.03.009>
- Tsan, M. F., Gao, B. (2009) Heat shock proteins and immune system. *Journal of Leukocyte Biology*, 85(6), 905–10.
- Taylor-Robinson DC, Maayan N, Soares-Weiser K, Donegan S, Garner P. (2015) Deworming drugs for soil-transmitted intestinal worms in children: effects on nutritional indicators, haemoglobin, and school performance. *Cochrane Database of Systematic Reviews*, (11), 7: CD000371.
- Taylor-Robinson DC, Garner P. Campbell (2017) Replication confirms little or no effect of community deworming. *The Lancet Global Health*; 5: e2–e3.
- Teklemariam, D., Legesse, M., Degarege, A., Liang, S., & Erko, B. (2018). *Schistosoma mansoni* and other intestinal parasitic infections in schoolchildren and vervet monkeys in Lake Ziway area, Ethiopia. *BMC Research Notes*, 11(1), 146. <https://doi.org/10.1186/s13104-018-3248-2>

- Tikasingh, E. S., Chadee, D. D., & Rawlins, S. C. (2011). The control of hookworm disease in Commonwealth Caribbean countries. *Acta Tropica*, 120(1), 24–30. <https://doi.org/10.1016/j.actatropica.2011.07.005>
- Turner, D. G., Wildblood, L. A., Inglis, N. F., Jones, D. G. (2008). Characterization of a galectin-like activity from the parasitic nematode, *Haemonchus contortus*, which modulates ovine eosinophil migration in vitro. *Veterinary Immunology and Immunopathology*, 122(1):138–45.
- Umur, S., Moravec, F., Gurler, A., Bolukbas, C., & Acici, M. (2012). First report on *Aonchotheca annulosa* Dujardin, 1845 (Nematoda, Capillariidae) in a Hamadryas baboon (*Papio hamadryas*) from a zoo in northern Turkey. *Journal of Medical Primatology*, 41(6), 384–387. <https://doi.org/10.1111/jmp.12020>
- Utzinger, J., & Keiser, J. (2004). Schistosomiasis and soil-transmitted helminthiasis: Common drugs for treatment and control. *Expert Opinion on Pharmacotherapy*, 5(2), 263–285. <https://doi.org/10.1517/14656566.5.2.263>
- Valenta, K., Twinomugisha, D., Godfrey, K., Liu, C., Schoof, V. A. M., Goldberg, T. L., & Chapman, C. A. (2017). Comparison of gastrointestinal parasite communities in vervet monkeys. *Integrative Zoology*, 12(6), 512–520. <https://doi.org/10.1111/1749-4877.12270>
- Vercauteren, I., Geldhof, P., Peelaers, I., Claerebout, E., Berx, G., Vercruyse, J. (2003). Identification of excretory-secretory products of larval and adult *Ostertagia ostertagi* by immunoscreening of cDNA libraries. *Molecular and Biochemical Parasitology*, 126(2):201–8.
- Vos T, Allen C, Arora M, Barber RM, Bhutta ZA, Brown A. (2016). Global, regional, and national incidence, prevalence, and years lived with disability for 310 diseases and injuries, 1990–2015: a systematic analysis for the Global Burden of Disease Study 2015. *The Lancet*, 388(10053), 1545–602.
- Wammes L. J., Mpairwe H., Elliott A. M., Yazdanbakhsh M. (2014). Helminth therapy or elimination: epidemiological, immunological, and clinical considerations. *The Lancet Infectious Diseases*, 14(11), 1150–62.

- Wang, T., Yang, G., Yan, H., Wang, S., Bian, Y., Chen, A., & Bi, F. (2008). Comparison of efficacy of selamectin, ivermectin and mebendazole for the control of gastrointestinal nematodes in *rhesus macaques*, China. *Veterinary Parasitology*, 153(1), 121–125.
- Wang, Y., Cheng, Z., Lu, X., Tang, C. (2009). *Echinococcus multilocularis*: Proteomic analysis of the protoscoleces by two-dimensional electrophoresis and mass spectrometry. *Experimental Parasitology*, 123(2), 162–7.
- Wang, D., Wang, X., Wang, X., Wang, S., & An, C. (2013). Trichuriasis diagnosed by colonoscopy: Case report and review of the literature spanning 22 years in mainland China. *International Journal of Infectious Diseases*, 17(11), e1073–e1075.  
<https://doi.org/10.1016/j.ijid.2013.02.008>
- Wang, J., Zhao, F., Yu, C. X., Xiao, D., Song, L. J., Yin, X. R., Shen, S., Hua, W. Q., Zhang, J. Z., Zhang, H. F., He, L. H., Qian, C. Y., Zhang, W., Xu, Y. L., Yang, J. (2013). Identification of proteins inducing short-lived antibody responses from excreted/secretory products of *Schistosoma japonicum* adult worms by immunoproteomic analysis. *Journal of Proteomics*, 87, 53–67.
- Wang, Y., Bai, X., Zhu, H., Wang, X., Shi, H., Tang, B., Boireau, P., Cai, X., Luo, X., Liu, M., Liu, X. (2017). Immunoproteomic analysis of the excretory-secretory products of *Trichinella pseudospiralis* adult worms and newborn larvae. *Parasites and Vectors*, 10(1), 579.
- Wharton, D. A., & Jenkins, T. (1978). Structure and Chemistry of the Egg-Shell of a Nematode (*Trichuris Suis*). *Tissue and Cell*, 10(3), 427–440. [https://doi.org/10.1016/S0040-8166\(16\)30338-X](https://doi.org/10.1016/S0040-8166(16)30338-X)
- White, M., Whiley, H., & E. Ross, K. (2019). A Review of *Strongyloides* spp. Environmental Sources Worldwide. *Pathogens*, 8(3). <https://doi.org/10.3390/pathogens8030091>
- WHO (2012) a. Helminth Control in School-Age Children: A Guide for Managers of Control Programmes, second ed. World Health Organization, Geneva.
- WHO (2012) b. Soil-Transmitted Helminthiasis: Eliminating Soil-Transmitted Helminthiasis as a Public Health Problem in Children. Progress Report 2001–2010 and strategic plan 2011–2020. World Health Organization, Geneva.
- WHO (2013). Assessing the efficacy of anthelmintic drugs against schistosomiasis and soil-transmitted helminthiasis.

- WHO (2017). Nutrition for Health and Development, World Health Organization, Department of Control of Neglected Tropical Diseases, & World Health Organization. *Preventive chemotherapy to control soil-transmitted helminth infections in at-risk population groups: Guideline*. <http://www.ncbi.nlm.nih.gov/books/NBK487927/>
- WHO (2018). Soil-Transmitted Helminth Infections. Retrieved 29 August 2018, from <http://www.who.int/news-room/fact-sheets/detail/soil-transmitted-helminth-infections>.
- Wilkinson, T. S., Roghanian, A., Simpson, A. J., & Sallenave, J.-M. (2011). WAP domain proteins as modulators of mucosal immunity. *Biochemical Society Transactions*, 39(5), 1409–1415. <https://doi.org/10.1042/BST0391409>
- Williams, A. R., Dige, A., Rasmussen, T. K., Hvas, C. L., Dahlerup, J. F., Iversen, L., Stensvold, C. R., Agnholt, J., & Nejsum, P. (2017). Immune responses and parasitological observations induced during probiotic treatment with medicinal *Trichuris suis* ova in a healthy volunteer. *Immunology Letters*, 188, 32–37. <https://doi.org/10.1016/j.imlet.2017.06.002>
- Woo, W-M., Goncharov, A., Jin, Y., Chisholm, A.D. (2004). Intermediate filaments are required for *C. elegans* epidermal elongation. *Developmental Biology*, 267(1), 216–29
- Wren, B. T., Gillespie, T. R., Camp, J. W., & Remis, M. J. (2015). Helminths of Vervet Monkeys, *Chlorocebus aethiops*, from Loskop Dam Nature Reserve, South Africa. *Comparative Parasitology*, 82(1), 101–108. <https://doi.org/10.1654/4712RR.1>
- Yang, J., Pan, W., Sun, X., Zhao, X., Yuan, G., Sun, Q., Huang, J., Zhu, X. (2015). Immunoproteomic profile of *Trichinella spiralis* adult worm proteins recognized by early infection sera. *Parasites and Vectors*, 8(1):20.
- Yang, J., Zhu, W., Huang, J., Wang, X., Sun, X., Zhan, B., Zhu, X. (2016). Partially protective immunity induced by the 14-3-3 protein from *Trichinella spiralis*. *Veterinary Parasitology*, 231:63–8.
- Yao, C., Walkush, J., Shim, D., Cruz, K., & Ketzis, J. (2018). Molecular species identification of *Trichuris trichiura* in African green monkey on St. Kitts, West Indies. *Veterinary Parasitology: Regional Studies and Reports*, 11, 22–26. <https://doi.org/10.1016/j.vprsr.2017.11.004>
- Young, A. R., Meeusen, E. N. (2002) Galectins in parasite infection and allergic inflammation. *Glycoconjugate Journal*, 19(7), 601–6



Zajac, A. M., & Conboy, G. A. (2012). *Veterinary clinical parasitology*. John Wiley & Sons.

## 9 Annexes

### 9.1 Supplementary table 1





UDP glucose pyrophosphorylase	A0A077YYW4	15.7	6	53	-	Nucleotidyltransferase, UTP:glucose-1-phosphate uridylyltransferase activity	UDP-glucose metabolic process	unknown
UDP glucuronosyltransferase ugt 58	A0A077ZDR2	9.3	3	46	-	Transferase, transferase activity, transferring hexosyl groups	Transmembrane helix	integral component of membrane
Vitellogenin N and VWD and DUF1943 domain containing	A0A077ZE83	56.3	205	199	1 to 19	lipid transporter activity	unknown function	unknown
WAP domain containing protein, SLP1-like [Source:UniProt	A0A077YXJ8	6.3	1	29	1 to 25	peptidase inhibitor activity	unknown function	extracellular region or secreted
WAP domain containing protein, SLP1-like [Source:UniProt	A0A077ZDD4	6.8	1	14	1 to 18	peptidase inhibitor activity	unknown function	extracellular region or secreted
ZF-C2HG4 and Lactamase B and zf-C2CH domain containing	A0A077Z6W1	6.6	3	69	-	hydroxyacylgutathione hydrolase activity, metal ion binding	methylyglyoxal catabolic process to D-lactate via S-lacto	unknown
ZF-CDGSH domain containing protein [Source:UniProtKB/Tr	A0A077Z600	34.1	2	10	-	2 iron, 2 sulfur cluster binding	unknown function	intracellular membrane-bounded organelle
Uncharacterized protein	A0A077Z2Z2	25.1	3	16	1 to 17	GPI anchor binding	positive regulation of voltage-gated channel activity, re	Cell membrane, GPI-anchor
Uncharacterized protein	A0A077ZMT5	14.1	20	84	-	lipid binding	unknown function	unknown
Uncharacterized protein	A0A077Z2P1	13.4	2	19	1 to 16	unknown function	unknown	unknown
Uncharacterized protein	A0A077Z906	13.0	4	39	1 to 17	unknown function	unknown	unknown
Uncharacterized protein	A0A077ZG91	32.3	3	14	-	unknown function	unknown	integral component of membrane
Uncharacterized protein	A0A077Z4J9	5.2	2	26	-	unknown function	unknown	integral component of membrane
Uncharacterized protein	A0A077Z2Q3	52.2	7	51	1 to 15	unknown function	unknown	unknown
Uncharacterized protein	A0A077YWH5	3.0	1	30	-	unknown function	unknown	unknown
Uncharacterized protein	A0A077ZJW0	12.8	1	11	1 to 24	unknown function	unknown	unknown
Uncharacterized protein	A0A077ZNL3	18.6	3	65	-	unknown function	unknown	unknown
Uncharacterized protein	A0A077YVW5	3.5	1	37	1 to 27	unknown function	unknown	integral component of membrane
Uncharacterized protein	A0A077ZDH0	37.0	13	66	-	unknown function	unknown function	integral component of membrane
Uncharacterized protein	A0A077Z544	48.8	19	34	1 to 23	unknown function	unknown function	unknown
Uncharacterized protein	A0A077YXT2	16.1	10	70	1 to 18	unknown function	unknown function	unknown
Uncharacterized protein	A0A077Y1L1	21.8	6	28	-	unknown function	unknown function	unknown
Uncharacterized protein	A0A077Z0R1	42.7	6	18	1 to 19	unknown function	unknown function	unknown
Uncharacterized protein	A0A077YX18	20.4	10	33	1 to 18	unknown function	unknown function	unknown
Uncharacterized protein	A0A077YXJ5	25.7	5	174	-	unknown function	unknown function	unknown
Uncharacterized protein	A0A077ZCJ0	7.6	1	12	-	unknown function	unknown function	unknown